

courtesy Carolina Pool Management

OPTIMIZATION
OF THE AQUATIC
SPINAL BOARD

Final Report

Jennifer Dowling-Medley, Christopher Dulhanty, Matthew Tieng ENGG 4120 Winter 2015, Group 42

# **Executive Summary**

Secondary injury may occur during immobilization in a spinal board. The key issue with the conventional spinal board design includes their ability to immobilize patients, comfort, and their ease of use and lack of modularity. Deficiencies in these areas could contribute to poor patient outcomes, which in the case of spinal injury has an immense economic impact upon patients, families, lifeguards and pool operators.

The optimization of the aquatic spinal board was conducted to aid in the immobilization process during emergency response and allow for easier maneuverability of the board, and its patient, to exit the pool and to allow for greater comfort and reduce possible secondary injury.

The main objective of this project was to optimize current spinal boards by:

- modification of physical structure for optimal ergonomics during lifesaving procedures;
- material selection for optimal patient comfort, performance and environmental considerations;
- design of modular harnessing system for spinal immobilization of a wide range of body types.

The alternative design solution for each objective was critiqued to select a design that not only fulfil the constraints set by the project group but also standards pertaining to spinal boards. The criteria must also be fulfilled to allow the optimization to demonstrate the intended improvement over current conventional spinal boards.

The major constraints of the spinal board design were that it comply fully with ASTM Standard F1557, allow for current lifesaving procedures as outlined by the Lifesaving Society of Canada to be performed, be comprised of materials that are compatible with diagnostic imaging technology and that it must be easily sanitized without deterioration. The board must also not obstruct the use of AED while still allowing immobilization of the spinal column.

The major criteria for the material selection was that the selected material must have lower net density than that of conventional spinal boards, increased Young's Modulus and yield strength, increased durability in common aquatic and terrestrial conditions and a reduction in CO₂ footprint. The board ergonomics must have simplicity in design, capacity to immobilize, perform knife and slant rescue, land rescue and permit easier maneuverability relative to current spinal boards. Lastly, the harnessing system must maintain closeness in design to current board, allow higher variability in strapping conditions, and be easy and intuitive to use.

The alternative designs were selected prior to the interim report and implemented as a prototype. The report examines the experimental testing and simulations conducted to analyze the various aspects of the prototype to be implemented into a final, comprehensive design.

## Nomenclature

ABS – Acrylonitrile butadiene styrene

AED - Automated external defibrillator

BC – Board center marker

BL – Board left marker

BTOP - Board top marker

CPR - Cardio-pulmonary resuscitation

FBD - Free body diagram

FEA – Finite element analysis

FH – Forehead marker

HDPE - High-density polyethylene

LC – Left cheek bone marker

LCA - Life cycle analysis

LCLAV – Left clavicle marker

MA – Manubrium marker

PHB – Polyhydroxybutyrate

PLA - Polylactide (Polylactic acid)

PVC - Polyvinyl chloride

RC – Right cheek bone marker

RCLAV – Right clavicle marker

ST – Sternum marker

TPU – Thermoplastic polyurethane

tSCI - Traumatic spinal cord injury

# **Table of Contents**

Execu	tive Sun	nmary	ii
Nome	nclature	e	iii
1.0	Introd	uction	1
1.1	Pro	blem Statement	1
1.2	Obj	ectives	3
2.0	Backg	round	4
2.1	Cur	rent State of Technology in the Field	4
2.2	Con	straints	6
2.3	Ass	umptions	6
2.4	Crit	eria	6
2.5	Oth	er Considerations	7
3.0	Metho	odology	8
3.1	Har	ness System Prototype	8
3	.1.1	Construction	8
3	.1.2	Motion Capture Data Collection	9
3	.1.3	Unused Experimental Trials	12
3	.1.4	Data Processing	12
3	.1.5	Head Range of Motion – KineMat MATLAB Toolbox	12
3	.1.6	Longitudinal and Lateral Body Displacement	14
3	.1.7	Survey of Lifeguards	15
3.2	Boa	rd Geometry Design	16
3	.2.1	Static Buoyancy Optimization	17
3	.2.1	Analysis of Curved Profile	19
3	.2.3	FEA Analysis of Structural Integrity	23
3.3	Boa	rd Surface Material Optimization	24
4.0	Result	s & Discussion	26
4.1	Har	ness System Prototype	26
4	.1.1	Modified Harness System Motion Capture Results	28
4	.1.2	Modified Harness System Motion Capture Discussion	31
4	.1.3	Modified Harness System Survey Results	33
4	.1.4	Modified Harness System Survey Discussion	33

4.2 Sp	oinai Board Geometry	34
4.2.1	Static Buoyancy Optimization	35
4.2.2	Analysis of Curved Profile	36
4.2.3	FEA Analysis of Structural Integrity	38
4.3 M	laterial Selection	40
4.3.1	Alternative Analysis	41
4.3.2	Selected Alternative	42
4.3.3	Modified Board Surface Motion Capture Results	43
4.3.4	Modified Board Surface Discussion	44
4.5 Ov	verall Spinal Board Design	45
4.5.1	Bill of Materials	45
4.5.2	Implementation Cost	45
4.5.3	Risk and Uncertainties	46
4.5.4	Life Cycle Analysis	47
5.0 Cond	clusions	49
6.0 Reco	ommendations	50
References		51
Appendices		54
Appendix	A – ASTM Standards	54
Appendix	B – Excerpt from a Canadian Lifeguard Manual	56
Appendix	C – Sensitivity Analyses for Decision Matrices	59
Spinal I	Board Geometry	59
Harnes	ssing System	60
Appendix	D – Static Fluids Calculations for Board Geometry Design	61
Appendix	E – Sample SolidWorks FEA Summary	64
Appendix	F – Lifeguard Survey	74
Appendix	G – LCA Results	76
Spinal I	Board LCA (QTY 1)	76
Spinal I	Board LCA (QTY 1000)	77
Appendix	H – KineMat MATLAB Toolbox	79
Angle p	peak-to-peak determination	79
Cardan	ı.m	80

	Soder.m	.81
	Screw.m	.83
Αı	ppendix I – Full Experimental Results	. 85

# List of Figures

Figure 1 Slant rescue (left) and knife rescue (right)	2
Figure 2: Schematic of typical aquatic spinal board [22]	5
Figure 3 Modified spinal board with harnessing system rail and padding	9
Figure 4: Vicon motion capture tests	10
Figure 5: Custom marker set	11
Figure 6: Proof-of-concept helical axis experiment	14
Figure 7: Preliminary board geometry design	16
Figure 8: FBD for static analysis of knife rescue	18
Figure 9: FBD for static analysis of slant rescue	18
Figure 10: Dynamic motion of conventional board during knife rescue	21
Figure 11: Dynamic motion of curved board during knife rescue	21
Figure 12: Boundary Conditions, Mesh and Loading Conditions of FEA Analysis	24
Figure 13 Final design of the optimized spinal board	26
Figure 14: Comparative representative example of tip test peak-to-peak ROM	27
Figure 15: Representative example of tip test cumulative longitudinal body displacement	27
Figure 16: Mean peak-to-peak ROM and 95% confidence intervals for drag test with conventional and	d
modified harness designs	28
Figure 17: Mean cumulative longitudinal displacement and 95% confidence intervals for drag test wit	th
conventional and modified harness designs	28
Figure 18: Mean peak-to-peak ROM and 95% confidence intervals for tip test with conventional and	
modified harness designs	29
Figure 19: Mean cumulative longitudinal displacement and 95% confidence intervals for tip test with	
conventional and modified harness designs	29
Figure 20: Mean peak-to-peak ROM and 95% confidence intervals for puke test with conventional an	d
modified harness designs	30
Figure 21: Mean cumulative lateral displacement and 95% confidence intervals for puke test with	
conventional and modified harness designs	30
Figure 22: 3D reconstruction of puke test trials for conventional and modified harness systems	32
Figure 23: Mean survey score and 95% confidence intervals for lifeguard survey of conventional and	
modified harness systems	33
Figure 24: Optimized Board Geometry Design	34
Figure 25: Final Configuration of Ports with Dimensions	36
Figure 26: Estimated drag forces of different board profiles during knife rescue	37
Figure 27: Displacement of Spinal Board with 2mm Shell, 200kg Load	39
Figure 28: Mean peak-to-peak ROM and 95% confidence intervals for drag test with conventional and	d
modified surface designs	43
Figure 29: Mean peak-to-peak ROM and 95% confidence intervals for tip test with conventional and	
modified surface designs	44

## **List of Tables**

Table 1: Summary of FEA Results	39
Table 2 Material properties of thermoplastic alternatives	41
Table 3 Components to be manufactured for the construction of the spinal board	45
Table 4 Components for purchase from other manufacturers.	45
Table 5 Cost of PLA for production processing per 1 spinal board assembly (assume 10% waste)	45
Table 6 Injection moulding cost for 1000 spinal boards (materials, labour and tools)	46
Table 7 Total cost of purchased parts not manufactured	46
Table 8 Summarized LCA for the production of 1 spinal board	47
Table 9 Summarized LCA for the production of 1000 spinal boards	48
Table 10 Overview of the CO2 emission of a spinal board	76
Table 11 Manufacturing and disposal of a spinal board	76
Table 12 CO2 emissions from the transportation of PLA from supplier	77
Table 13 Overview of the CO2 emission of 1000 spinal board	77
Table 14 Manufacturing and disposal of 1000 spinal board	77
Table 15 CO2 emissions from the transportation of PLA from supplier	78
Table 16: Full results of peak-to-peak angles	85
Table 17: Full results of body displacement	85

## 1.0 Introduction

## 1.1 Problem Statement

Emergency care in the aquatic environment poses a number of unique challenges from the perspective of medical equipment design. Because of this, specialized or modified equipment is often required in order to overcome the challenges afforded by this environment. One notable example of this is the aquatic spinal board. Like a land-based spinal board, aquatic spinal boards aim to provide total immobilization of a patient's body in preparation for hospital transportation. In addition to this, aquatic spinal boards must be able to be effective for use in-water, and be able to facilitate patient removal from water, which may be complicated by ramps, deck or dock ledges, and steps.

As a result of these constraints, aquatic spinal board design has converged around a number of common features, while maintaining the same basic functionality as a regular land spinal board. Some of these unique features include the use of buoyant materials such as HDPE and wood in the construction of the rigid backboard, the existence of sled-like rails on the bottom surface, and the existence of a rubber flap ("beaver tail") [1]. Like a land-based spinal board, aquatic spinal boards feature handle holes along the outside edge of the board, a number of lateral straps and a headpiece or cervical collar [1]. The strapping system typically involves 3-4 straps, which are anchored on the board at fixed locations that correspond to the average location of the chest, hips, knees and ankles [1].

Procedures that are performed with or assisted by the use of an aquatic spinal board tend to fall into four categories:

- Deep water rescue (above rescuer standing depth)
- Shallow water rescue (rescuer standing depth)
- Very shallow water or land rescue (water too shallow for patient to float)
- Non-spinal rescues or procedures

Because most spinal injuries result from diving in shallow water or slipping and falling, shallow water and land rescues are the most commonly performed rescues [2]. Spinal boards may also be used in non-spinal rescues as a lever to facilitate removal of larger persons or to raise a patient above the deck level to keep them dry during AED use.

For true in-water rescues, lifeguards may elect to use either a "knife rescue" or "slant rescue" in order to mount the patient on the board, as depicted in Figure 1. Typically, a spinal board's geometry and buoyancy will dictate which type rescue will be performed, however other factors such as lifeguard confidence in one procedure over another, number of rescuers available and patient circumstance can also dictate this choice. For example, a knife rescue tends to require more rescuers in order to ensure the board is pushed under the patient in a controlled manner, and to stabilize the length of the board during immobilization [3]. A knife style rescue however, can be performed in deep water, or where there does not exist a ledge on which to slant the board (such as a waterfront facility or lagoon-style pool).

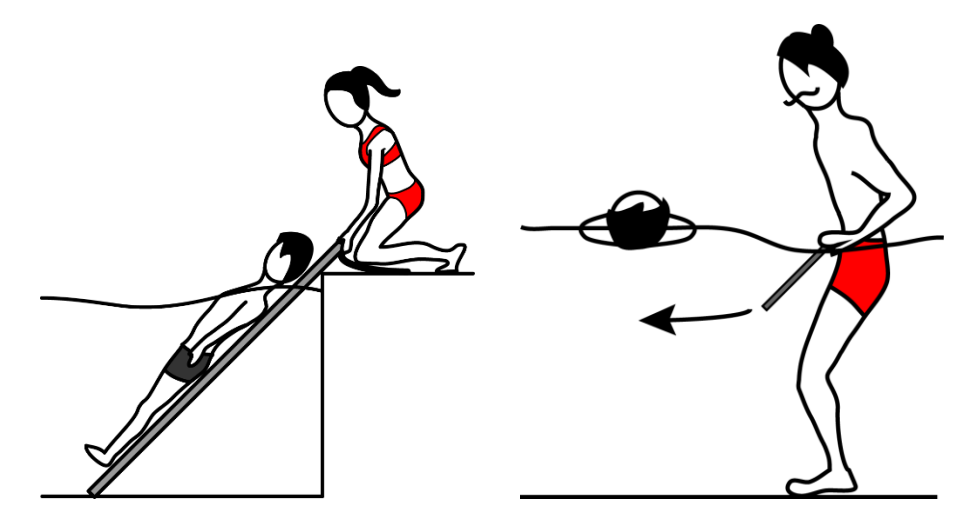


Figure 1 Slant rescue (left) and knife rescue (right).

A slant board is designed to sink slightly at the foot-end, and has a beaver tail to facilitate stability and lifeguard comfort during mounting immobilization. A knife board is designed to be more buoyant, so that the patient floats horizontally in the water after mounting on the board without excessive need for support by the lifeguard team.

In spite of these aquatic-specific design features, current spinal board designs tend to pose a number of issues for lifeguards, pool operators and patients. For lifeguards and pool operators, there is a great deal of concern with poor patient outcomes from a legal perspective and also with time spent in training on spinal rescue procedures, both during training courses and at seasonal in-house sessions [3]. In-house sessions are often paid, and involve the full lifeguarding staff, and may involve extra training sessions for newer staff to be trained on the facility's specific spinal board. From this perspective, an improved spinal board could have a great economic impact in reduced operating costs and in lowering the likelihood of lawsuits from injured parties.

For patients, there is considerable concern with poor outcomes, as spinal cord injury can have devastating physical and economic consequences [4]. Most spinal cord injuries sustained in an aquatic environment are a result of diving, and occur to the cervical spine, which often leads to death or permanent disability if improperly managed [5]. Improper management of such injuries during the rescue procedure may also cause secondary injuries [5]. For example, excessive movement of the limbs or head during the immobilization and removal process may cause further injury to the spine [5]. There is also concern for serious soft tissue injury, such as bed sores, as result from being immobilized for long periods of time post-rescue [6].

Main issues that contribute to these concerns include:

- Necessity to compromise immobilization for quick removal due to time consuming procedure
- Confinement to rescue styles permitted by individual board design
- Lifeguard unfamiliarity with individual design

- Inability to attain adequate immobilization for all body types
- Hard, non-compliant surfaces contacting bare skin, pressure risers

Through improvement of spinal board design, many of these issues could be addressed. For example, lifeguard unfamiliarity, which could lead to improper or slower rescue techniques, is largely a result of the great variability in spinal board design at different facilities. These different designs exist because there is no one design that manages to perform all types of rescues to a high degree, and thus designing a board that better accommodates all rescue styles and situations would lead to greater homogeneity, and less potential for inadequate rescues due to unfamiliarity. This would also mean that there would be less chance of having to compromise immobilization for speed, as lifeguards would be able to choose the optimal rescue style in a given situation.

With this in mind, the creation of an optimized aquatic spinal board design solution has been proposed in order to remedy these issues. The scope of this project will include will include the creation and testing of various prototypes in order to ascertain their individual effectiveness. Results from this testing will be used to refine the final design recommendations.

## 1.2 Objectives

This optimized spinal board design will aim to address the key issues previously outlined, with the endresult of improving patient outcomes and alleviating the stress felt by lifeguards and pool operators who are responsible for these outcomes.

Three different aspects of board design were identified whose improvement would contribute most to these goal. These areas will be the focus of the design optimization process.

- modification of physical structure for optimal ergonomics during lifesaving procedures;
- material selection for optimal patient comfort, performance and environmental considerations;
- design of modular harnessing system for spinal immobilization of a wide range of body types.

In order to arrive at the optimized design solution, the best solution for each of these features was selected from various alternative design solutions that was then combined to form an overall design recommendation. This recommendation represents a novel product that would ideally replace spinal boards used at Canadian aquatics facilities if put into mass production.

Implementation of the optimized design solution employed a combination of physical and computer-based prototypes that provided quantitative evaluation of each design feature, as appropriate. Through the use of these evaluations, refinement and further optimization of each design feature occurred, and improvement over existing designs was assessed. Results from this is to be used to render the overall design recommendation, which will serve as the final result of design.

# 2.0 Background

It is estimated that 3 spinal cord injuries per million persons occur each year in the United States as a result of swimming or water-related incidences [2]. Assuming such a comparison is valid, this would correspond to around 105 aquatics-related spinal cord injuries per year in Canada. Aquatic traumatic spinal cord injuries (tSCI) are almost exclusively located in the cervical spine, with several epidemiological studies accounting for 95% or higher of aquatic tSCI in this region. Males under 25 years of age are the most common demographic that is injured [2].

In Canada a lifeguard is legally defined as one who is certified by the National Lifeguarding Service (NLS) and is certified in Standard First Aid [7]. From a legal perspective, lifeguards must follow the most recent protocols outlined by the recognized governing body they received training from, such as the Canadian Red Cross or Lifesaving Society [7]. These protocols include a variety of techniques relating to management of spinal injuries and use of spinal boards.

In general, there are three situations in which a lifeguard may use a spinal board: deep water, shallow water and on land [1]. Depending on the situation, different board characteristics become more or less desirable [1]. Each of these situations requires a minimum of two, but ideally three to four lifeguards to perform the rescue [7]. The end goal of any spinal rescue is to mount the patient securely and move them out of and away from water in preparation for the arrival of paramedics [7].

## 2.1 Current State of Technology in the Field

A spinal board is a flat piece of wood or high-density polymer material with a number of hand holes. A retention system is present, comprised of a number of straps that are fastened with buckles or Velcro, and a device to secure the head and neck, such as a cervical collar or a "headpiece". Runners run longitudinally on the back of the spinal board, allowing it to sit above the ground and to be dragged easily across the pool deck. In addition, some spinal boards feature a rubber flap near the head of the board known as a "beavertail", which enables a guard kneeling on deck to provide additional stability while the straps and headpiece are fastened [1]. Figure 2 displays the schematic of a typical aquatic spinal board. Exact protocols for immobilization can vary depending on the board design, and some pools might have special boards designed for children or very large persons. Metal is typically avoided in designs to allow for diagnostic imaging to be used without transferring the patient to another board at the hospital.

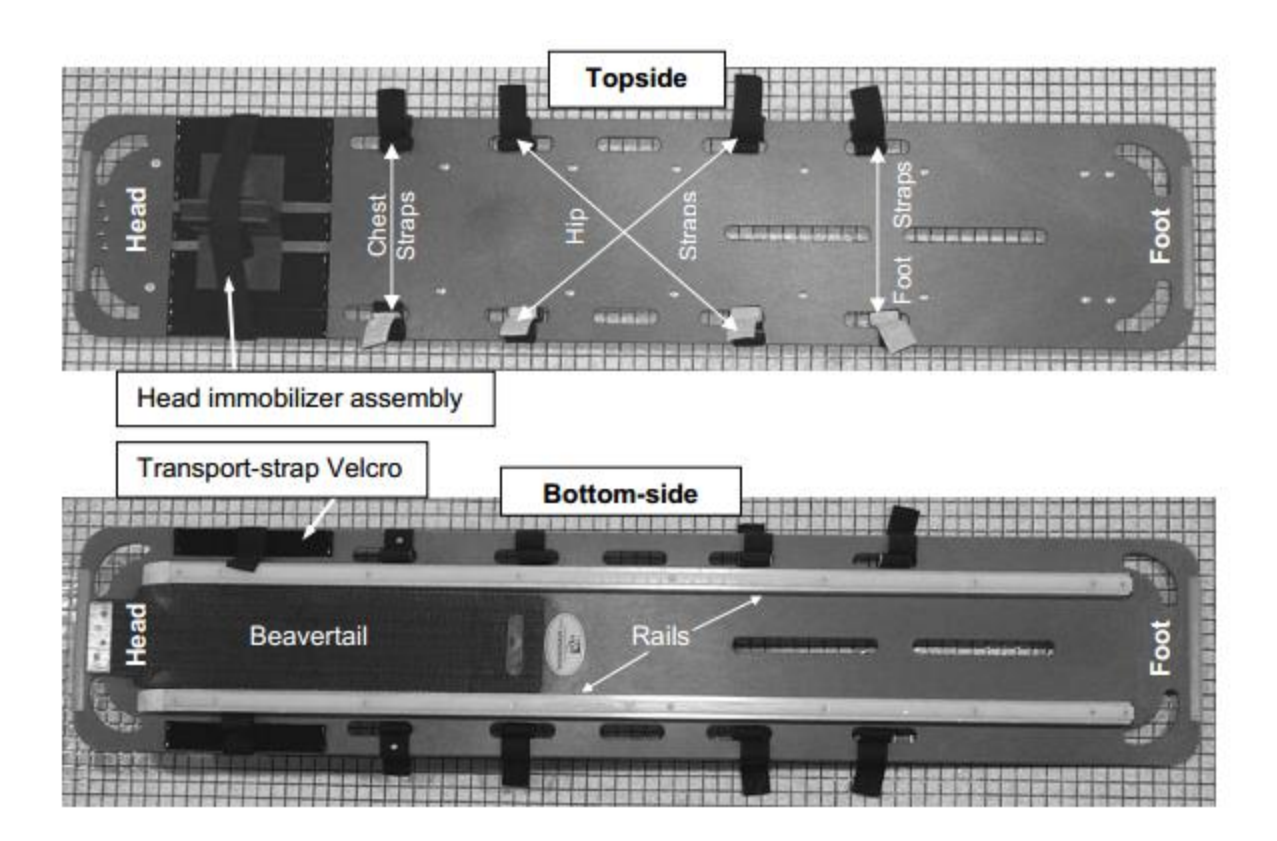


Figure 2: Schematic of typical aquatic spinal board [22].

There exist two styles of aquatic spinal board recoveries; the "side-knife" and "slant-board" procedures. In a side-knife procedure, the board is brought to the horizontal of the patient in the water and is pushed underneath them [7]. In a slant-board recovery, the board is stabilized on the deck with a beavertail, angled downwards from the edge of the pool, and the patient is guided on to it as the board is raised [7]. After this initial mounting on the board, the rescue continues in the same manner [7].

An existing alternative to the traditional flat spinal board design is the vacuum mattress, which is commonly employed for land-based spinal rescues. This type of equipment tends to score better in terms of patient comfort and level of immobilization [8], but is not commonly employed in aquatic environments due to unfamiliarity. Other similar strategies include the use of padding on rigid spinal boards [6].

Aside from spinal injury rescues, spinal boards are sometimes used for other procedures. For example, a spinal board may be used to elevate a patient above a wet deck during the use of an automated external defibrillator (AED).

Complications may arise during a spinal board rescue that can pose risks to the quality of care during immobilization. For example, as a patient's airways and breathing are prioritized over other injuries, the immobilization procedure may be critically abbreviated in order to perform cardio-pulmonary resuscitation (CPR) as quickly as possible [7]. Additionally, if the patient starts to vomit during CPR or the

immobilization procedure, they and the board will be rotated sideways to prevent choking or aspiration, regardless of whether this might risk further damage to a spinal injury [7].

#### 2.2 Constraints

Constraints to be considered in the optimization of the aquatic spinal board include:

- Full compliance with "ASTM Standard F1557 94 (2007): Standards Guide for Full Body Spinal Immobilization Devices (FBSID)", as outlined in Appendix A ASTM Standards.
  - Of note, the spinal board must support, at a minimum, the full height and weight of the 95<sup>th</sup> percentile American male patient (6'3" 290lbs) [7]
- Current lifesaving procedures as outlined by the Lifesaving Society of Canada's "Alert:
   Lifeguarding in Action" must be accomplished without modification, including protocols in deep water, shallow water and on land. Appropriate sections of the manual can be found in Appendix B Excerpt from a Canadian Lifeguard Manual.
- Construction from materials that do not interfere with diagnostic imaging technology
- Construction from materials that can be easily sanitized, without product deterioration
- Access to areas of the body necessary for AED use must not be obstructed
- A retention system that includes a headpiece and at minimum three straps must be included in the design, as required by the "Public Pool Safety Standards for Canadian Public Swimming Pools" [1]
- Immobilization of the spinal column, analyzed through the use of VICON 3D motion capture on markers placed on the head and trunk of a subject, must be (at minimum) as successful at minimizing relative movement during a lift, turn and drag test as a currently available spinal board when compared to a control

## 2.3 Assumptions

Assumptions that are made in the design include:

- Users of the spinal board are fully educated on currently regulatory lifesaving procedures and proper immobilization techniques
- The board will be used primarily in an indoor pool environment, not an outdoor setting such as a beach or a lake
- Movement of the head and trunk accurately replicates the relative movement of the cervical spine in 3D motion capture

#### 2.4 Criteria

Criteria to evaluate the success of the design include:

- Material selection criteria:
  - Density: a lower density means a lower mass and therefore a lower weight, desirable for lifting and maneuvering the device – a lower density also means a greater buoyancy
  - Material cost: a lower material cost reduces manufacturing costs and lowers the barrier of entry for customer

- Young's Modulus: a measure of the stiffness of the material higher is desirable to ensure the device does not bend when weight is applied
- Yield Strength: a higher value means a greater force the material can withstand before plastic, permanent deformation begins, which is very undesirable in a piece of lifesaving equipment
- Durability: the ability of the material to withstand freshwater, saltwater, and ultraviolet light, as determined by documented qualitative figures provided by CES EduPack 2014
- Environmental Impact: the impact on the environmental of the primary production of the material, measured in its equivalent CO2 footprint
- Board ergonomics criteria
  - Simplicity
  - Capacity to immobilize
  - Knife and slant rescues
  - Land rescue
  - o Ease of maneuverability in water
- Harnessing system criteria:
  - Maintain closeness in design to current board to allow easier training methods
  - o Modularity of design: the number of discrete ability for the spinal board to adjust
  - Intuitiveness of features/ ease of use: a qualitative measure determined from survey results of certified lifeguards conducting training sessions

#### 2.5 Other Considerations

In Canada, the annual economic burden of all spinal cord injuries is \$2.67 billion, encompassing healthcare costs, legal costs and indirect costs [10]. The estimated individual lifetime economic burden of tSCI ranges from \$1.5 million to \$3.0 million for incomplete paraplegia and complete quadriplegia, respectively [10]. Lifeguards and pool operators can also face financial and judicial repercussions from incidences of spinal injuries if they are deemed criminally negligent [7]. Thus, ensuring aquatic spinal boards are optimally designed and used correctly is of critical importance to patients, lifeguards, pool operators and society.

From an environmental standpoint, the material selection is taken into consideration to not only allow lowered environmental impacts during the primary production of the material, but also the material's biodegradability will lead to more environmentally friendly disposal of old or damaged spinal boards.

# 3.0 Methodology

## 3.1 Harness System Prototype

In order to properly assess the success of the modular harness system, it was determined that a prototype would be constructed, as simulations would be both complex and require too many assumptions to be successful in modelling the system. The final design specifies the harness system to be built into the sides of the spinal board itself through an injection-molding process, however it was not possible to construct a full prototype of the spinal board in this manner due to time and money limitations of the project. Therefore, a harness system prototype would have to be a modification to the conventional spinal board.

This modification would come along with it a few assumptions. The harness system would be affixed to the spinal board along its sides using risers and pipe clamps, therefore sitting higher vertically than the current system on the spinal board. It was assumed that this higher vertical position would not have a large impact on spinal immobilization tests. As the final board design specifies a curved geometry for ergonomic purposes, the sides of the board sit at a higher position relative to the middle of the board. The modification would therefore be a more accurate representation of the final design with respect to the vertical position of the harness system.

As most aquatic spinal injuries involve the cervical spine, it was assumed that motion in this area was the most important area to assess. Due to this, only one harnessing system was constructed for use in spinal immobilization testing. In contrast to the three modular harnessing systems for the chest, hip, and leg straps that the final design specifies, the prototype would have only one. It was assumed that this would not have a large impact on the spinal immobilization results, as the head and trunk segments were the only areas assessed for movement.

#### 3.1.1 Construction

Construction of the prototype harness system was done with the aid of Ken Graham in the School of Engineering Machine Shop. Two 12-inch nylon rods of 1-1/2 inch diameter were machined with a longitudinal groove along with 10 strapping positions, each separated by one inch. This would allow for a much greater range in harnessing position.

The sliding belt clip was intended to be 3D printed, but difficulties in accessing a 3D printer capable of printing the components in a proper timeframe lead to an alternate construction method. 1-1/2 in. Sch. 40 PVC pipe was cut to 50 mm length and drilled with a central 5 mm diameter hole. A circular head bolt was chosen to act as the interior mechanism of the belt clip, allowing it to move and lock into place within the machined grooves. Two small holes were drilled into the ends of the belt clip to allow for zip ties to hold the belt into place. A 3-pronged buckle and thick seatbelt-grade polyester webbing was chosen as the belt material.

The rods were attached to the board through the use of pipe clamps and 20 mm risers at the top and bottom of the rods. The risers would provide the sliding component proper clearance to move freely along the length of the rod. The pipe clamps were fastened very tightly as to ensure that stress placed on the rod from the seatbelt would not alter the position of the rods on the board during testing. It was

assumed that during experimental trials the rods themselves did not move and compromise the integrity of the modified harness system.

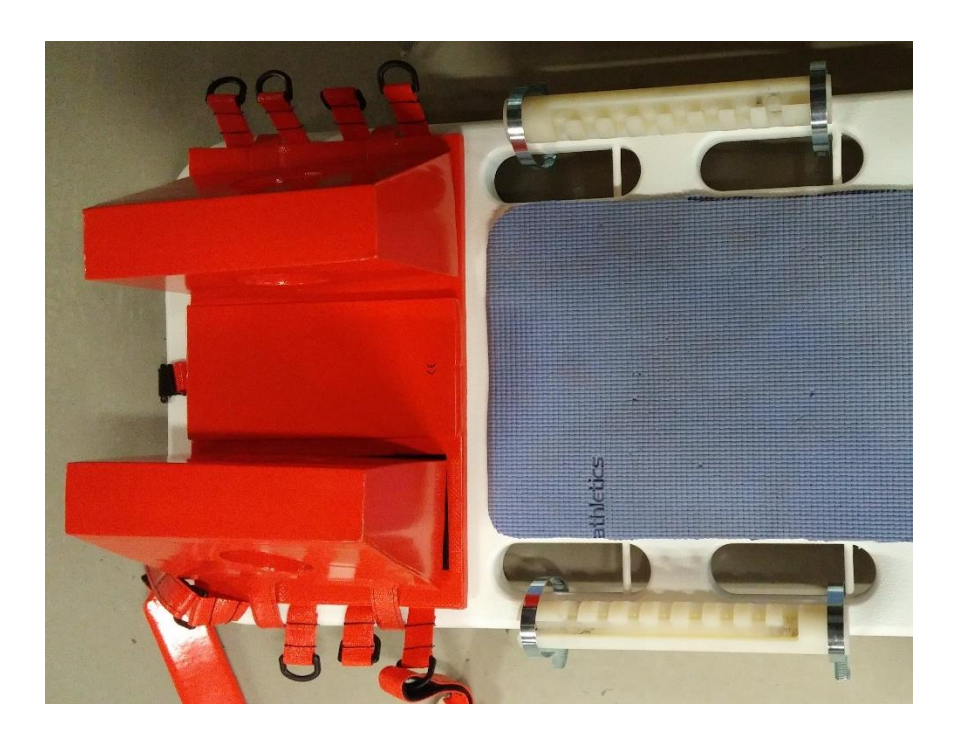


Figure 3 Modified spinal board with harnessing system rail and padding.

#### 3.1.2 Motion Capture Data Collection

The modified harnessing system was tested using a Vicon motion capture system to determine the success in spinal immobilization when compared to the conventional model. The Vicon motion capture system used was located in the School of Engineering Biological Engineering Lab, THRN 2135. The system utilizes seven infrared cameras to locate passive markers within a capture volume, which can then be reconstructed using Vicon Nexus software to determine positional data. Data was sampled at 100 Hz.

Static calibration and dynamic calibration of the Vicon system took place as well as efforts to minimize artifacts within the capture volume by removing reflective materials and light sources. Care was taken when determining the orientation in which experiments were performed as to allow for a maximum number of cameras to be in sight of each marker for the entire duration of the test.

Three different tests were performed on a male subject (67 kg, 182 cm) to simulate spinal immobilization protocols that are derived from the Royal Canadian Lifesaving Society [7]. The Tip Test, seen in Figure 4A, saw the spinal board lifted longitudinally to a 45° angle. This test sought to simulate the slant style rescue. The Puke Test, as seen in Figure 4B, saw the spinal board lifted laterally to a 90° angle. This test sought to simulate the act of rolling the victim on their side if an airway were to become

constructed due to vomit during immobilization or CPR. The Drag Test, as seen in Figure 4C, saw the spinal board dragged three meters in the longitudinal direction. This test sought to simulate the act of moving a victim who was already on land in order to position them in a more advantageous position for supplementary care or extraction by paramedics.

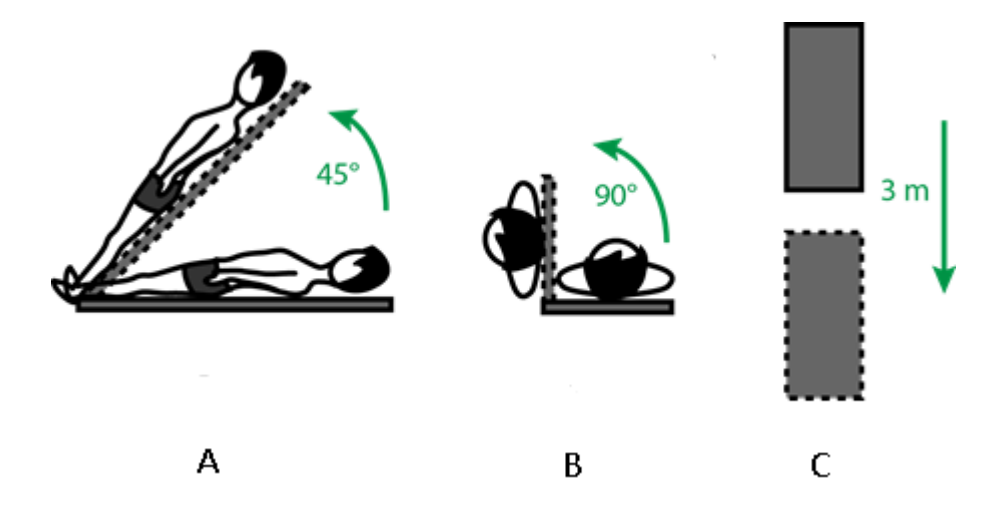


Figure 4: Vicon motion capture tests

Three trials of drag, tip, and puke tests were performed with the conventional harness system and then with the modified harness system. In addition, three trials of each test were performed with a padded spinal board condition with the conventional harness system. In doing so, direct comparisons between the conventional board and the performance of each modification could be made. It should be noted that as testing was performed manually, there were inherent differences from trial to trial in gross board movement. In order account for this lack of trial standardization, the same researcher performed all manual lifting tasks for all trials of the same subject.

In order to adequately measure spinal immobilization, a custom marker set was used to create a free joint between the head and trunk. Three markers corresponding to the forehead (FH), right cheek bone (RC) and left cheek bone (LC) were used for the head segment. Four markers corresponding to the sternum (ST), manubrium (MA), right clavicle (RCLAV) and left clavicle (LCLAV) were used for the trunk segment. Anatomical locations of the markers can be seen in Figure 5.

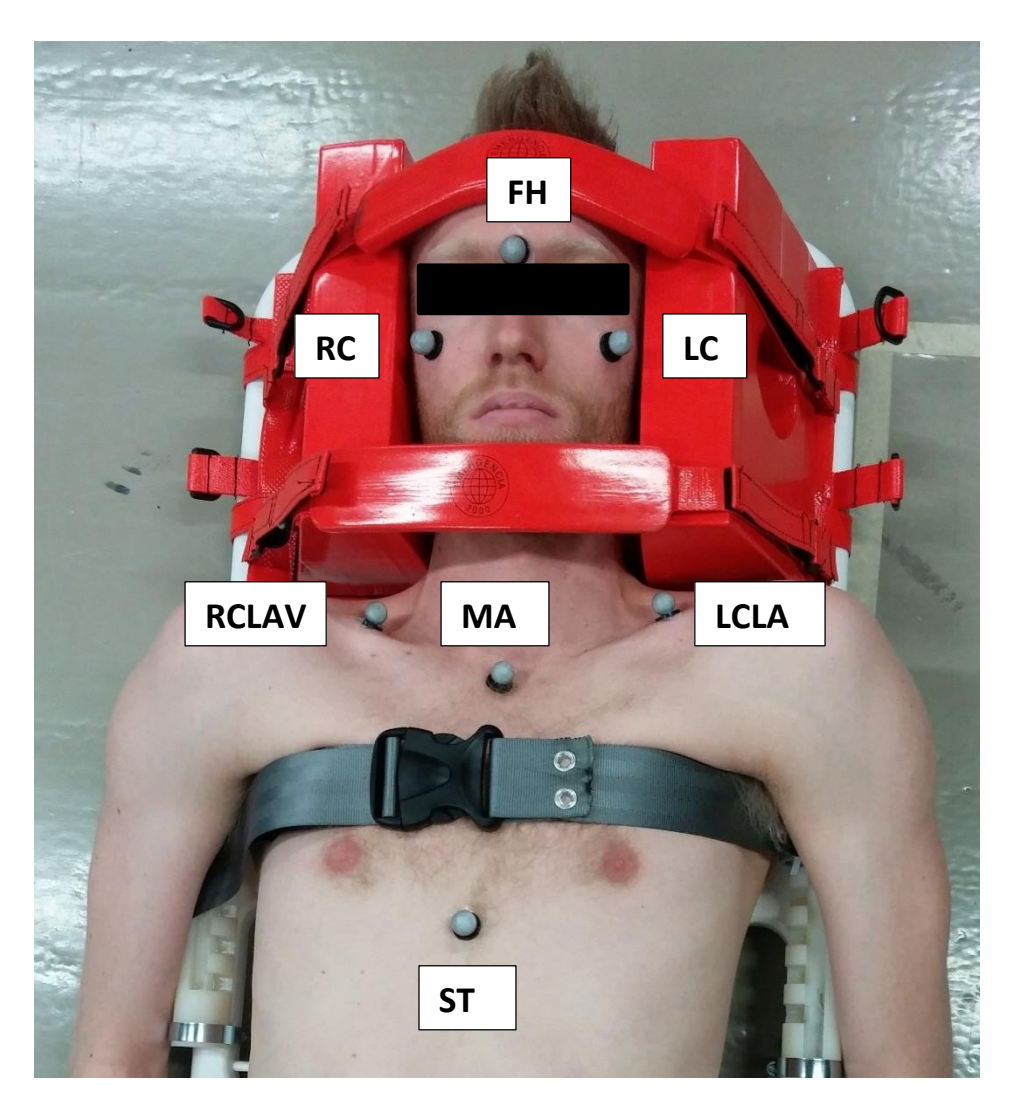


Figure 5: Custom marker set

In addition to the markers placed on the subject, three markers were affixed to the spinal board itself as to determine the relative movement of the subject with respect to the board during a trial. One marker was affixed at the bottom of the board in the centre (BC), one was affixed at the bottom of the board in the left corner (BL), and one was affixed 15 cm directly above the BL marker (BTOP).

As the consistent location of markers on a subject's body was instrumental to the successful collection of data, efforts were made to complete the entirety of trials within the same session. All data presented in this report represent trials performed solely on March 27, 2015, without the removal of markers on a subject between trials.

In order to ensure that the subject was restrained to the spinal board to meet regulatory standards, a researcher with 3 years' experience in lifeguarding and experience teaching Bronze Cross and Bronze Medallion courses preformed the spinal immobilizations for all trials. It was assumed that the restrainment technique was performed successfully for all trials. In addition, straps were adjusted to a consistent tightness based on the best judgement of the researcher with lifeguarding experience.

#### 3.1.3 Unused Experimental Trials

It should be noted that a preliminary set of nine trials that corresponded to drag, tip, and puke tests for the conventional spinal board took place on March 11, 2015, but were not included in subsequent analysis as markers were not affixed to the spinal board for this session.

Additional trials involving one male subject (64 kg, 168 cm) and one female subjects (61 kg, 175 cm) were performed on March 27 to analyze the performance of the modified harness system for additional anatomies. The tip test was chosen to be replicated by the two additional subjects as this test was determined to have the largest ROM and lateral displacement, thus it would be the best representation of potential improvements to these areas for a wide range of body types. Unfortunately, this data was not collected in a successful manner, as large gaps within marker data sets were present. There were not, at minimum, three markers per segment available for each frame, and therefore data could not be calculated using data processing methods. Marker gaps in the trials were large and it was therefore deemed inappropriate to perform interpolation as the result would not be an accurate representation of the true movement during the trial. As this error in data collection was widespread, it was concluded that no results could be drawn from these additional trials.

## 3.1.4 Data Processing

Motion capture data was generally complete but marker gaps were sporadically present in trials. These gaps represented instances in which fewer than two infrared cameras were able to determine the location of the marker in question. Two gap filling methods were used in the Vicon Nexus software to estimate missing data; spline interpolation was used primarily for gaps smaller than 20 frames, and trajectory duplication was used for gaps larger. Trajectory duplication involved the selection of a secondary marker and the copying of the secondary marker's trajectory to estimate the trajectory of the primary marker. In using this method of gap filling, a rigid body assumption was in place, as markers within the head segment or trunk segment were used to fill in data for missing markers only within their segments.

A second-order low-pass Butterworth filter with a 5 Hz cut-off frequency was applied to raw data in order to attenuate unwanted noise in the high-frequency range.

The Vicon motion capture system used in the lab had an image error of  $\pm$  0.17 mm, as determined through the dynamic calibration process.

Experimental trials sought to assess the spinal immobilization of a variety of conditions, however, metrics by which to assess spinal immobilization were necessary to be determined. Spinal immobilization was determined to encompass both rotations of the head about the x- y- and z-axes as well as longitudinal and lateral displacement of the body with respect to the board.

#### 3.1.5 Head Range of Motion – KineMat MATLAB Toolbox

The Vicon motion capture system output trials as position data within the global coordinate system. In order to determine the joint angles between the head and trunk body segments within 3D space, coordinate transformations were necessary. As this proved to be a complex process, an online resource

from the Human Performance Laboratory at the University of Calgary was used to determine the flexion / extension, rotation, and lateral bending of the head.

Researchers Christoph Reinschmidt and Ton van den Bogert developed KineMat, a MATLAB toolbox for 3D kinematic analysis, and the toolbox allowed for the calculation of intersegmental motion between the head and trunk. We opted to use helical angles to describe the motion between these two segments.

The helical axis system allows for the description of any finite movement from a reference position in terms of a rotation about an axis. A position vector and an orientation vector are calculated for each axis of rotation. The instantaneous position of one local coordinate system can be described with respect to another. Helical angles are therefore highly representative of relative position of the head to the trunk, as both segments move through several planes during the tip, drag, and puke tests.

Code used for the determination of the helical angles from global coordinates is provided in Appendix H – KineMat MATLAB ToolboxThe algorithm will now be briefly discussed.

The code required four inputs to calculate angles during a trial; neutral positions for the head and trunk segment markers as well as marker positions for the head and trunk segment markers during movement. The neutral positions were used to align the segmental coordinate system to the global coordinate system. Using these four inputs, 4x4 matrices containing a rotation matrix (3x3) and a translation vector (3x1) were calculated for each segment (A and B) using a singular value decomposition method as first described by Soderkvist and Wedin [11]. The linear system was then solved by *inv(A)\*B*. The resulting matrix was used to calculate the finite helical angle descriptors, including the angle of rotation, translation along the axis and the location of the axis in space, as first described by Spoor and Veldpaus [12].

In order to orient ourselves as to the anatomical representation of the helical angles as outputted by the code, a proof-of-concept experiment was constructed. The custom marker set displayed in Figure 5 was adopted and four test were conducted; a static test to establish the neutral position, a test in which the subject moved their head exclusively in flexion/extension, one exclusively in rotation, and one in exclusively lateral bending. By controlling how many axes the head was rotating in, information could be

gathered as to the anatomical representations of each column of the helical angle output matrix. Results are displayed below in Figure 6.

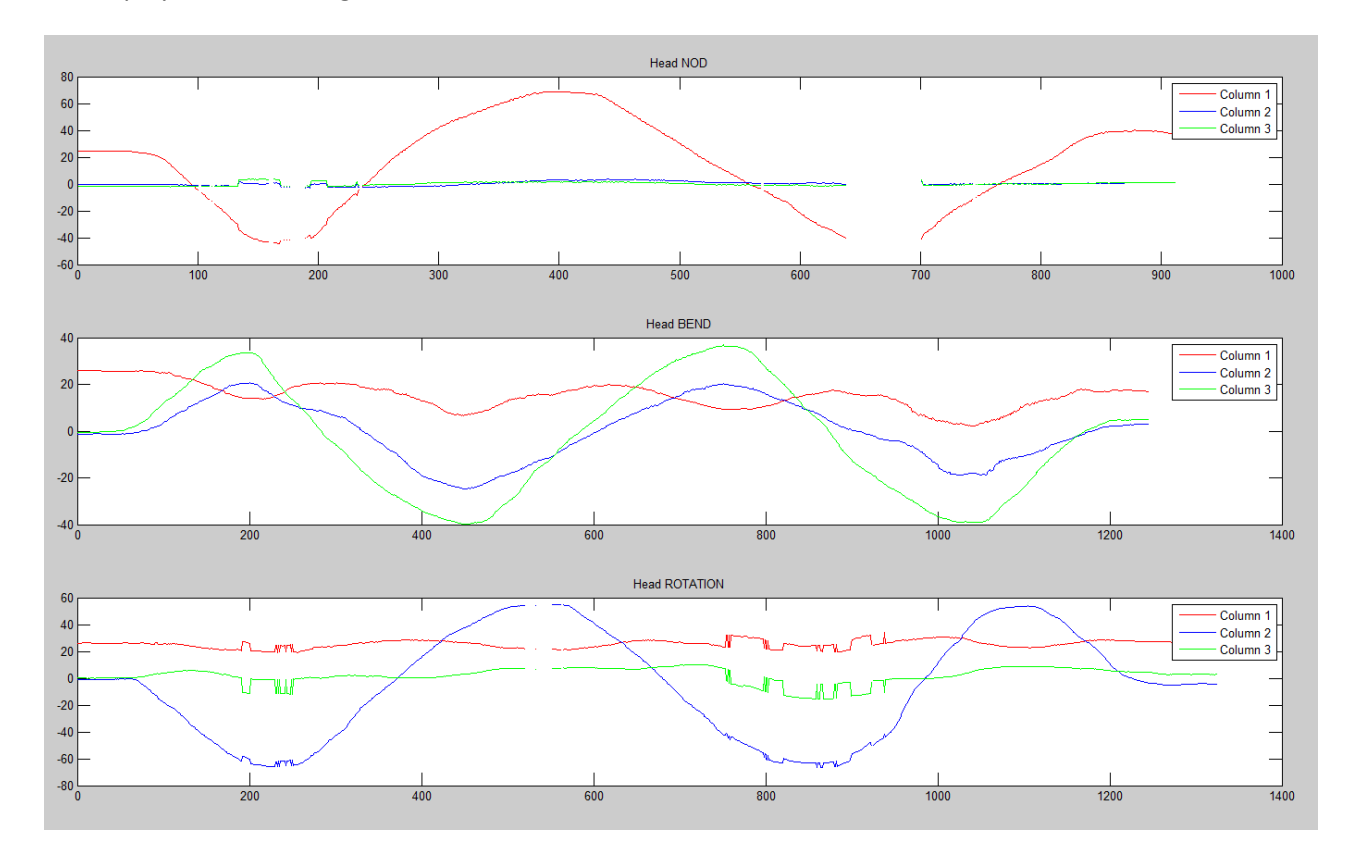


Figure 6: Proof-of-concept helical axis experiment

As shown above, movement was seen primarily within only one axis of rotation for each of the tests. It should be noted that the second plot, 'Head BEND' demonstrates some movement in Columns 2 and 1, however as it is difficult to perform a lateral bend of the head solely within the frontal plane due to the anatomy of the neck, it was determined as Column 3 had the greatest range, it represented lateral bending. Column 1 was deemed to represent flexion / extension and Column 2 was deemed to represent rotation.

## 3.1.6 Longitudinal and Lateral Body Displacement

Displacement of the body with respect to the board was determined from the position data in the global coordinate system. As tip and drag tests had movement only in the longitudinal direction of the board, and the puke test had movement only in the lateral direction, it was decided that displacement in these respective directions would be calculated for each test.

Longitudinal displacement was calculated by calculating a vector between the ST marker and the board's central marker (BC) marker for the duration of a test trial. The magnitude of this vector was then calculated. Across all trials, a distinct pattern was apparent. Magnitude decreased as the board was lifted during the trial, magnitude reached a minimum, then increased when the board was lowered back to the ground at the end of the trial, but did not reach the same magnitude at the beginning of the trial.

Cumulative body displacement equaled the sum of the displacement 'down' the board, and the subsequent displacement 'up' the board. The following equation was used to determine the cumulative displacement:

```
%Net longitudinal displacement
A = mean(MAG(1:200));
B = mean(MAG1(end-200:end));
C = min(MAG1);
NET = (A - C) + (B - C);
```

As the first and last 2 seconds consisted of no trial movement, it was determined that the mean of these frames would be an accurate measure of starting and ending body position.

Lateral displacement during the puke test was calculated in the same manner, but the board's bottom left marker (BL) was used in place of BC. Although this did not create a vector that was parallel with the axis of movement, it was assumed that there was no movement in the longitudinal direction during the puke test, thus the change in magnitude of the diagonal vector would represent the lateral body displacement.

#### 3.1.7 Survey of Lifeguards

An important consideration in the design of the aquatic spinal board is how it is received by the intended user group. Because aquatic spinal rescues require specific, specialized training, the intended user group of the design was assumed to be trained lifeguards exclusively. As such, the opinions of trained lifeguards with working experience was sought to evaluate the more subjective design criteria, such as the intuitiveness of the design and simplicity of the design, with specific focus on the strapping system.

Five trained lifeguards with  $2.6 \pm 2.13$  years of working experience completed a modified Likert scale survey, where 1 was "bad/worst" and 5 was "good/best" for all questions. The survey asked the lifeguards to rate the conventional, unmodified board purchased by the research team (with modifications hidden or removed) in a number of categories. The lifeguards were then asked to answer the same questions in relation to the modified prototype, after receiving a brief demonstration of its functionality.

Lifeguards were recruited randomly from the University of Guelph student population, and were not known to the research team in order to minimize biases. The mean numerical response for each question across all participants was taken, and a confidence interval was calculated with a student T test and an alpha of 0.05. Differences between the corresponding questions for the conventional and prototype board were considered statistically significant if the difference between the maximum accumulations of error was less than the average difference in response for the question pair.

A copy of the survey questions may be found in Appendix F – Lifeguard Survey.

## 3.2 Board Geometry Design

The aim of the board geometry design optimization was to address the following key issues:

- Inability to perform both knife and slant rescues
- Physical difficulty experienced while submerging the board during knife rescued
- Discomfort felt by patients during prolonged immobilization

With the constraints and criteria for a successful spinal board design as detailed previously in mind, a number of design options were proposed, detailed in Figure 7. Its main novel features include a curved transverse profile, a sliding sink/float port and a compliant, removable top mat.

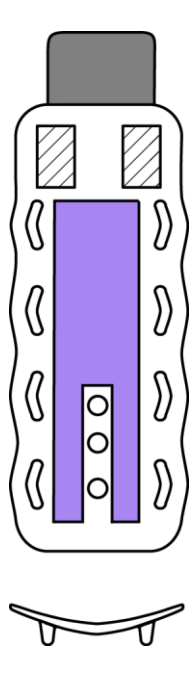


Figure 7: Preliminary board geometry design

In the interest of the constraint that the design not interfere with current rescue procedures and the criteria that the design should be simple and not depart excessively from the expectations, a number of features scattered amongst the collective variety of existing spinal boards were retained. These include the beaver tail, gross dimensions, rails and perimeter handle holes.

In order to ensure that the proposed design addressed the outlined issues in such a way that satisfied the established constraints and criteria for a successful design, a number analyses were performed. In addition to assessing the proposed design's success, the analyses were also used to determine the optimal configuration of certain features, such as the precise number, location and size of the handle holes and sink/float port and the precise construction details of the board.

Three major analyses were performed in terms of the board geometry: a static buoyancy analysis, a fluid dynamics analysis and an FEA analysis of the board's structural integrity. The first two analyses address

the issues of modularity between slant and knife rescues, and the issue of difficult during board submersion respectively. While structural integrity is not a key concern with existing technology, FEA analysis was performed to ensure that changes resulting from the geometric optimization did not adversely affect its strength.

Although patient comfort was identified as a key design issue, the effectiveness of the removable top pad in terms of pressure riser reduction was not formally evaluated due to non-availability of appropriate testing equipment. However, implementation of similar systems has been supported in the literature for land spinal boards [13].

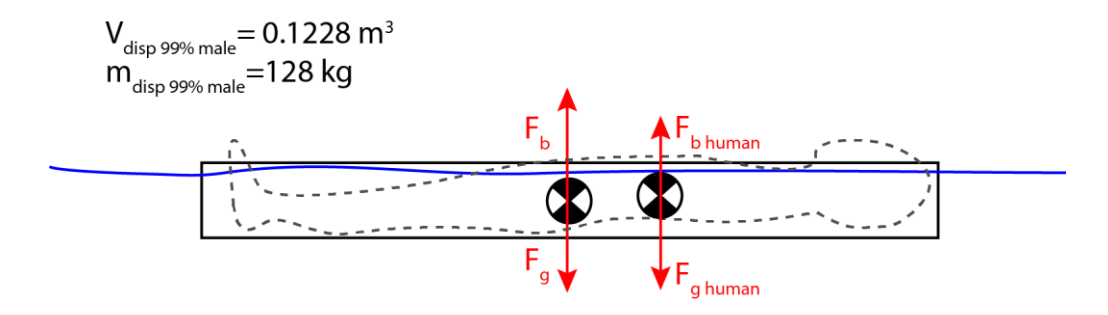
Similarly, the curved profile was not assessed in terms of provision of patient comfort due to limitations in modelling of human factors. The implementation of this design feature has also had some support in the literature in terms of comfort through testing of an existing land spinal board product with a similar curvature profile [14].

## 3.2.1 Static Buoyancy Optimization

The desirable characteristics for a spinal board during a knife and a slant rescue are divergent. During a knife rescue, it is desirable for the board to float parallel to the water's surface when loaded with a patient, while during a slant rescue it is desirable for the board to sink to the bottom at the foot end of the board both during the approach phase and when loaded. Because of these divergent design requirements, boards are designed to favour one type of rescue at the expense of the other.

The implementation of the sink/float port design provides a solution for this by allowing lifeguards to change the centre of buoyancy of the submerged part of the board by opening or closing the port. The goal of this analysis was to determine the dimensions, position, number and size of ports that would result in a board that floats horizontally when the port is closed and that sinks at the distal (foot) end when opened. Other factors that might also affect the desired properties, such as the average board density, mass and thickness were also given consideration.

In order to do this, a static, 2D analysis of the board during the two rescues was first performed to iteratively narrow in on geometric properties that would yield the desired result. This was considered to be an appropriate means of assessment as the board should be stationary during these steps of the rescue, and all net forces are acting through the centre of symmetrical objects. Free body diagrams used to perform the analyses of the two rescues can be seen in Figure 8 and Figure 9.



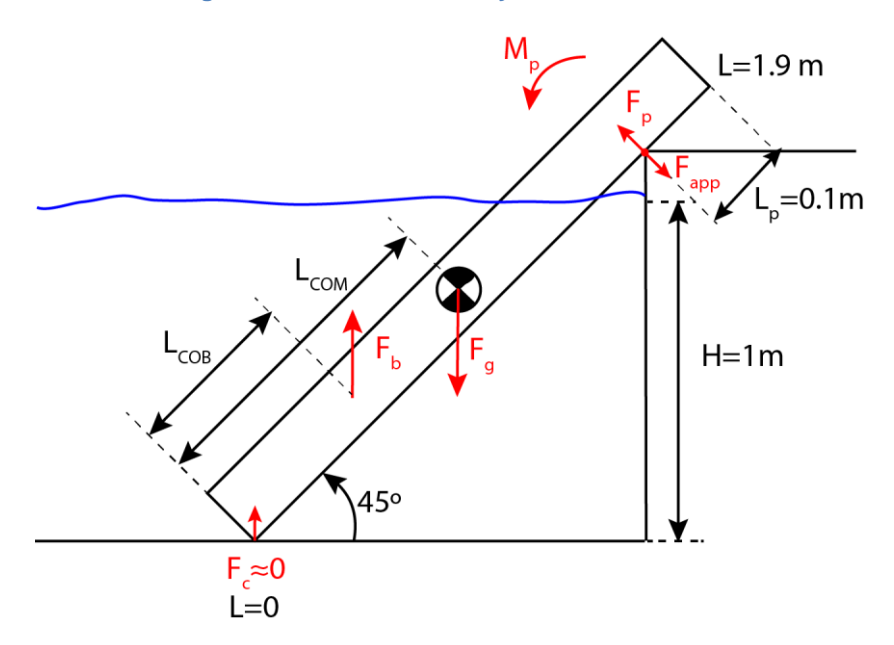


Figure 8: FBD for static analysis of knife rescue

Figure 9: FBD for static analysis of slant rescue

In Figure 8, it is assumed that the entire volume of the patient is submerged to simplify analysis. Moments created by the forces acting through the patient's centre of mass/buoyancy about the board centre were considered to be negligible as these would likely be circumvented by the rescuer stabilizing the board at the head/proximal end.

In Figure 9,  $F_p$  is the contact force between the deck ledge and the board, and  $F_{app}$  is the stabilizing force provided by the rescuer holding the board from the deck. In order to simplify the slant rescue analysis, it was assumed that  $F_{app}$  and  $F_p$  are applied through the same point, P.  $F_{app}$  is assumed to be of such a magnitude and direction as to result in an  $F_{net}$  of 0. A water depth of 1m and slant angle of 45 degrees were assumed to be representative of the circumstances in which a slant rescue is ideally performed.

After creating a preliminary full-scale CAD of the design in SolidWorks, the approximate requisite average density and volume of the unloaded board were determined for the board to float unloaded (ie. have  $F_{\text{net}}$  y $\geq$ 0). Results from this analysis were then used to refine the board's thickness and construction of the board, until this requirement was achieved while maintaining the mass of the board within the same range as other commercially available boards (6-10 kg). Significant changes to parameters such as length, width and number of handle holes were avoided as changes to these parameters would reduce the functionality and ease of use of the board.

Following this, a static analysis of the board loaded was performed to determine the maximum body mass that could be supported by the board in the water without lifting action from the rescue team. In this case, the displaced volume of patient was based on the average density of a healthy male and the body mass of a 99<sup>th</sup> percentile American male. This assumption presents a worst-case scenario in terms of loading, as this calculation likely underestimates the volume of the maximal load, resulting in a lower buoyant force than would be likely for a person with a large body mass. A margin of safety of 0.1 was

then applied to this mass to account for possible errors such as differences in body composition. A larger margin was not used as if the board is unable to support a person's mass independently in the water, lifeguards are able to provide support to the board during the rescue.

While changes that increased the buoyancy and maximum supported mass of the board were considered positive for the knife analysis and optimization, some consideration was given to the possibility of creating a board that was too buoyant, and thus too difficult to push underwater during a knife rescue and too buoyant to sink during a slant rescue. To avoid this possibility, the ideal board mass, general geometry and maximum supported mass were considered to be values that were similar to existing boards.

Following the analysis of the board in the knife rescue position, a similar static analysis was performed in the slant position. Using the previously refined board geometry, the angular acceleration of the board about point P (point of contact between the board and the deck ledge), was determined without any portholes, to determine if the end of the board would rotate upwards (in the negative, clockwise direction).

Using the results from this, ports of increasing size and then numbers were added iteratively to determine their effect until a desirable configuration that resulted in a net moment about P that was greater than or equal to zero was obtained. Changes to parameters other than the shape, location and number of portholes were avoided in order to preserve the ideal characteristics achieved from the previous knife rescue analysis.

For both static analyses, the properties such as moments of inertia, volume, mass and centres of were determined accurately for each geometric iteration using the SolidWorks "mass properties" function. Similarly centres of buoyancy and submerged volumes were determined by sectioning the complete board below the water line, and running the "mass properties function" on the submerged section. Accurate material properties were assigned within SolidWorks in order for these parameters to be determined. Sample calculations may be found in Appendix D – Static Fluids Calculations for Board Geometry Design.

#### 3.2.1 Analysis of Curved Profile

Aside from increasing the ease with which patients are positioned on the board and providing some increased lateral immobilization, the curved aspect of the board geometry was designed to improve the ease with which the board may be pushed under a patient during a knife rescue.

This theoretical improvement is based upon the principles of fluid drag, where the coefficient of drag  $(C_d)$  is a dimensionless description of the resistance of an object's movement through a fluid. The coefficient of drag is the combination of the coefficient of skin drag  $(C_{skin})$  and the coefficient of form drag  $(C_{form})$  of the object. Skin drag is caused by the wall shear stress of the fluid against the entire wetted surface of the object, while the form drag is caused by the pressure differential from the area of the leading edge of the object, according to:

#### **Equation 1: Derivation of coefficient of drag**

$$C_d = C_{form} + C_{skin} = \frac{1}{\rho v^2 A_{front}} \int_{S} \left[ (P - P_0) \cdot \hat{n} \cdot \hat{i} \right] dA + \frac{1}{\rho v^2 A_{surf}} \int_{S} \left[ \tau_w \cdot \hat{t} \cdot \hat{i} \right] dA$$

Equation 2: Relationship between drag force and coefficient of drag

$$F_{drag} = \frac{C_d \rho v^2 A_{front}}{2}$$

Because of the complexity of determining an object's coefficient of drag from Aside from increasing the ease with which patients are positioned on the board and providing some increased lateral immobilization, the curved aspect of the board geometry was designed to improve the ease with which the board may be pushed under a patient during a knife rescue.

This theoretical improvement is based upon the principles of fluid drag, where the coefficient of drag (Cd) is a dimensionless description of the resistance of an object's movement through a fluid. The coefficient of drag is the combination of the coefficient of skin drag (Cskin) and the coefficient of form drag (Cform) of the object. Skin drag is caused by the wall shear stress of the fluid against the entire wetted surface of the object, while the form drag is caused by the pressure differential from the area of the leading edge of the object, according to:

Equation 1,  $C_d$  values are commonly determined experimentally. Tabular  $C_d$  values for common, generalized shapes for certain dimension ratios and Reynolds numbers can be used to approximate an object's  $C_d$  by scaling according to the frontal area of the object, as seen in Equation 2 if experimental determination of  $C_d$  is impractical.

Based on the knifing method presented in Figure 10 and Figure 11, introducing a curved profile would greatly reduce the form drag component of  $C_d$  as the board is pushed underneath the floating, horizontal patient. This reduction would in theory provide a lower total coefficient of drag, and thus, a lower drag force. This lower drag force would reduce the force used by the rescue team to submerge the board.

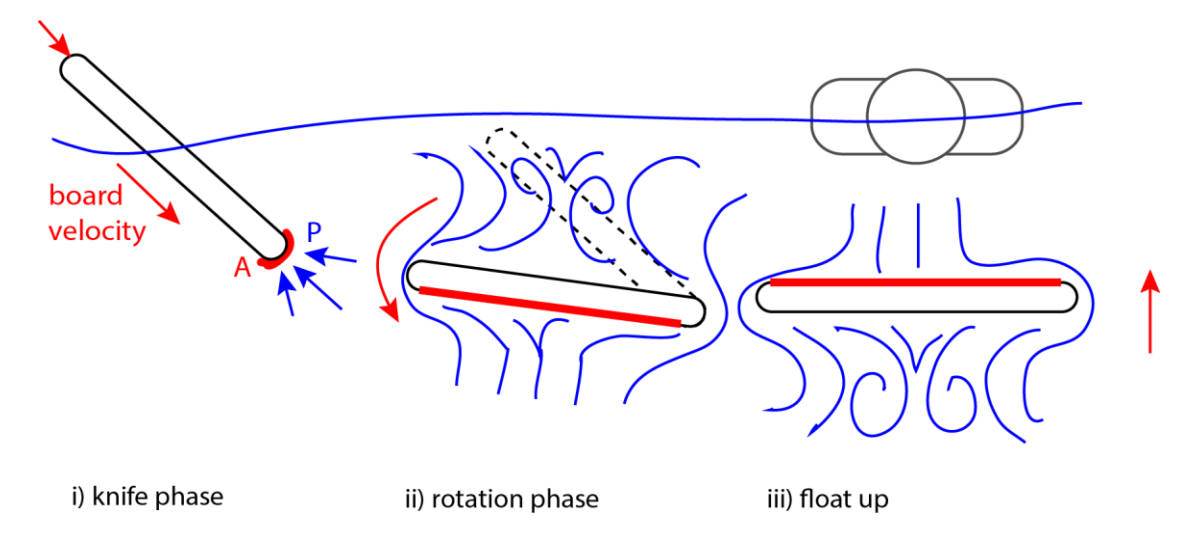


Figure 10: Dynamic motion of conventional board during knife rescue

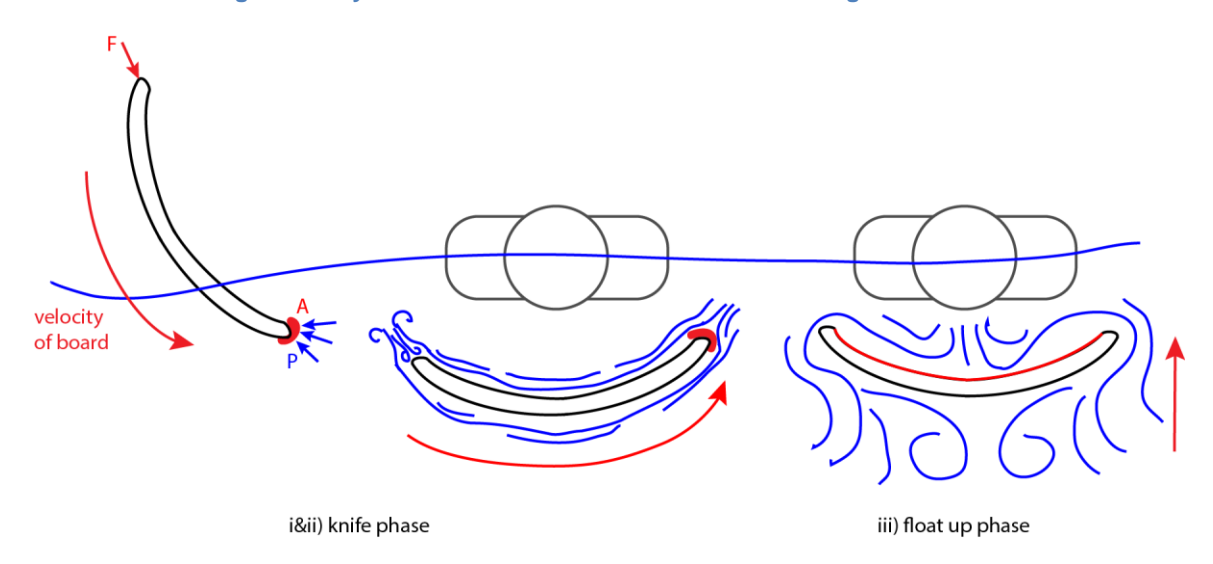


Figure 11: Dynamic motion of curved board during knife rescue

While a precise, quantitative analysis of this feature had been planned using a CFD model, it was determined that the number of assumptions or simplifications that would have to be made for the analysis meant that similar accuracy could be achieved using a 2D estimation of drag forces encountered during the knifing procedure. The disadvantage to this analysis is that by using generalized tabular C<sub>d</sub> values, one could not gain insight into the effect of the different curvature profiles. This aspect of the design was justified by determining appropriate dimensions based on anthropometric data from the two extreme ends of the expected patient (99<sup>th</sup> percentile male, 50<sup>th</sup> percentile 6 year old female). The 50<sup>th</sup> percentile 6 year old female was selected as the lower bound because children under age 6 are unlikely to engage in activities such as diving that put them at risk for a spinal injury in an aquatic environment due to their swimming competence and adult supervision requirements for young children at aquatic facilities.

2D motion of the board during a knife rescue using the curved and flat profiles was estimated and divided into phases, according to Figure 10 and Figure 11. The approximate drag, F<sub>d</sub> was calculated for each phase as a function of some unknown velocity, based on the known area of the leading edge for each phase and experimentally determined coefficients of drag C<sub>d</sub>, obtained from shape tables [15] [16]. Leading edge areas were determined using the measure tool in SolidWorks.

To simplify analysis and facilitate comparison, it was assumed that the flat profile and curved profile boards had comparable surface areas. It was also assumed that each phase accounted for exactly one third of the overall procedure for both boards, and that each phase took 1 second to perform.

In terms of  $C_d$ , the curved profile was approximated as a thin, flat plate parallel to fluid flow for phases 1 and 2, and as a concave C-section for phase 3. Although the curved profile is not flat, this assumption is reasonable if one assumes that the velocity vector of the streamline runs parallel to the board (ie. the board is pushed along a curved path matching its curvature).

The flat profile was approximated as a thin, flat plate parallel to fluid flow for phase 1, and as a thin, flat plate perpendicular to fluid flow for phases 2 and 3. For phase 2 of the flat profile, it was assume that at the beginning the board was positioned at a 45 degree angle relative to the water surface, and was rotated at a constant angular velocity until positioned at 0 degrees. Knowledge of this angular velocity was used to quantify the increasing drag forces that would result as the board rotates towards being a flate, perpendicular plate.

Laminar flow was assumed throughout, and effects of material roughness and geometric complexities such as the rail system, holes and straps were neglected to simplify analysis.

These approximated  $F_d$  values, expressed as a function of velocity, were plotted for comparison for each phase. The integral of each  $F_d \cdot v^2$  profile was taken over phase I and II, to express work done as a function of velocity. This approximation of the total work as a function of velocity was used to determine which board would require the lowest overall energy expenditure, assuming that velocities for each phase would be of a similar magnitude and that each phase would take roughly the same amount of time to perform. The difference between the two board profile W values were expressed as a ratio. A conservative adjustment factor of 0.5 was then applied to this to account for inaccuracies inherent in the model, which would all result in a reduction in the improvement of this factor if properly accounted for.

Equation 3: Relationship between drag force and coefficient of drag

$$F_{drag} = \frac{C_d \rho A_{front}}{2} v^2$$

Equation 4: Relationship between drag force and work

$$W = \int_0^2 (F_{drag} \cdot v) dt$$

Phase III was not considered in the integral describing expended effort as during phase III the board is allowed to float up by itself.

## 3.2.3 FEA Analysis of Structural Integrity

Because the selected board geometry design involved significant departures from conventional board construction, some consideration of its mechanical integrity was considered important to its viability as medical device in terms of safety and usage guidelines.

To determine the maximum safe loading for the design, the "worst case" scenario of normal use was modeled. During the rescue process, the instant of greatest mechanical stress on the board itself is during the removal process, where the entire load of the board and patient is concentrated through the contact force between the deck edge and the two runners on the rear of the board. It was assumed that any load that could be deemed safe in this particular configuration would be safe in all other configurations. Because the motions that occur during the rescue process are generally quite slow, a static analysis of this instant was considered appropriate.

In this case, the main concern would be the deflection of the board as well as the mechanical stress experienced throughout the board. While deflection in absence of excessive stress is not necessarily a concern, excessive deflection is undesirable because it might result in poor immobilization or undue alarm on the part of the patient or rescuers. Due to the short term and infrequent nature of spinal board use, fatigue and load cycling were not considered.

In order to determine the safe loading characteristics, an FEA analysis of simplified board geometry was performed using the SolidWorks Simulation toolbox. The body mass was modeled as a distributed load over the entirety of the top surface, with the gravitational force acting perpendicular to the top surface (the worst-case scenario). The distal, foot end edge of the both runners were considered as fixed geometry (6 degrees of freedom constrained), as were the proximal (head end) handle holes. The two board components (the outer shell and inner foam) were defined as a bonded contact pair. The "standard mesher" was used with an element size of 51.44mm.

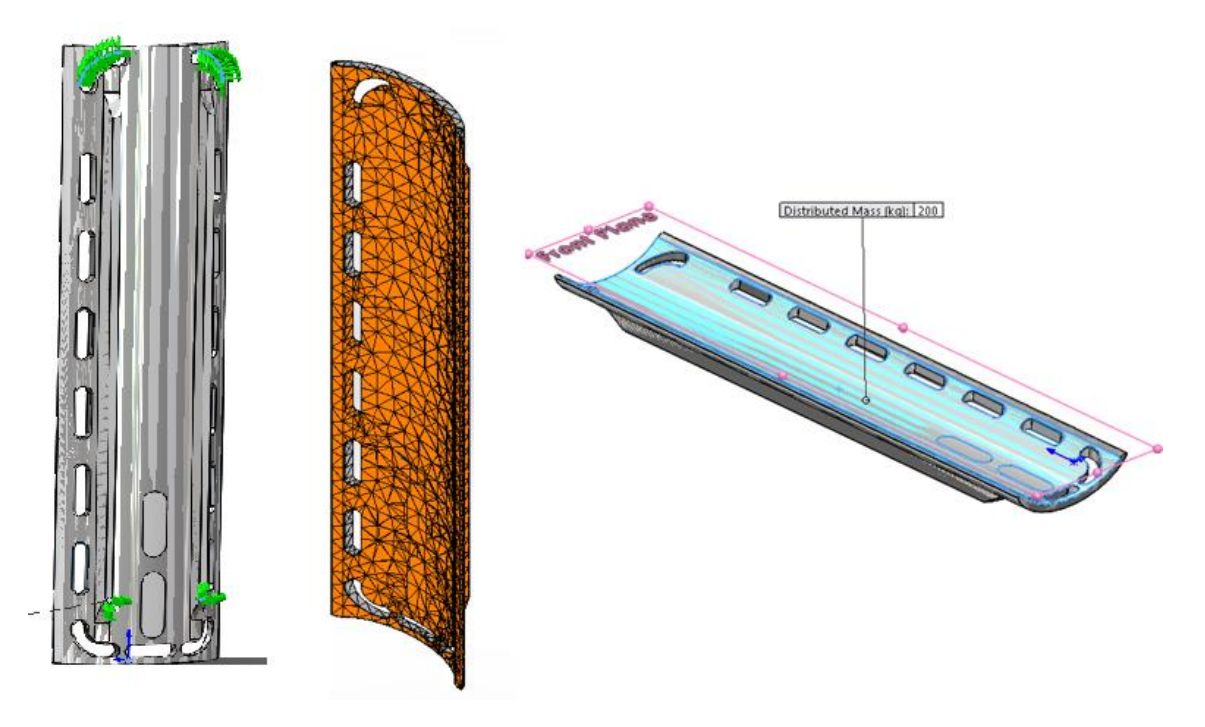


Figure 12: Boundary Conditions, Mesh and Loading Conditions of FEA Analysis

The simulation was run iteratively using various combinations of loads and outer shell thicknesses, in order to determine the maximum safe load for each shell thickness. While having a thicker outer shell would make the board stronger, having a thin outer shell is desirable in terms of buoyancy characteristics and the overall mass of the board. As such, a balance had to be struck for the determination of the thickness of the outer shell, where functional characteristics more pertinent to typical use such as the mass of the board and its buoyancy were given priority.

Determination of the safety cut-off was considered to be the earliest instance of the von Mises stress in any element exceeding the yield strength of the material (either PLA, 57.8 MPa or BioFoam, 300 kPa depending on location), or the deflection exceeding 15mm for a particular distributed load. A safety factor of 1.5 was then applied to any load exceeding this stress limit, which is the standard suggested safety factor for plastics experiencing static, short-term loads [17].

### 3.3 Board Surface Material Optimization

The addition of padding to a spinal board has been shown to decrease the development of pressure sores and increase patient comfort [12]. As such, an investigation into the impact of padding on the spinal immobilization was necessary to ensure that the inclusion of a padded top layer to our design would not negatively impact the main criteria of the project, immobilization of the spine.

A prototype padded surface constructed from a PVC yoga mat which was cut to the dimensions of the spinal board and affixed with Velcro. The padded board condition was tested with Vicon motion capture in the same protocol as described in the above harness system methodology. The Drag and Tip tests were chosen as representative examples of the impact of padding on spinal immobilization. Three trials

were conducted for the padded spinal board condition and results in the peak-to-peak angle ranges were calculated.

## 4.0 Results & Discussion

The overall design of the optimized spinal board consists of all the components selected in the interim report. These include the construction material of PLA with a PLA derived, BioFoam padding. The board will also contain the adjustable harnessing system for the chest and the hips. Lastly, the spinal board will feature a curved form factor with the porthole to assist in knife style rescue and slant style rescue. The finalized board design is located in Figure 13. Note that the image does not display the foam padding attachment in the inner curvature of the board nor the polyester immobilization straps.



Figure 13 Final design of the optimized spinal board.

## 4.1 Harness System Prototype

Vicon motion capture mean results with 95% confidence intervals are plotted in the following figures. A representative example the calculated helical angles for one trial of the Tip Test for both the conventional and modified harness system is provided in Figure 14. A representative example of the

longitudinal body displacement during the Tip Test is provided in Figure 15. Full experimental results are provided in tables in Appendix I – Full Experimental Results.

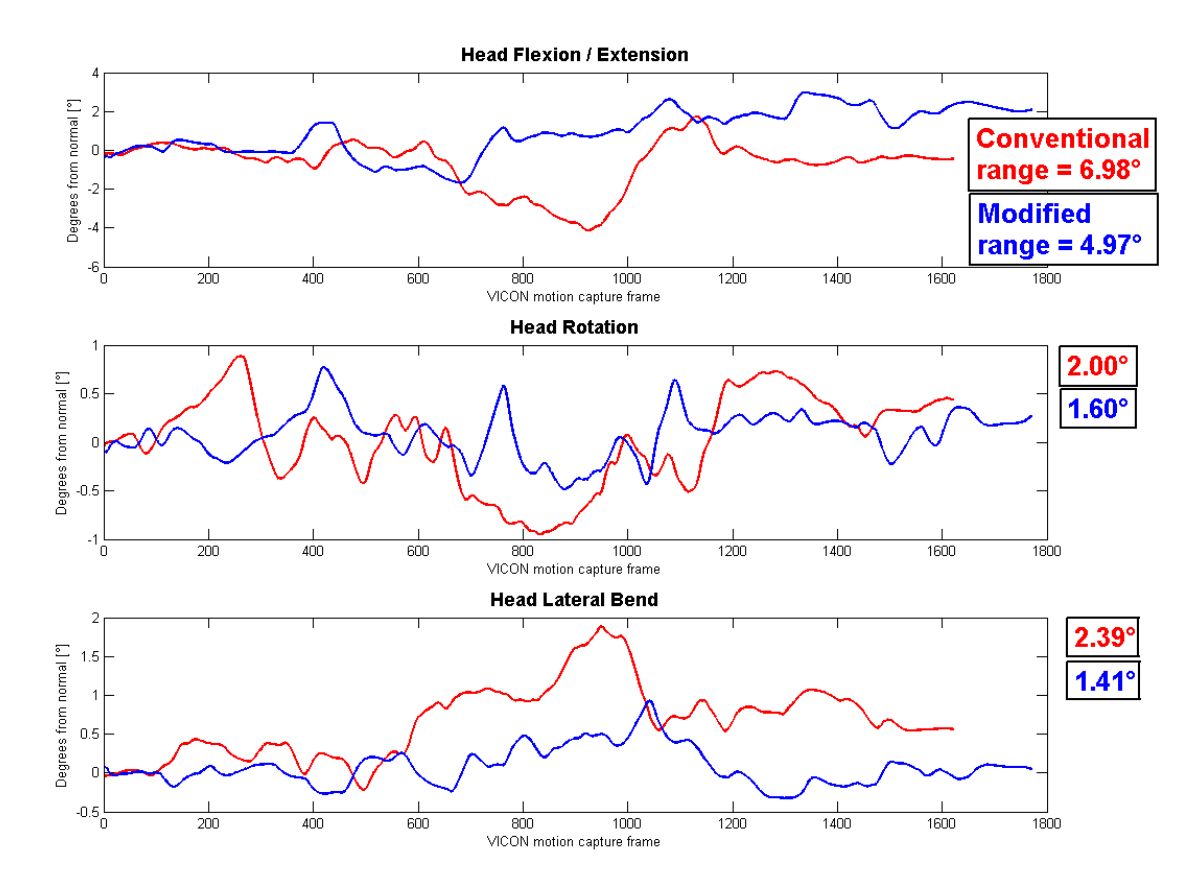


Figure 14: Comparative representative example of tip test peak-to-peak ROM

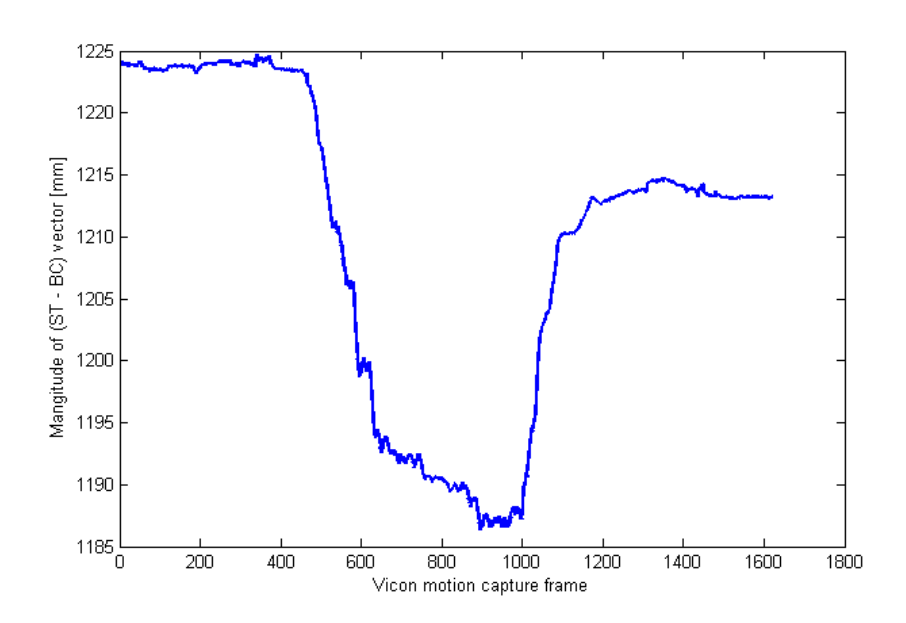


Figure 15: Representative example of tip test cumulative longitudinal body displacement

## 4.1.1 Modified Harness System Motion Capture Results

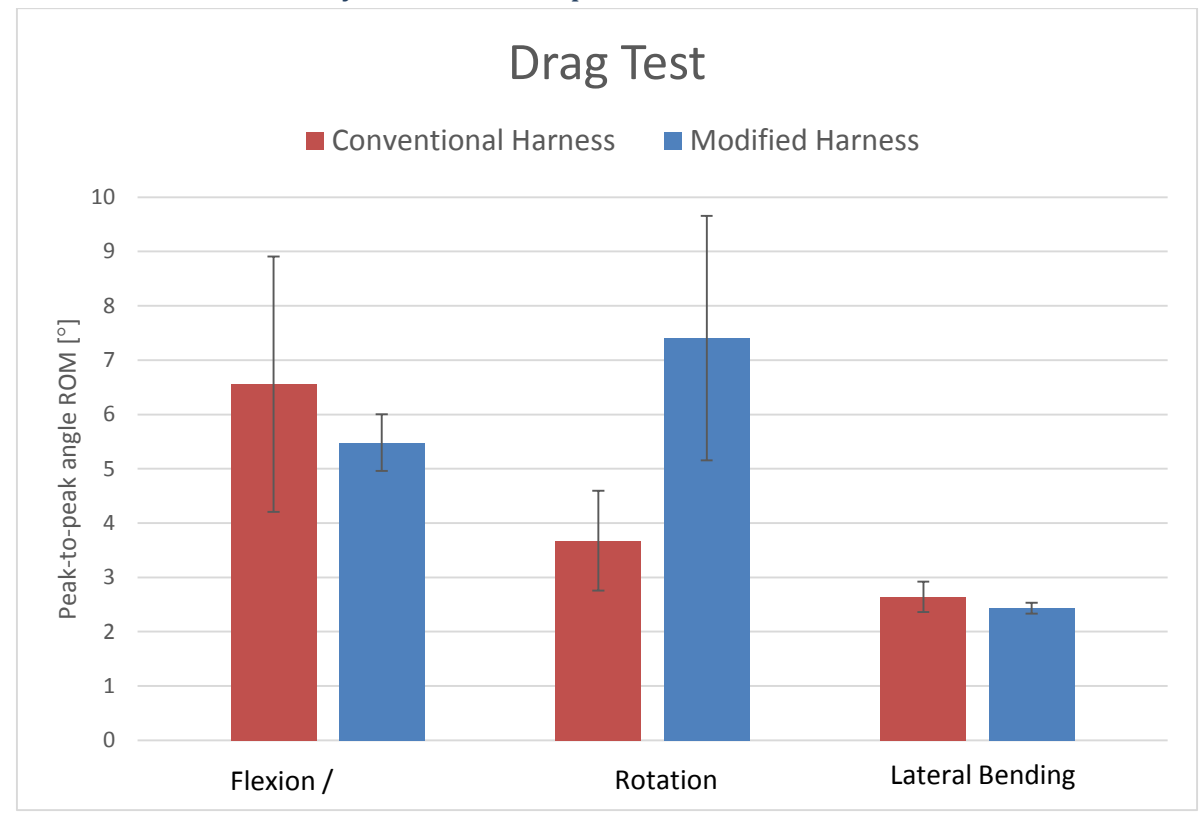


Figure 16: Mean peak-to-peak ROM and 95% confidence intervals for drag test with conventional and modified harness designs

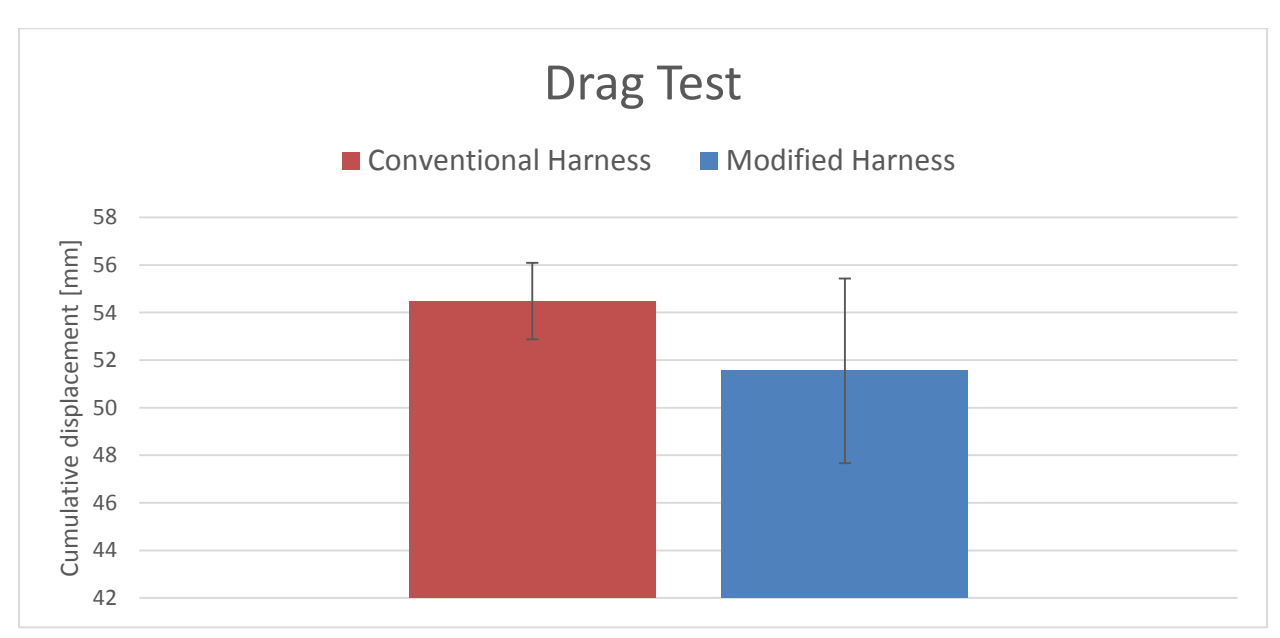


Figure 17: Mean cumulative longitudinal displacement and 95% confidence intervals for drag test with conventional and modified harness designs

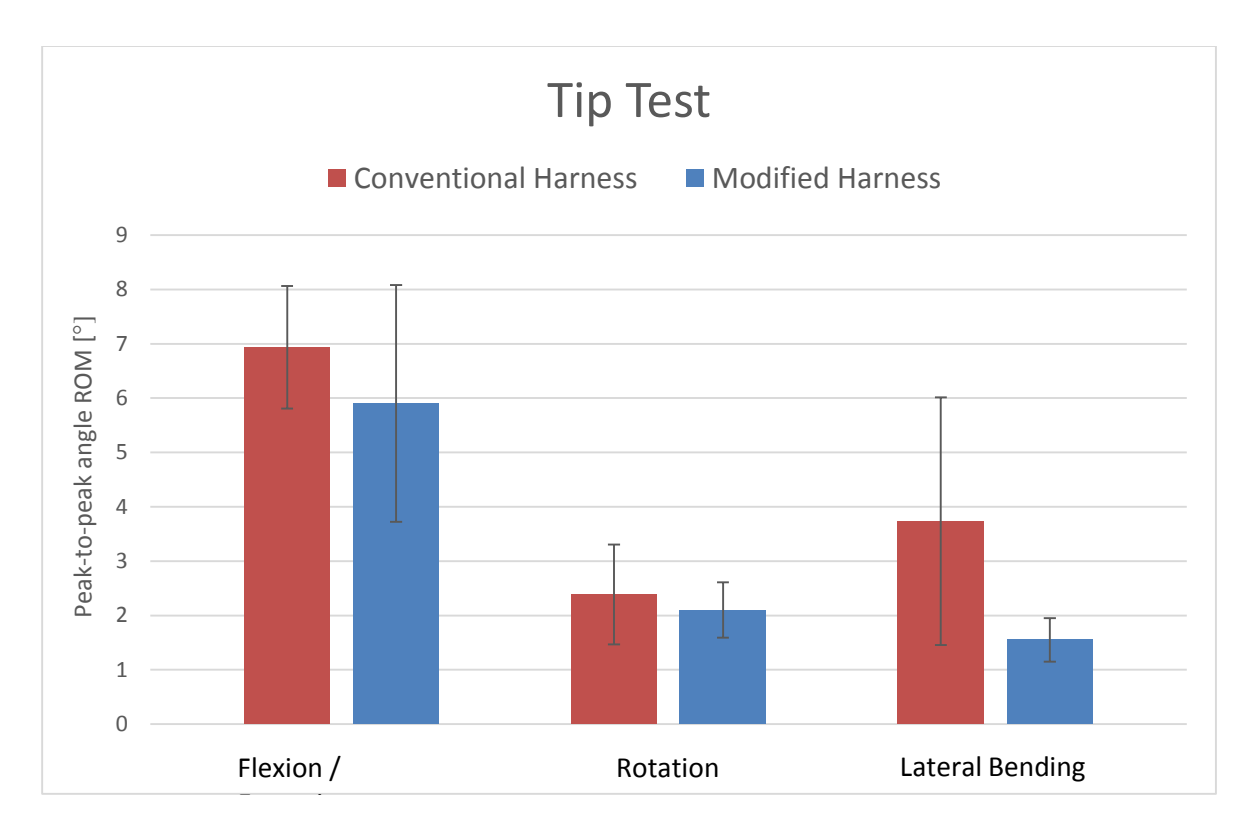


Figure 18: Mean peak-to-peak ROM and 95% confidence intervals for tip test with conventional and modified harness designs

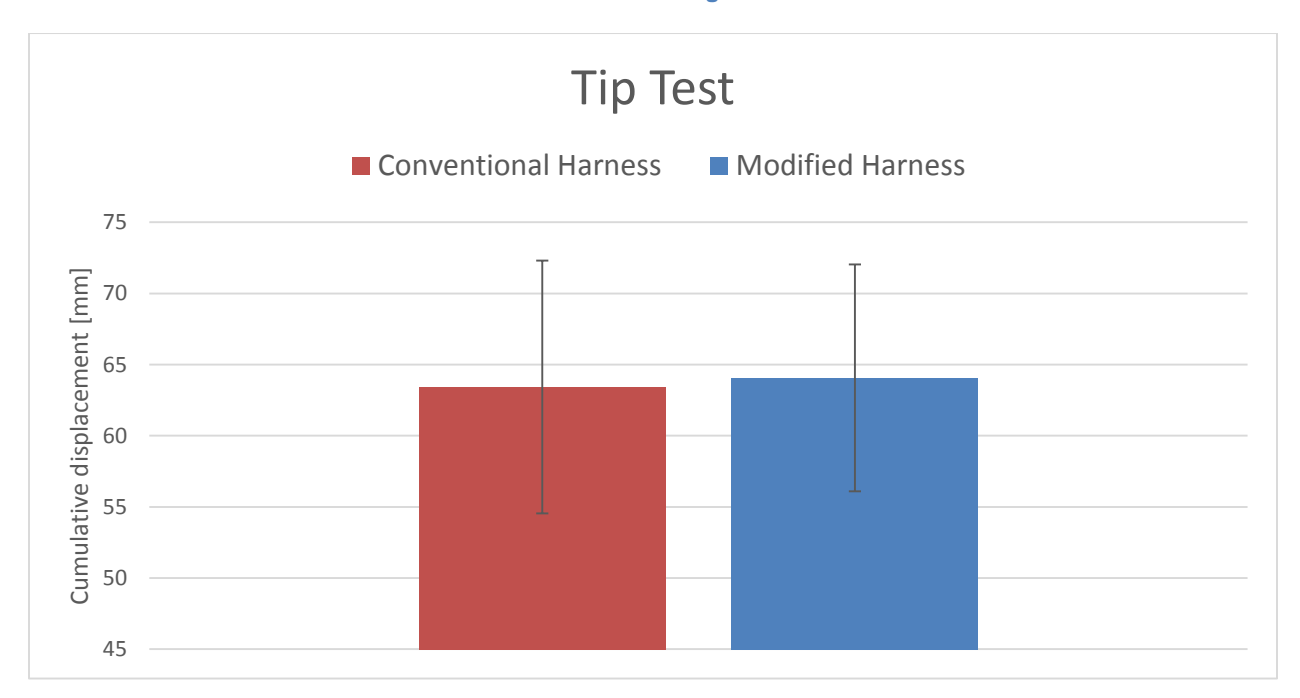


Figure 19: Mean cumulative longitudinal displacement and 95% confidence intervals for tip test with conventional and modified harness designs

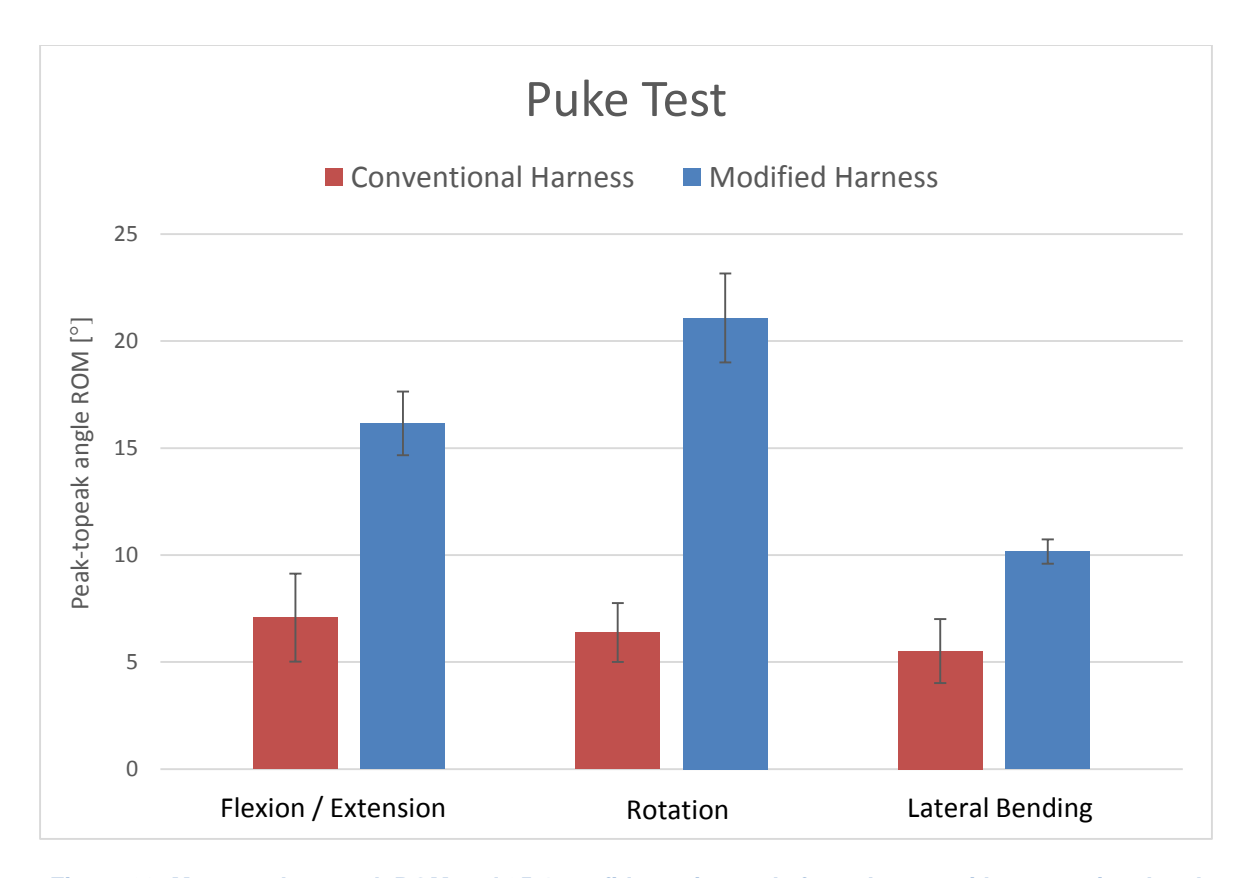


Figure 20: Mean peak-to-peak ROM and 95% confidence intervals for puke test with conventional and modified harness designs

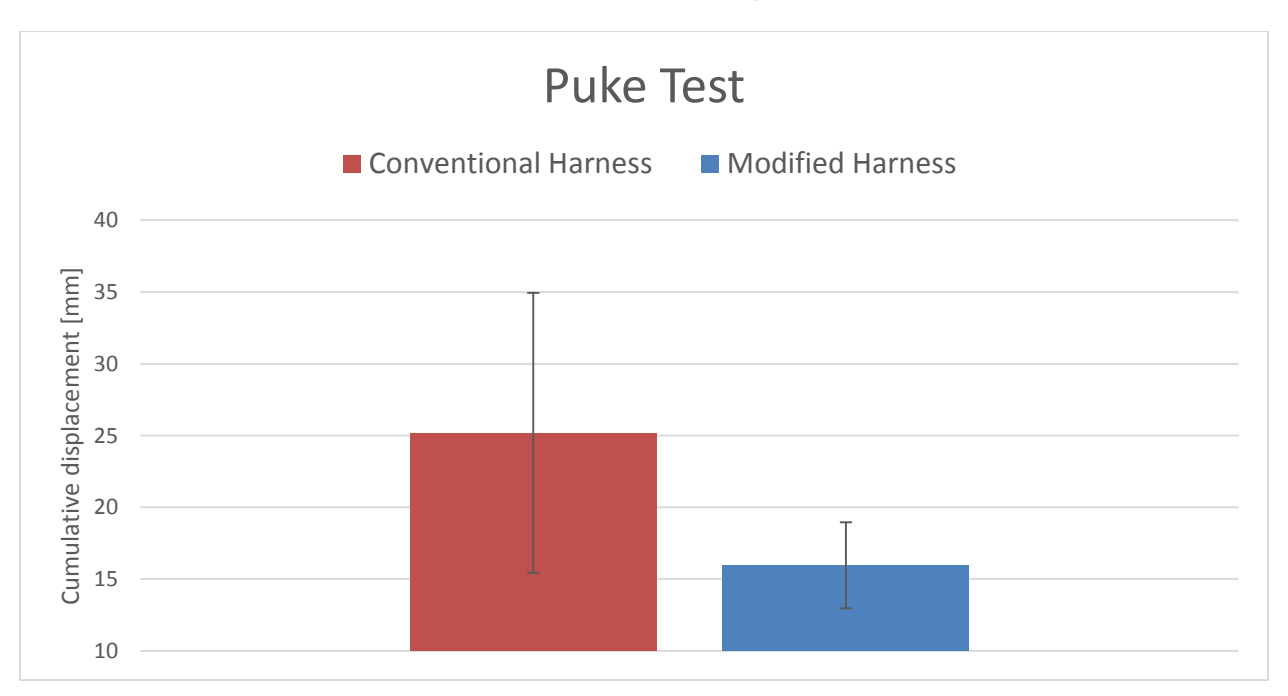


Figure 21: Mean cumulative lateral displacement and 95% confidence intervals for puke test with conventional and modified harness designs

#### 4.1.2 Modified Harness System Motion Capture Discussion

#### **Drag Test**

Peak-to-peak angle ranges of motion for head flexion / extension and lateral bending were found to have had a non-significant decrease with the addition of the modified harness system. Peak-to-peak angle range of motion for head rotation was found to have a significant increase. Longitudinal cumulative displacement was found to have a non-significant decrease with the addition of the modified harness system.

These results, along with all of the subsequent motion capture results, have to be taken with a grain of salt, as the sample size was very small (n=1). It would be difficult to draw any large implications as to the true performance of the modified system from the experimental data, however, there are some conclusions to be made.

The lack of change in the translation meets the constraint that the design immobilize the patient at least as well as the conventional board. While the increase in rotation with the prototype design does not meet this criteria, the data for this particular trial is somewhat suspect as for both the prototype and the conventional design, 1 trial had to be discarded as an outlier. The resulting error from using only two samples was high, and thus the result may not be reflective of the true performance.

#### Tip Test

Peak-to-peak angle ranges of motion for head flexion / extension, rotation, and lateral bending were all found to have had a non-significant decrease with the addition of the modified harness system. Longitudinal cumulative displacement was found to be non-consequential, as means were very similar (within 1 mm) and the confidence intervals for both conditions were similarity large.

Reduction in translation and rotation in the tip test means that the design met both the constraint of providing at least the same amount of immobilization as the conventional design and the criteria that it perform better in terms of immobilization. In a realistic sense, this result is the most meaningful of the three rescue procedure tests as this motion is performed every time an aquatic spinal rescue is performed.

#### Puke Test

Peak-to-peak angle ranges of motion for head flexion / extension, rotation, and lateral bending were all found to have had a significant *increase* with the addition of the modified harness system. Lateral displacement was found to have a non-significant decrease with the addition of the modified harness system.

The increase in angle ranges of motion was an unexpected result, as anecdotal reports of these tests did not find any noticeable increase in movement at these axes. These result was further investigated by looking back at raw data, and 3D representations of the head and trunk segments in Vicon Nexus software allowed for an explanation, as shown in Figure 22.

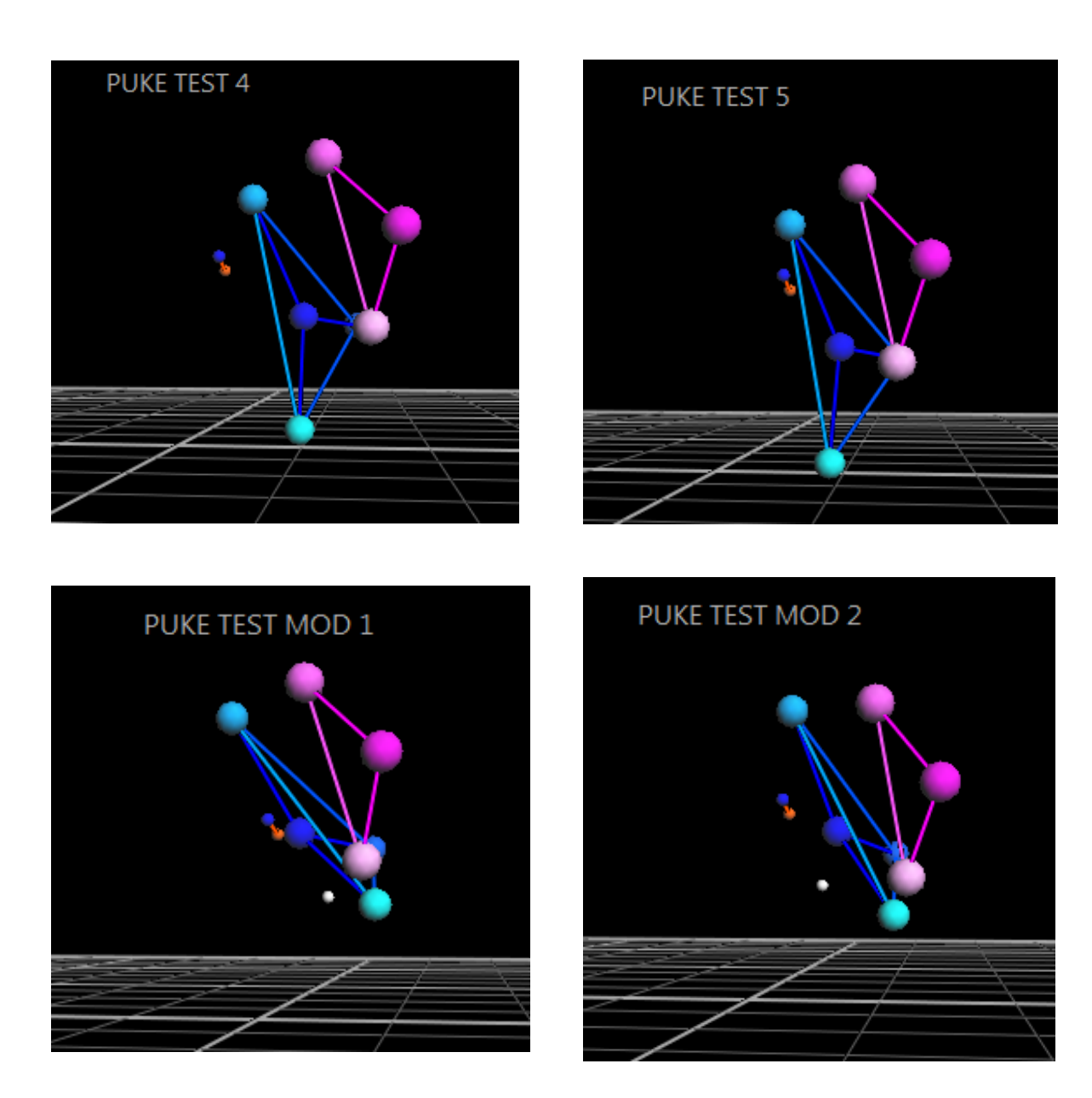


Figure 22: 3D reconstruction of puke test trials for conventional and modified harness systems

The above figures demonstrate the positions of the head and trunk at the full rotation of the spinal board laterally,  $\sim 90^{\circ}$ . It can be seen that while the conventional spinal board allowed for the head and trunk to be relatively parallel, the modified spinal board had a large difference in the angle of the head and trunk at the full board rotation.

This fundamental difference was deemed to be due to the fact that the modified harness system altered the body's position when the board was rotated during the Puke Test. As the modified harness system sat above the surface of the spinal board on risers, secured by pipe clamps, this decreased the available same horizontal length for the subject to lie on the board. When the board was rotated laterally, there

was not sufficient space for the subject to displace, and therefore the subject's body was forced to compensate by rotating, instead continuing to displace.

This explanation is supported by both the increase in angle ranges of motion and the decrease in displacement.

It was determined that due to the physical structure of the prototype harness system, results of the puke test did not reflect the true ability of the system to immobilize the subject. Therefore, these results were not considered when assessing the performance of the modified harness system.

## 4.1.3 Modified Harness System Survey Results

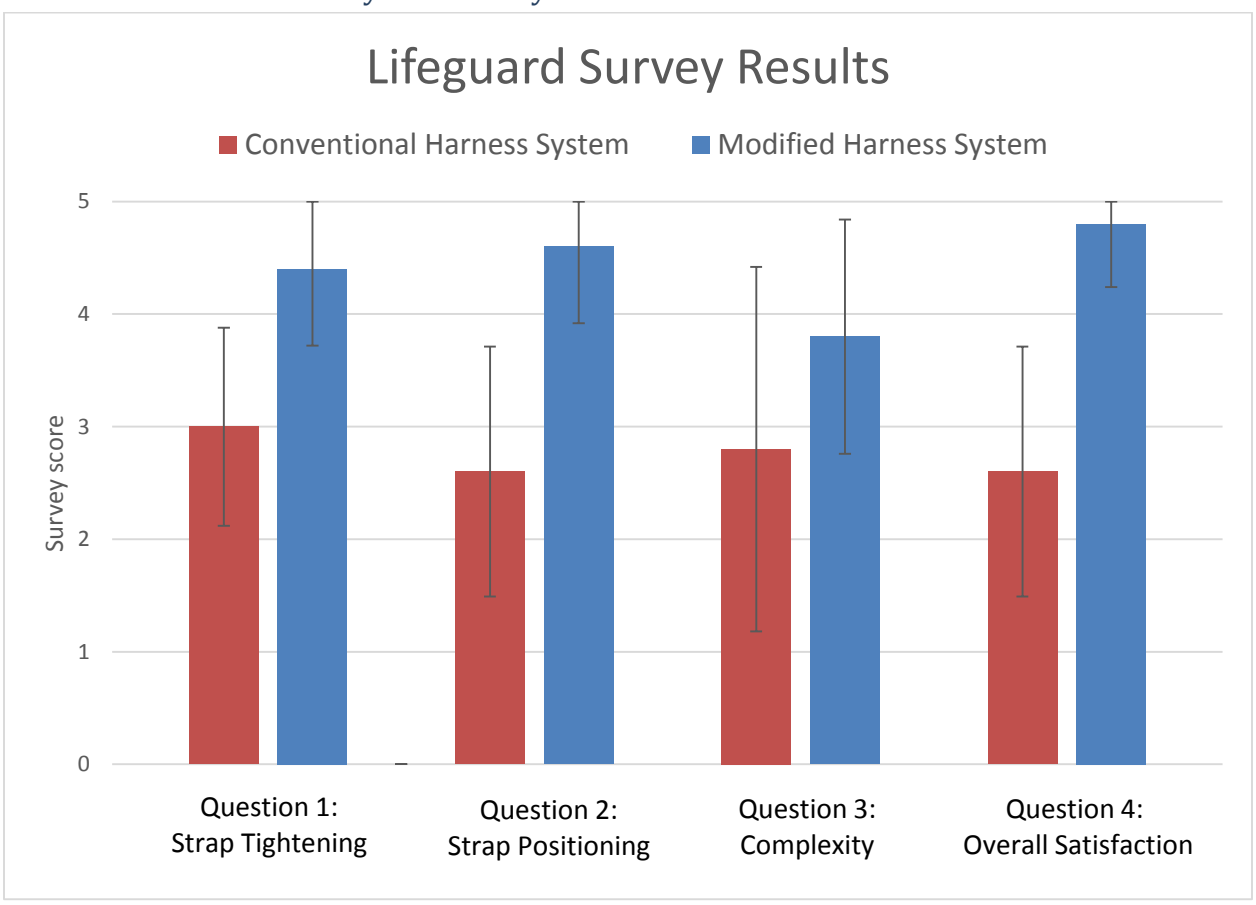


Figure 23: Mean survey score and 95% confidence intervals for lifeguard survey of conventional and modified harness systems

#### 4.1.4 Modified Harness System Survey Discussion

Results from the survey of the lifeguards were generally favourable, with average improvements seen on each question between the conventional board and the prototype. Of these improvements two were considered statistically significant: an 8% improvement in question 2 and a 20% improvement in question 4 were seen for the prototype board. Question 2 pertained to the ease with which proper positioning could be obtained during a rescue and question 4 pertained to overall satisfaction with the design.

These results are encouraging, and support the implementation of the strapping system from the perspective of the intended user group. This result is important, because regardless of the objective effectiveness of the strap system, this feature cannot be effective if those using feel that the feature would not be useful or easy to use.

While the results suggest a unanimous preference for the prototype over the conventional board, some consideration should be given to the limitations of the survey methodology. Given a small sample size and homogeneity of lifeguards surveyed, it cannot be declared that those sampled represent a true cross-section of the Canadian lifeguards. Additionally, a certain amount of bias was inherent in the survey, as participants knew that their results were for a student design project, and were thus less likely to provide unfavourable or critical feedback.

## 4.2 Spinal Board Geometry

Based on the results from the spinal board geometry analyses, specific design recommendations were finalized as detailed in Figure 24.

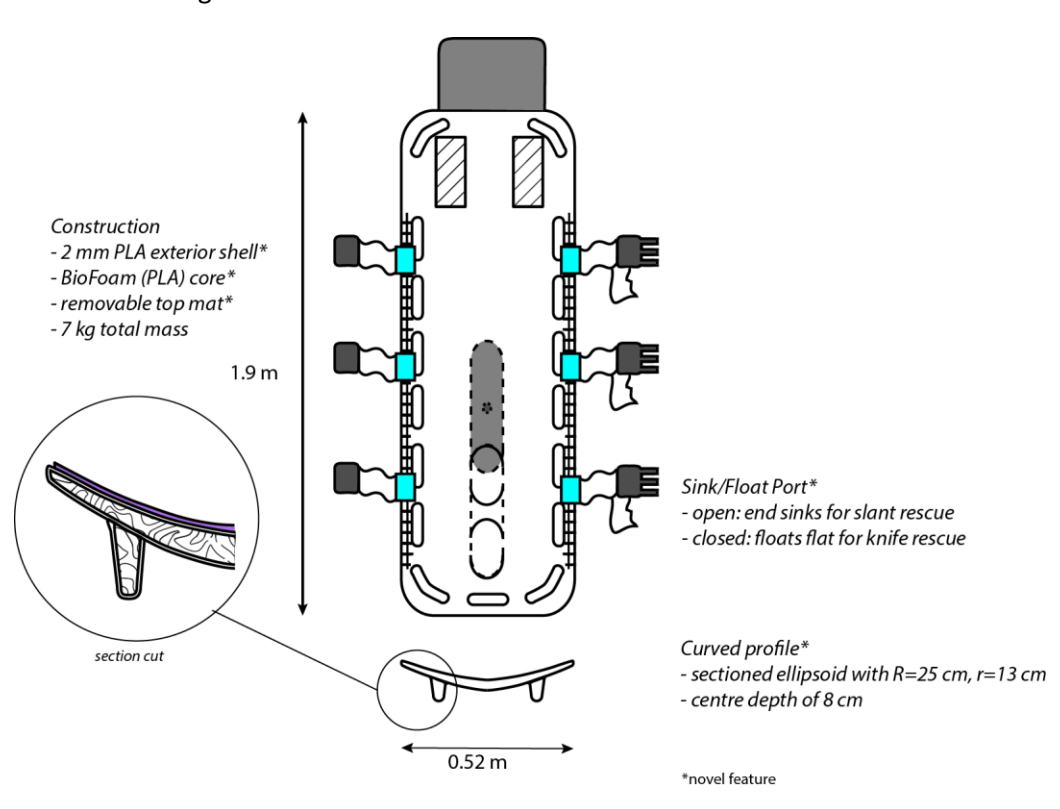


**Figure 24: Optimized Board Geometry Design** 

To summarize, the results of the static buoyancy analysis converged upon the implementation of a 2mm thick PLA shell with a BioFoam core, and the creation of two slot-shaped sink/float ports with dimensions of 190 mm x 70 mm. The results from the fluid dynamics analysis indicate that the general case of the curved profile would reduce drag forces over the course of the knife procedure by up to 5-

fold. Meta-analysis of existing products and anthropometric tables resulted in the selection of an ellipsoid profile with radii of 25 cm and 13 cm, with a centre depth of 8 cm. Finally, the results of the FEA analysis demonstrated that this geometric configuration was structurally sound in terms of deflection and von Mises stress for patients up to 200 kg.

#### 4.2.1 Static Buoyancy Optimization

After a number of CAD and buoyancy calculation iterations in which overall thickness, width, number and size of handle holes were altered, a board volume displacement and mass that would allow floatation of a patient of at least the 99<sup>th</sup> percentile male was ascertained. Assuming the material properties of PLA (which has a density greater than that of water), it was determined that the board would have to be constructed as a thin shell with a foam core to attain the requisite average density to allow for reasonable floatation. This was determined to be in the region of 200-350 kg/m³ on average. BioFoam, a derivative of PLA was selected for the core, which has a density of 40 kg/m³ [18].

At a mass of 7kg, with overall dimensions of 1.9 m x 0.52 m x 25.4 mm, and average density of 209.6 kg/m $^3$ , the optimized geometry is able to float a patient of up to 134 kg without external assistance. This exceeds criterion that the board be appropriate for 99<sup>th</sup> percentile male. Unloaded, the board would also float flat with the sink/float port, as the centre of mass and centre of buoyancy lie at the geometric centre of the board. This fulfills the criterion that the board float, and the criteria that it float flat to facilitate a knife rescue.

In terms of the sink/float port design, a number of iterations of different configurations and numbers of ports analyzed. Through this analysis, it was found that it would be mathematically impossible to converge upon a reasonable configuration that achieved the required change in centre of buoyancy for sinking at the distal end. Short of making the board so full of holes that it lost functionality or adding a large countersink to the board, unloaded distal end sinking could not be achieved through opening the port alone.

According to calculations, it was determined with the maximum reasonable size and number of ports that the distal end would sink if an equivalent of 10 kg of submerged weight were to be applied at the distal end. This configuration is detailed in FIGURE. Assuming average human centre of mass proportions (0.44 of body length from head) and volume, this means that the board would sink at the distal end when loaded with an adult. This would not occur with the ports closed, or in a similar board without ports.

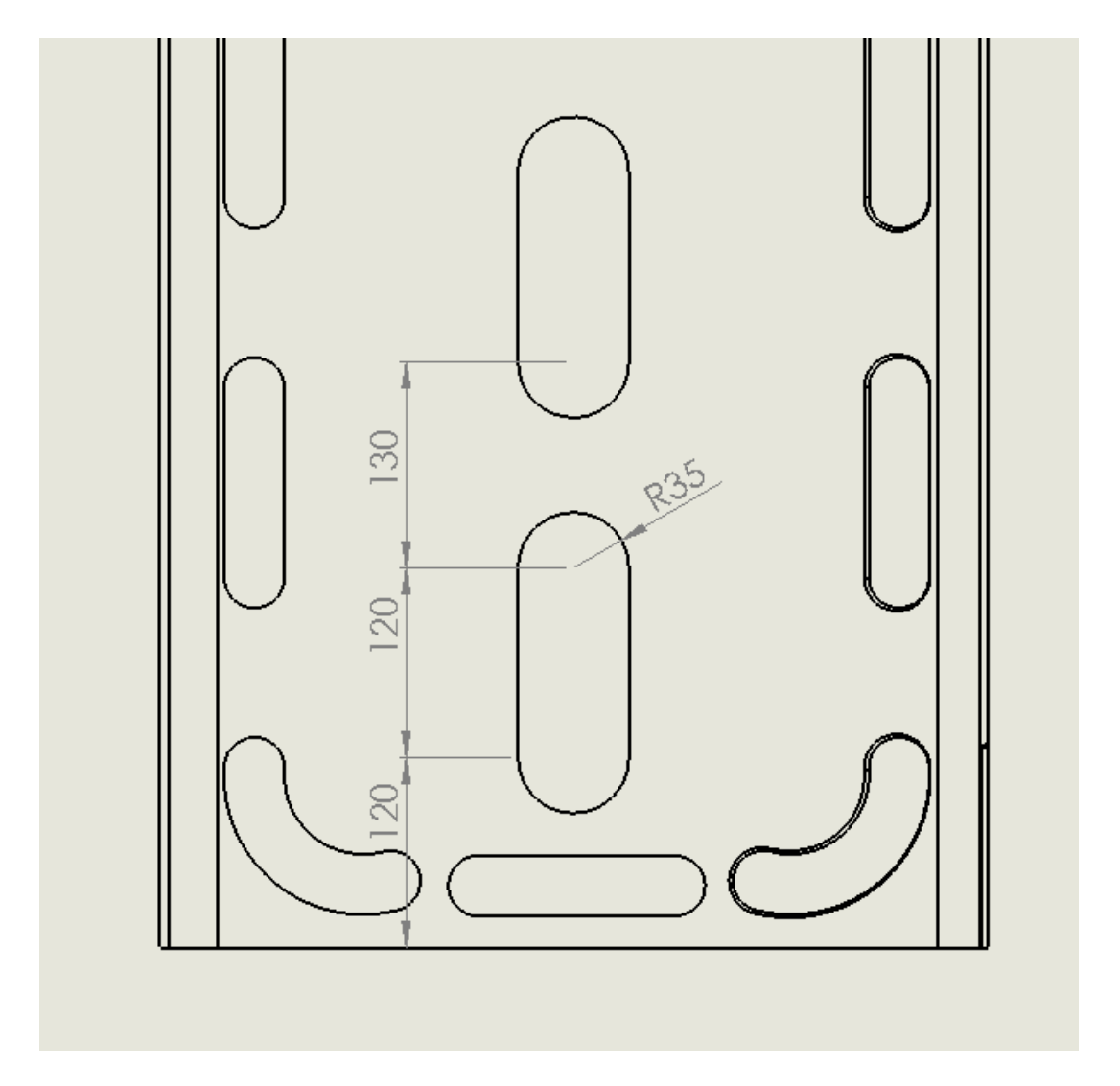


Figure 25: Final Configuration of Ports with Dimensions

While sinking at the distal end only if loaded does not satisfy the criteria to the highest degree, this design feature is retained as it does improve the board's capacity to perform both slant and knife rescues. Although ideally the board would sink unloaded, sinking when loaded represents an improvement over designs without the port feature. In terms of ramifications for the rescue team, this would mean that one of the rescuers would have to push the board downwards at the distal end with their foot until the patient was loaded on to the board. This is an existing strategy used in slant rescues, and would not introduce additional complexity. Because this strategy would typically have to be adopted for the entirety of the in-water rescuer procedure, only having to adopt this strategy in the initial stages of the rescue with the port design would represent an improvement.

#### 4.2.2 Analysis of Curved Profile

From the fluid dynamics analysis of estimated drag forces during the knife procedure, detailed in Figure 26, it was found that with theoretical improvement of up to 10-fold would result from adopting the generalized curve profile. Applying an adjustment factor of 0.5 would suggest up to a 5-fold

improvement. This result satisfies the criteria that the board design improve the capacity to perform both slant and knife rescues, and the criteria that the board design allow for easier use by the rescue team.

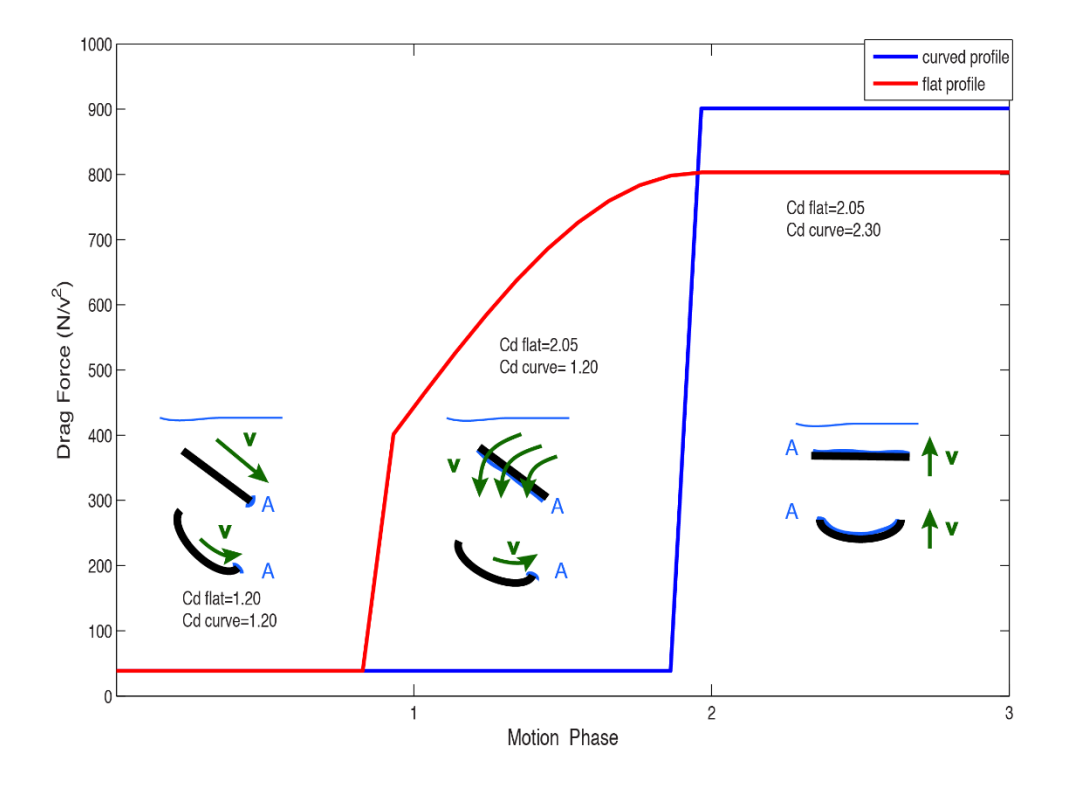


Figure 26: Estimated drag forces of different board profiles during knife rescue

For the flat board, an integral of 689v³ was projected for phases I and II, and an integral of 1491v³ was projected for phase I-III. For the curved board, integrals of 52.8v³ and 960v³ were projected. The ratio of the integrals of phases I and II formed the basis for the improvement as it is during these phases that the rescue team is actively pushing the board beneath the water. During phase III, it might actually be desirable to have greater drag forces, as this would slow the upward motion of the board, making it the motion more controlled.

In considering this analysis, it should be noted that all forces and work projections were made as a function of some unknown velocity, which is assumed to be approximately the same regardless of board profile or phase. If a velocity of 0.5 m/s is assumed, this would correspond to a peak drag force of 200N for the flat profile board and 6.6 N and 225 N for the curved profile during phase I-II and phase III respectively. Keeping in mind that the board is generally pushed underwater by two persons, these forces are reasonable. These forces represent only the contribution from the drag force, and are not necessarily representative of the total force required to push the board underwater, which would also include some contribution of increasing static pressure forces as the board is pushed deeper.

Due to the number of simplifications made in the drag force calculations, the true improvement given by the curved profile is likely lower than 5-fold. Use of tabular coefficients of drag based on shapes that do

not give an entirely accurate representation of design geometry or usage conditions results in board geometric simplification, and likely results in an underestimation of the skin drag of the board. From a conceptual standpoint, skin friction is the major contributor to the curved profile's drag force through phases I and II, meaning that this force was likely underestimated. For example, geometric features that would increase the drag forces such as the handle holes, rails, straps and material roughness were not included in this analysis, but would likely result in an upwards shift of the curved force profile, leading to a smaller improvement ratio.

Other assumptions that must be considered for this analysis include the assumption of constant velocity, and the velocity direction of the water relative to the board. In the analysis, it is assumed that the rescuer performs the motion ideally for the given board profile. This may not be realistic, especially for the curved profile where some training or experimentation with angles of approach for the design curvature would be necessary. The ability of the rescuers to attain this ideal motion pattern may also be affected by the specific curvature of the curved profile.

The specific curvature of the curve profile was determined to be a sectioned ellipsoid with radii of 25 cm and 13 cm, sectioned to have a centre depth of 8cm. This was arrived at based on the biacromial breadth of the 99<sup>th</sup> percentile male, which was found to be 45 cm, and the chest depth of the 50<sup>th</sup> percentile 6 year old female, which was found to be 12 cm [19] [20]. Thus, this profile would allow for proper and comfortable immobilization of a wide array of patients. The results of the search for existing products revealed the existence of a land spinal board with a similar curved profile with similar dimensions (width of 43 cm, centre depth of 8 cm, 25 degress of curvature) [14]. This result meets the constraint that the board be suitable for persons at the anatomical extreme ends of the patient population.

#### 4.2.3 FEA Analysis of Structural Integrity

From the static buoyancy analysis, it became apparent that in order for the board to have a reasonable mass and proper buoyancy characteristics, a PLA shell of 3mm or less would have to be used. While the conventional HDPE spinal boards are typically hollow, no data could be found about typical thickness of the shell structure. Because of this, a supporting foam interior made of BioFoam was proposed to prevent collapse of the structure. This construction method was inspired by existing surfboard technology, where an interior core of expanded polystyrene (EPS) is coated with a fiberglass outer shell [21]. BioFoam was selected as it possesses similar physical and material properties to EPS [18], but without significant environmental and health concerns associated with EPS production and disposal [22].

As summarized in Table 1, different combinations of shell thickness and distributed loads were tested. It was found that with a 2mm thick PLA shell the maximum suggested safe load could be 200 kg. With a shell thickness of 3 mm, this would increase to just over 300 kg. In both cases, the deflection would be the limiting factor.

**Table 1: Summary of FEA Results** 

shell thickness (mm)	total board mass (kg)	Distributed Load (kg)	Maximum von Mises stress (MPa)	Maximum deflection (mm)	Acceptable
2	6.85	200	14.5	14.73	Yes
2	6.85	300	21.5	21.86	No
3	15.9	300	14.9	13.94	Yes
3	15.9	350	17.3	16.21	No

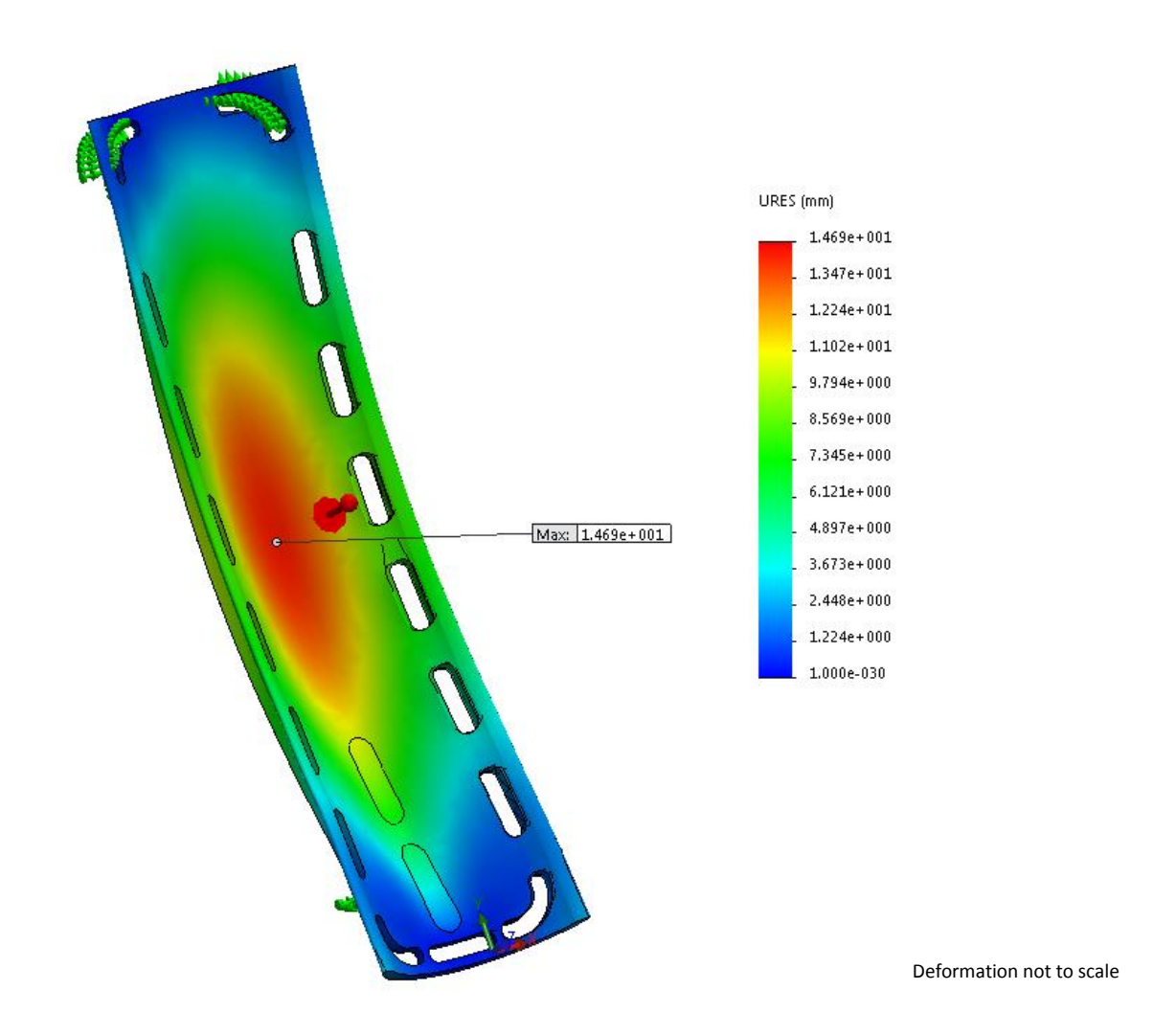


Figure 27: Displacement of Spinal Board with 2mm Shell, 200kg Load

Although having a larger maximum load is more desirable, the margin of improvement seen between 2 and 3 mm shell thickness is not justified when one considers the effect this change would have on the

mass of the board. Making the shell 3 mm thick would result in the board having a total mass of 15.9 kg, which is much heavier than a typical spinal board. A board of this weight would be undesirable in a rescue environment, and would also have poorer buoyancy properties.

Given that a maximum safe load of 200 kg is reasonable, as it is well above the 99<sup>th</sup> percentile male weight (128 kg), a 2 mm shell thickness is justified. This maximum safe load recommendation for the design meets the constraint that the design be suitable for patients up to the 99<sup>th</sup> percentile male.

Though some commercially available boards claim a maximum safe load of upwards of 1100 kg, this is likely a result of the application of different safety constraints. Because no mention of deflection limit is made, it is assumed that only yield stress criterion were considered for the determination of the maximum load. Since this stress limit was not approached in the present analysis, the true maximum safe load is likely in line with currently available boards. Such large body masses were not tested in the FEA analysis because aside from the excessive deflection caused, these loading scenarios would likely limit the rescue procedure in ways unrelated to the board design (strength of rescue team, physical size of person).

Because no appropriate deflection limit could be ascertained from the literature or from existing products, the deflection limit of 15 mm was selected based on the assumption that deflections in excess of this would be both noticeable and potentially compromising in terms of immobilization. Further testing to ascertain a more validated deflection limit would be recommended.

#### 4.3 Material Selection

An analysis of spinal boards presently on the market demonstrates that they are produced from a variety of different thermoplastic materials. However, as the designs are often proprietary, specific details of the materials used in production are seldom disclosed by the manufacturer. In selecting the optimal material for the spinal board, a variety of options that are currently in place on the market were selected for analysis of their material properties. High-density polyethylene (HDPE) is a polymer used by spinal board manufacturer Laerdal Medical Corporation. It has a high strength-to-density ratio and is a low cost material with a wide variety of applications. Thermoplastic polyurethane (TPU) a polymer used in the Lifeguard Master line of spinal boards, having a relatively high yield strength. Acrylonitrile butadiene styrene (ABS) is a polymer used by spinal board manufacturer Kiefer and has applications that include automotive interiors, luggage, toys and boats.

In addition to the design alternatives discussed above, consultation with graduate students at the Bioproducts Discovery and Development Centre at the University of Guelph provided insight into opportunities to incorporate bio-polymers into the design of the optimized spinal board. Polylactic acid (PLA) is a polymer derived from corn starch that has good strength, stiffness and a relatively low cost. Polyhydroxybutyrate (PHB) is a polymer that is the product of bacterial anaerobic growth that is both biodegradable and water insoluble.

The five selected materials demonstrate available thermoplastics that are capable of undergoing injection molding on an industrial scale. They were selected as alternates for the material of the spinal board.

#### 4.3.1 Alternative Analysis

In order to conduct a thorough analysis of the material properties of the alternatives mentioned above, a dataset with reliable information on a variety of polymer materials was necessary. CES EduPack 2014 is a software package developed by Granta Design, a leading materials information management company, with detailed information and properties for over 3,900 materials from handbooks, textbooks, Internet, and software sources. The software allows for the comparison and analysis of a variety of materials given constraints and criteria.

Table 2 demonstrates properties that were tabulated to aid in this decision making process. In order to have a comprehensive analysis of the best material alternative, a fractional score was developed for the performance of each polymer in each property category. The polymer with the 'best' performance for a given property was given a 1, and each other polymer was given a fractional score in comparison to the best value. Properties were weighted based on importance, and fractional scores were multiplied by weights to determine the total weighted score for each polymer.

Table 2 Material properties of thermoplastic alternatives.

Material Class		Polymers		Bio-Pol	vmers
Material	HDPE	TPU	ABS	PLA	PHB
Density [kg/m^3]	952-965	1120-1240	1020-1080	1240-1270	1230-1250
Fractional Score	1	0.8123	0.9129	0.7637	0.773
Weighted Score @ 0.2	0.2	0.16246	0.18258	0.15274	0.1546
Cost [\$/kg]	1.81-2	6.04-6.64	2.77-3.05	2.27-2.73	6.18-7.21
Adjusted cost [\$/m^3]	1723-1930	6465-8234	2825-3294	2815-3467	7601-9013
Fractional Score	1	0.2485	0.597	0.5815	0.2199
Weighted Score @ 0.2	0.2	0.0497	0.1194	0.1163	0.04398
Young's modulus [GPa]	1.07-1.09	1.31-2.07	2-2.9	3.3-3.6	3.5-4
Fractional Score	0.288	0.4507	0.653	0.92	1
Weighted Score @ 0.1	0.0288	0.04507	0.0653	0.092	0.1
Yield strength [MPa]	26.2-31	40-53.8	29.6-44.1	55-72	35-40
Fractional Score	0.4504	0.7386	0.5803	1	0.5906
Weighted Score @ 0.3	0.13512	0.22158	0.17409	0.3	0.17718
Durability, salt water				Acceptable	Acceptable
[E/A/L]	Excellent	Excellent	Excellent	Acceptable	Acceptable
Fractional Score	1	1	1	0.5	0.5
Weighted Score @ 0.05	0.05	0.05	0.05	0.025	0.025
Durability, fresh water [E/A/L]	Excellent	Excellent	Excellent	Acceptable	Acceptable
Fractional Score	1	1	1	0.5	0.5
Weighted Score @ 0.05	0.05	0.05	0.05	0.025	0.025
Durability, UV radiation [E/G/F/P]	Fair	Fair	Poor	Good	Good
Fractional Score	0.5	0.5	0.25	0.75	0.75
Weighted Score @ 0.05	0.025	0.025	0.0125	0.0375	0.0375
CO2 footprint [kg/kg]	2.64-2.92	3.52-3.89	3.64-4.03	3.43-3.79	4.14 - 4.58

Fractional Score	1	0.753	0.7249	0.7701	0.6376
Weighted Score @ 0.05	0.05	0.03765	0.036245	0.038505	0.03188
Material	HDPE	TPU	ABS	PLA	PHB
<b>Total Weighted Scores</b>	0.73892	0.64146	0.690115	0.787045	0.59514

#### 4.3.2 Selected Alternative

The material with the highest total weighted score was PLA, a biopolymer with good strength, stiffness, and a relatively economical cost. However, there are a few issues to address in the selection of this alternative, as the biopolymer is relatively new in commercial applications.

The biodegradability of the material is a desirable attribute from an environmental standpoint, but it can be problematic if the material begins to degrade when the device it is still in use. For this purpose, further research will be done into the lifespan of PLA and if there are constituents that have the possibility of forming a composite material to extend its lifespan. In addition, surface treatments will be evaluated to assess their performance in increase the material's resistance to environmental effects.

In addition, the density of PLA is the highest of the alternates selected for analysis, approximately 1255 kg/m^3. The material is not inherently buoyant if it is made into a spinal board. This higher density, however allows for the inclusion of another aspect of the design to augment the high density. Padding in the form of closed-cell polyethylene foam and a HDPE top-layer has the ability to decrease the overall density of the spinal board, and to increase the comfort during immobilization. As an influential study by Walton et al. demonstrated that the inclusion of closed-cell foam significantly increased comfort without compromising cervical spine immobilization of the patient, this addition to the design would achieve two objectives. No further changes in the selected material for the spinal board has been made since the submission of the interim report. However, instead of a closed-cell polyethylene foam used for padding, a PLA derived BioFoam is to be used instead.

## 4.3.3 Modified Board Surface Motion Capture Results

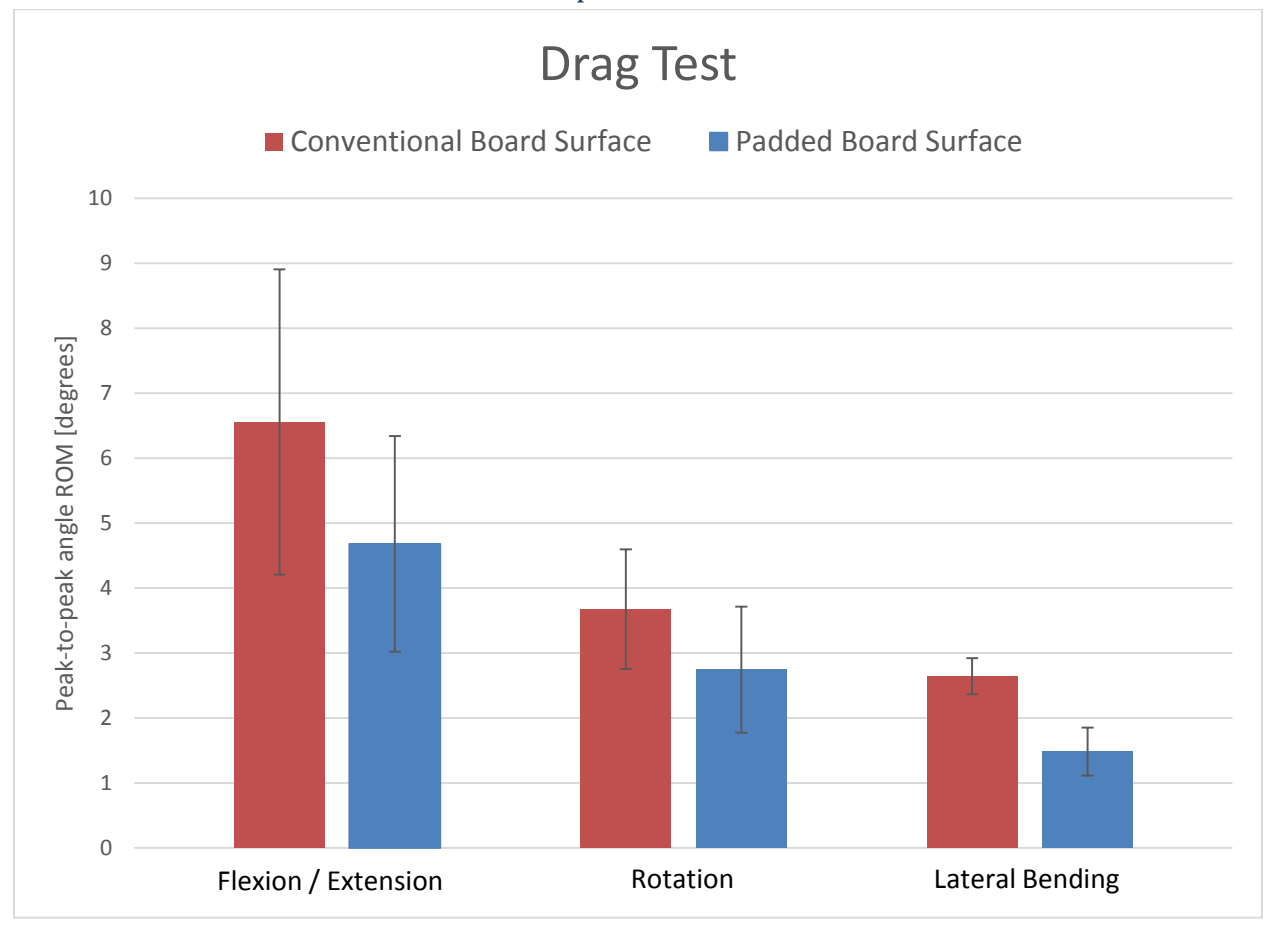


Figure 28: Mean peak-to-peak ROM and 95% confidence intervals for drag test with conventional and modified surface designs

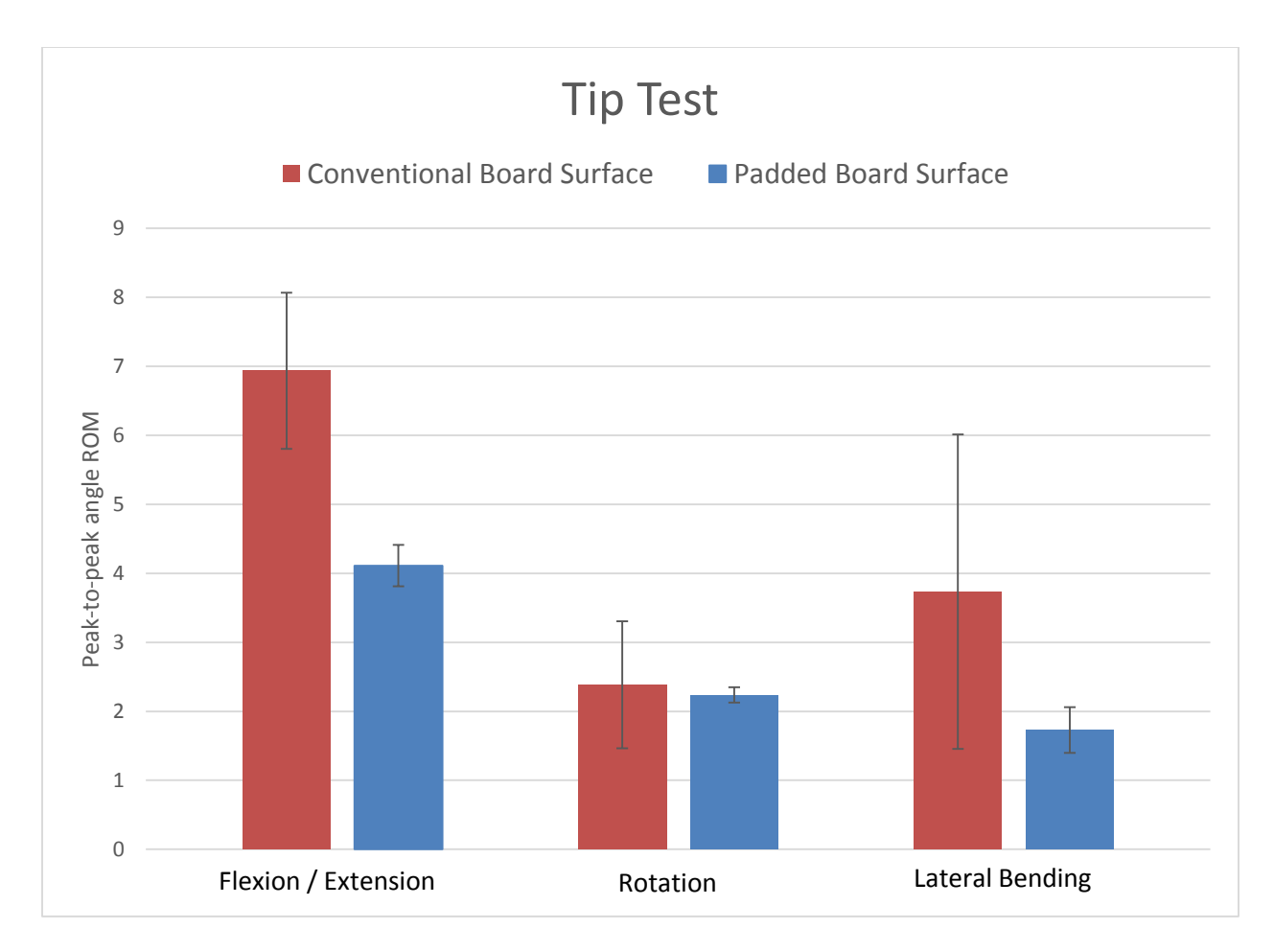


Figure 29: Mean peak-to-peak ROM and 95% confidence intervals for tip test with conventional and modified surface designs

#### 4.3.4 Modified Board Surface Discussion

It was found that there was a decrease in the range of motion of the head all three axes of rotation for both the drag test and the tip test. The decrease in lateral bending in the drag test was found to be statistically significant, as was the decrease in flexion / extension in the tip test.

These results were unexpected, but welcomed, as the addition of padding to the surface of the spinal board was found to be successful in increasing immobilization. The underlying mechanism for this increase may have been due to a difference in the static coefficient of friction of the conventional HDPE spinal board and the PVC yoga mat. As the function of a yoga mat is to decrease slippage between the floor and the yogi, this relatively higher coefficient would potentially decrease displacement. Literature values for the static coefficient of friction were found to be 1 for the surface of a spinal board [23], and approximately 1.75 for a polyvinyl yoga mat [24], which agreed with this analysis.

In addition to the increases in spinal immobilization, the addition of a removable padded surface would be advantageous in terms of sanitization, as it could be washed or replaced readily. This aspect addresses the criteria that it be easy to maintain and sanitize.

## 4.5 Overall Spinal Board Design

### 4.5.1 Bill of Materials

The final spinal board design consists of several components in its assembly. Most of the components are to be manufactured on-site in the facility where it will be stored prior to shipment once a purchase is made, as seen in Table 3.

Table 3 Components to be manufactured for the construction of the spinal board.

Item #	Part Name	Material	Production Process	Qty
1	Spinal board	PLA	Injection Moulding	1
2	Mounting unit	PLA	Injection Moulding	4
3	Strap buckle	PLA	Injection Moulding	6
4	BioFoam insert	BioFoam (PLA)	Injection Moulding	1

The components of the assembly for purchase are the straps and padding. Each assembly will have 6 straps, each with a length of 610mm (2ft) and a  $1.370m \times 0.305m$  (4.5ft x 1ft) sheet of BioFoam from Synbra Technology.

Table 4 Components for purchase from other manufacturers.

Item #	Part Name	Manufacturer	Description	Qty
5	Strap	Outdoor Fabrics	A 610mm long polyester strap for	6
		Canada	the use of immobilization.	
6	Padding	Synbra Technology	BioFoam sheet for padding	1

#### 4.5.2 Implementation Cost

PLA will be supplied by NatureWorks LLC, Minnetonka, Minnesota, USA. The total mass of PLA to be used for the components in Table 3 is 7.5kg. Assuming 10% waste during the production processing, a total of 8.33kg of PLA will be used. BioFoam, which is PLA in a lower net density through means of adding air bubbles is to be used as the inner shell of the spinal board.

Table 5 Cost of PLA for production processing per 1 spinal board assembly (assume 10% waste).

Item #	Part Name	Material	Mass(kg)	Qty	Cost (\$/kg)	Total (\$)
1	Spinal board	PLA	7.778	1	2.73	21.23
2	Mounting unit	PLA	0.0333	4	2.73	0.97
3	Strap buckle	PLA	0.0889	6	2.73	0.55
4	BioFoam insert	BioFoam	0.728	1	2.73*	1.99
					Total	\$24.74

<sup>\*</sup>the price used is the price of regular PLA rather than BioFoam. Assumption of same price was made using the mass of BioFoam.

The process used to manufacture the components is injection molding. For the spinal board component, the injection molding involves thin-walled of 2mm outer layer with a BioFoam inner core to provide structural support. The thin-walled outer layer will be made prior to injecting the BioFoam. An assumed defect rate of 5% was used to calculate the total injection moulding cost. The salaries of the labourers to

create the components and the moulds were estimated using the national average for those professions. These were the mould-making labour that cost of \$65/hr, this includes direct and indirect labour costs, setup labour and direct labour at \$23.37/h and post labour (post processing and quality assurance) of \$20.6/h. The cost of injection moulding to produce 1000 spinal boards with each consisting of 1 spinal board and 4 mounting units is estimated in Table 6. 1000 spinal boards is used as the initial inventory to be created using the moulds.

Table 6 Injection moulding cost for 1000 spinal boards (materials, labour and tools).

Part #	Required Resource	Cost (\$/1000 Product)	Cost(\$/Product)
1	Moulding Tooling	79,189	79.19
	Injection Moulding (incl. tooling)	82,946	82.95
2	Moulding Tooling	7,386	1.85
	Injection Moulding (incl. tooling)	8,717	2.18
		Total (injection moulding)	\$85.13

Lastly, two parts are ordered directly from manufacturers are the straps and padding. The total cost of these can be seen in Table 7. The padding provider is Synbra Technology, a supplier of specialized PLA BioFoam stationed in Etten-Leur, Netherlands. The polyester immobilization straps will be purchased from Outdoor Fabrics Canada for their durable polyester seatbelt webbings.

Table 7 Total cost of purchased parts not manufactured.

Item #	Part Name	Manufacturer	Qty	Part Cost(\$)	Total(\$)
5	Strap	Outdoor Fabrics Canada	6	1.00	6.00
6	Padding	Synbra Technology	1	15.00	15.00
				Total (all)	\$21.00

Therefore, the total cost to manufacture and assemble one complete spinal board is \$130.87. This does not include facility rental and other personnel not included in the processing and assembly of the spinal board. The cost of some products, such as the padding may be reduced further with larger volume purchases for increased spinal board production.

#### 4.5.3 Risk and Uncertainties

The optimization of the spinal board resulted in the alteration of the current conventional spinal board whose technology has remained relatively static for several years. The introduction of radically different components, shape and material may incur risks and uncertainties. These may result in future legal complications such as lawsuits, to which the engineers will be liable.

Since the technology for spinal boards have been static for many years, the alterations introduces a new immobilization methodology that includes steps that were never mentioned in training manuals. This will require the retraining lifeguards to use the products and may ultimately prove difficult to be worth investing both time and money in. Improper usage of the board due to changes made to the spinal board's form factor and mechanism may result in significant wear and tear lowering the board's life

expectancy. Improper usage of the board may also result in injury to the personnel or further increase the severity of spinal injury of the patient.

The introduction of PLA as the material used to manufacture the spinal board instead of the commonly used HDPE may result in risks involving expedited fatigue failure or other mechanical failure due to different environmental conditions. This could be prevented through extensive testing conducted on the spinal board however, at the current standing of the project, there is inadequate amount of supporting literature to fully eliminate the possibility of failure due to varied conditions.

The experimental data procured from Vicon motion capture testing provides some understanding on the improvements made by the spinal board. However, there remains the uncertainty that the data is inaccurate in representing the actual impact of the optimized spinal board and its changes. The board design may actually do more harm than good causing an increase in severity of spinal injury. Similarly, the improvements may only be apparent on similar body types to those tested in the lab. Body types that do not conform to the tested conditions may not be accommodated. Lastly, the experimental procedure was conducted on land which may not represent loading conditions present in aquatic environment that the spinal board was intended for.

Lastly, other uncertainties present with the design is the possibility of imperfections created at the numerous stages of the manufacturing of the spinal board. Quality assurance at each stage may allow prevention, however this may prove too costly, especially for a new product.

While not fully preventable, proper training on the use of the spinal board and further experimental tests, as well as sufficient time of the spinal board in the market, the risks and uncertainty outlined above will be greatly reduced.

#### 4.5.4 Life Cycle Analysis

Similar to current conventional spinal boards, the optimized design has a life expectancy of 15 years for the board given proper use and maintenance. Accessories such as the immobilization straps and buckles will last for 5 years depending on usage. The life expectancy will be equivalent or better than the comparable spinal board due to PLA's higher Young's Modulus and yield strength compared to HDPE. Similarly, PLA has better UV durability allowing longer life when stored in outdoor or high sun exposure conditions.

A life cycle analysis (LCA) was conducted using LCAcalculator.com. This calculator does not have PLA as an option for plastic components, as with most LCA calculators currently available. Therefore, HDPE was used for the estimated environmental impact during the manufacturing process. HDPE was chosen as the alternative for the simulation due to its similar properties with PLA. The CO<sub>2</sub> emission was calculated for each phase of the production of 1 spinal board and 1000 spinal boards as seen in

Table 8 and Table 9. Full LCA for each part of the assembly is located in Appendix G – LCA Results.

Table 8 Summarized LCA for the production of 1 spinal board.

Phase

Manufacture	29.8
Transport	2.92
Use	0
Disposal	0.102
Cumulative CO <sub>2</sub>	32.8

Table 9 Summarized LCA for the production of 1000 spinal boards.

Phase	_ Total CO <sub>2</sub> (kg)
Manufacture	160000
Transport	2920
Use	0
Disposal	102
Cumulative CO <sub>2</sub>	163000

From the analyses, the manufacturing process results in the highest amount of CO<sub>2</sub> emission. However, this value may not be entirely accurate as HDPE was used for estimation. The emission to create PLA should be lower than HDPE by a significant factor. For 1 kg of PLA, approximately 57 MJ of energy must be spent from fossil fuel while LDPE (low density polyethylene) requires 82 MJ to manufacture 1 kg [25]. Manufacturing HDPE will slightly higher energy than LDPE, resulting in the doubling of the energy required compared to PLA [11]. While not necessarily half the LCA estimation's result, it is assumed that the manufacturing CO<sub>2</sub> emission will be significantly lower, unless a large majority of the CO<sub>2</sub> emission originated during the injection molding procedure.

The  $CO_2$  emission due to transportation will not vary as the factor of consideration to calculate this was the mass of the components and the distance travelled. The two major travel distance is from the PLA supplier in Minnesota, USA which carries a large volume of PLA and the air freight from the BioFoam provider in the Netherlands. Because of the factors taken into consideration, HDPE provides an adequate estimation of the  $CO_2$  emission for the transportation component.

Typically for an application, the required amount of PLA and HDPE will result in similar masses, thus, the disposal options practiced may be largely similar [25]. While virgin PLA will take up majority of the production especially during the initial production of 1000 units, recycled PLA may later be used once PLA recycling methods are procured. This will reduce the CO<sub>2</sub> emissions from the disposal of the spinal board. PLA also has biodegradability and therefore may be disposed of using a controlled environment requiring less energy than HDPE, thus lowering CO<sub>2</sub> emission.

Overall, the optimized spinal board design does not have environmental impacts throughout its usage. The major environmental impact is derived from the manufacturing process and transportation. However, the estimated values will be lower for the manufacturing process proving more environmentally friendly than the common HDPE spinal board available in the market.

## 5.0 Conclusions

The design alternatives three components of the project design were assessed and an appropriate solution was chosen that satisfy the criteria determined in the proposal and those added in the interim report. The three aspects of the board that was considered for optimization were the material selection for the construct of the spinal board, the physical board mechanics and ergonomics, and the harnessing system of the spinal board. Decision matrices and sensitivity analyses were conducted to reach a conclusion for the alternative design to be used. It was determined that the optimized board will include:

- a twist locking mechanism that allows adjustments to immobilization strap location;
- a combination design that incorporates a curved spinal board structure and a porthole for adjusted buoyancy;
- the material selected is polylactic acid for its relatively lower cost, high strength and durability, and environmental effects.

The harness system was well received by others from the surveys conducted. General census of the survey show persons found the design to have easier strapping positioning and increased overall satisfaction to the spinal board. The Vicon data collected resulted in non-statistically significant improvement in peak-to-peak angle in head flexion-extension and lateral bending. Further studies may be needed with a larger sample size to gather more accurate results.

The modified board geometry was successful in allowing both slant and knife style rescue methods. The addition of a curvature along the frontal plane of the spinal board resulted in reduced drag force while performing the knife style rescue when compared to conventional flat spinal board.

Although ideally the board would sink unloaded, sinking when loaded represents an improvement over designs without the port feature. To perform slant rescue, a second lifeguard would be required to push the board downwards at the distal end. This is an existing strategy used in slant rescue. Therefore, the design still complies with the criterion of the ability to perform slant rescue and the constraints the board must follow current lifesaving procedures as outlined by the Lifesaving Society of Canada.

Through calculations and simulations, it was found that PLA is a justifiable material for the construction of an aquatic spinal board. The FEA results determined that a thin-walled PLA spinal board with a BioFoam inner core is able to withstand significant deflection from a 200 kg load. This maximum safe load recommendation for the design meets the constraint that the design be suitable for patients up to the 99<sup>th</sup> percentile male.

## 6.0 Recommendations

It is recommended that further study be conducted on the effects of immobilization on a spinal board using a larger sample size that includes a greater variance of height, weight and body types. It is also recommended to conduct trials in aquatic environments to better represent actual emergency response spinal immobilization. These will allow further improvement, if needed, on the aspects of the board contributing to immobilization such as the spinal board shape and harnessing system.

## References

- [1] City of Winnipeg, "Lifeguarding Training Manual," 2013. [Online]. Available: http://www.winnipeg.ca/cms/aertraining/Docs/AERmanual/aer\_manual\_10th\_web.pdf. [Accessed 08 01 2015].
- [2] World Health Organization, "Drowning and Injury Prevention," N.D.. [Online]. Available: http://www.who.int/water\_sanitation\_health/bathing/srwe2chap2.pdf. [Accessed 08 01 2015].
- [3] Royal Lifesaving Society of Canada, Canadian Lifesaving Manual, 5 ed., Royal Lifesaving Society of Canada, 2004.
- [4] Rick Hansen Institute, "Canadians Unaware of Staggering Costs of Spinal Cord Injury and Paralysis," 2012. [Online]. Available: http://www.rickhanseninstitute.org/media-room/archives/313-canadians-unaware-of-staggering-costs-of-spinal-cord-injury-and-paralysis. [Accessed 08 01 2015].
- [5] B. Green, M. Gabrielsen, W. Hall and J. O'Heir, "Analysis of Swimming Pool Accidents Resulting in Spinal Cord Injury," *Paraplegia*, vol. 18, pp. 94-100, 1980.
- [6] W. Cordell, J. Hollingsworth, M. Olinger, S. Stroman and D. Nelson, "Pain and Tissue-Interface Pressures During Spine-Board Immobilization," *Ann Emerg Med*, vol. 26, no. 1, pp. 31-36, 1995.
- [7] Royal Lifesaving Society of Canada, Alert: Lifeguarding in Action, 8 ed., Royal Lifesaving Society of Canada, 2007.
- [8] M. D. Luscombe and J. L. Williams, "Comparison of a long spinal board and vacuum mattress for spinal immobilisation," *Emerg Med J*, vol. 20, no. 4, pp. 476-478, 2003.
- [9] ASTM Standard F1557-94, Standard Guide for Full Body Spinal Immobilization Devices (FBSID) Characteristics, West Conshohocken: ASTM International, 2007.
- [10] V. K. N. L. M. T. P. J. C. S. R. H. Krueger, "The economic burden of traumatic spinal cord injury in Canada," *Chronic Diseases and Injuries in Canada*, vol. 33, no. 3, pp. 113-122, 2013.
- [11] S. I. and W. P. -A., "Determining the movements of the skeleton using well-configured markers.," *Journal of Biomechanics*, vol. 26, pp. 1473-1477, 1993.
- [12] C. Spoor and F. Veldpaus, "Rigid body motion calculated from spatial co-ordinates of markers," *Journal of Biomechanics*, vol. 13, no. 4, pp. 391-393, 1980.

- [13] H. Baukje, P. Martijn and P. Brink, "Reduced Tissue-Interface Pressure and Increased Comfort on a Newly Developed Soft-Layered Long Spineboard," *Journal of Trauma-Injury Infection & Critical Care*, vol. 68, no. 3, pp. 593-598, 2010.
- [14] J. Krell, M. McCoy, P. Sparto, G. Fisher, W. Stoy and D. Hostler, "Comparison of the Ferno Scoop Stretcher with the Long Backboard for Spinal Immobilization," *Prehospital Emergency Care*, vol. 10, no. 1, pp. 46-51, 2006.
- [15] R. Fox and A. McDonald, Introduction to Fluid Mechanics, Wiley, 1985.
- [16] B. Munson, A. Rothmayer and T. Okiishi, Fundamentals of Fluid Mechanics, Wiley Global Education, 2012.
- [17] Plastics Institute of America, Plastics Engineering Manufacturing and Data Handbook, vol. 2, Norwell, MA: Kluwer Academic Publishers, 2001.
- [18] Synbra Technology, "BioFoam Physical and Thermal Properties," 2015. [Online]. Available: http://www.BioFoam.nl/index.php?page=physical-and-thermal-properties. [Accessed 01 03 2015].
- [19] Centers for Disease Control and Prevention, "Selected Body Measurements of Children 6-11 Years, United States," National Center for Health Statistics, Rockville, MD, 1973.
- [20] Centers for Disease Control and Prevention, "Anthropometric Reference Data for Children and Adults: United States, 1988-1994," National Center for Health Statistics, Hyatsville, MD, 2009.
- [21] J. Kinstle, Surfboard Design and Construction, Natural High Express Publishing , 1975.
- [22] D. Lithner, A. Larsson and G. Dave, "Environmental and health hazard ranking and assessment of plastic polymers based on chemical composition," *Science of the Total Environment*, vol. 409, no. 18, pp. 3309-3324, 2011.
- [23] C. W. J. Oomens, W. Zenhorst, M. Broek, B. Hemmes, M. Poeze, P. R. G. Brink and D. L. Bader, "A numerical study to analyse the risk for pressure ulcer development on a," *Clinical Biomechanics*, vol. 28, pp. 736-742, 2013.
- [24] A. Sutphen, "Friction Testing: Results and Analysis," Tufts University Future Technologies Lab, Medford, 2005.
- [25] K. R. R. D. A. G. P. R. G. Erwin T.H. Vink, "Applications of life cycle assessment to NatureWorks(TM) polylactide (PLA) production," *Polymer Degradation and Stability*, vol. 80, pp. 403-419, 2003.

- [26] L. Plueschow, "Lifeguard Training Supplemental Notes," lifeguardtrainer.com, 2010. [Online]. Available: http://www.lifeguardtrainer.com/lifeguardtrainer/Docs/SupNotes.pdf. [Accessed 12 February 2013].
- [27] US Department of Health and Human Services, "Anthropometric Reference Data for Children and Adults: United States, 2007–2010," Library of Congress, Hyatsville, MD, 2012.

## **Appendices**

## Appendix A – ASTM Standards



Designation: F1557 - 94 (Reapproved 2007)

#### Standard Guide for Full Body Spinal Immobilization Devices (FBSID) Characteristics <sup>1</sup>

This standard is issued under the fixed designation F1557; the number immediately following the designation indicates the year of original adoption or, in the case of revision, the year of last revision. A number in parentheses indicates the year of last reapproval. A superscript epsilon (n) indicates an editorial change since the last revision or reapproval.

#### INTRODUCTION

The objective of this guide is to begin to address the recognized need to support and immobilize the components of the spine or spinal cord. Although this guide does not quantitatively address performance standards for this device, it does address the characteristics of the device(s) used to provide support and immobilization of the components of the central nervous system for the patient suspected of receiving trauma to that body system.

#### 1. Scope

- 1.1 This guide establishes minimum standards for devices, designated here as full body spinal immobilization device(s) (FBSID), commonly known as long boards. The FBSID is designed to be used as the base structure for immobilization and transport of a patient with potential spine or spinal cord injury by emergency medical service personnel.
- 1.2 This guide does not identify specific degrees of limitation of motion achieved by placement of a FBSID on a patient. Definitive requirements for immobilization of the spine, and, in particular, the degree of limitation associated with the use of a FBSID, have not been established in the medical literature.
- 1.3 This standard does not purport to address all of the safety concerns, if any, associated with its use. It is the responsibility of the user of this standard to establish appropriate safety and health practices and determine the applicability of regulatory limitations prior to use.

#### 2. Referenced Documents

2.1 ASTM Standards:2

F1177 Terminology Relating to Emergency Medical Services 2.2 Centers for Disease Control Standard:

Guidelines for Prevention of Transmission of HIV and HBV to Healthcare and Public Safety Workers<sup>3</sup>

2.3 OSHA Standard:

29 CFR 1910.1030 Occupational Exposure to Bloodborne Pathogens; Final Rule<sup>4</sup>

#### 3. Terminology

- 3.1 Definitions:
- 3.1.1 retention system—a retention system is an adjunct to or an integral part of the primary platform that allows the patient to be securely attached to that platform, used in whatever configuration and size necessary to accomplish the goal, while still allowing reasonable and necessary access to the patient.
- 3.1.2 spinal immobilization—spinal immobilization refers to immobilization of the entire spine and its contiguous structures, the pelvis and skull.
- 3.1.3 spine—the spine shall include the cervical, thoracic, lumbar, and sacral vertebrae.
- 3.2 Definitions of Terms Specific to This Standard:
- 3.2.1 directions of movement—include flexion, extension, rotation, distraction, lateral motion, and axial compression motion
- 3.2.2 full body spinal immobilization device— a platform upon which a patient can be secured, that will support the entire length and weight of the patient during immobilization and transportation.

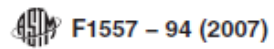
<sup>&</sup>lt;sup>1</sup> This guide is under the jurisdiction of ASTM Committee F30 on Emergency Medical Services and is the direct responsibility of Subcommittee F30.01 on EMS Equipment.

Current edition approved Feb. 1, 2007. Published February 2007. Originally approved in 1994. Last previous edition approved in 2002 as F1557 – 94(2002). DOI: 10.1520/F1557-94R07.

<sup>&</sup>lt;sup>2</sup> For referenced ASTM standards, visit the ASTM website, www.astm.org, or contact ASTM Customer Service at service@astm.org. For Annual Book of ASTM Standards volume information, refer to the standard's Document Summary page on the ASTM website.

<sup>&</sup>lt;sup>3</sup> Available from Centers for Disease Control & Prevention (CDC), 1600 Clifton Rd., Atlanta, GA 30333, http://www.cdc.gov.

<sup>&</sup>lt;sup>4</sup> Available from Superintendent of Documents, U.S. Government Printing Office, Washington, DC, 20402.



- 3.2.3 immobilization-limitation of motion.
- 3.3 For definitions of other terms used in this guide, refer to Terminology F1177.

#### 4. Significance and Use

- 4.1 The intent of this guide is to identify characteristics which a FBSID shall possess.
- 4.2 It is not expected that the FBSID will be used alone to provide the entire scope of required immobilization. Clinical situations may require differing combinations of devices for adequate total spinal immobilization. A FBSID may be one of the devices.
- 4.3 A device intended for use with adult patients shall accommodate the 95th percentile adult American male.
- 4.4 Devices that are labeled as intended for pediatric use shall not be required to accommodate an adult.
- 4.5 The device shall be able to be used by the practitioner in an ergonomically sound manner.

#### 5. Characteristics

- 5.1 The FBSID, when lifted in accordance with manufacturer's instructions, shall support the 95th percentile adult American male patient, full length in the supine position.
- 5.2 The FBSID shall incorporate a means to accommodate the ergonomically sound handling and lifting of the device when fully loaded.
- 5.3 The FBSID shall allow X-ray to be taken through it and be MRI compatible.

- 5.4 The FBSID shall allow for the use of adjunct devices as necessary such that immobilization is provided in the planes of motion as noted in 3.2.1.
- 5.5 The FBSID shall support lower extremities in such a manner that it prevents motion of the pelvis and spine.
- 5.6 There shall be a retention system used in conjunction with the immobilization platform.

#### 6. Durability

6.1 The FBSID shall maintain stated characteristics throughout its lifetime as indicated by manufacturer's recommendations.

#### 7. Maintenance

- 7.1 The FBSID shall be disposable, or easily cleaned, consistent with CDC and OSHA decontamination procedures, without deterioration of the product or the retention of cleaning agents that may be harmful to the patient.
- 7.2 The cleaning/decontamination procedure shall be explained in the manufacturer's product information.

#### 8. Capability

8.1 This guide does not presently quantify the limitation of motion expected to be imposed upon a patient as a result of the application of a SPINE device. This capability has not been omitted due to a lack of need, but as a result of the fact that such quantitative requirements have not been identified in the medical literature. It is hoped that such requirements can be developed, and included in this guide at its next review.

#### 9. Keywords

9.1 immobilization device; long board; spinal cord; spine

ASTM international takes no position respecting the validity of any patent rights asserted in connection with any item mentioned in this standard. Users of this standard are expressly advised that determination of the validity of any such patent rights, and the risk of intringement of such rights, are entirely their own responsibility.

This standard is subject to revision at any time by the responsible technical committee and must be reviewed every five years and if not revised, either reapproved or withdrawn. Your comments are invited either for revision of this standard or for additional standards and should be addressed to ASTM international Headquariers. Your comments will receive careful consideration at a meeting of the responsible technical committee, which you may attend. If you feel that your comments have not received a fair hearing you should make your views known to the ASTM Committee on Standards, at the address shown below.

This standard is copyrighted by ASTM international, 100 Barr Harbor Drive, PO Box C700, West Conshohocker, PA 19428-2959, United States. Individual reprints (single or multiple copies) of this standard may be obtained by contacting ASTM at the above address or at 610-832-9585 (phone), 610-832-9555 (fax), or service@astm.org (e-mail); or through the ASTM website (www.astm.org). Permission rights to photocopy the standard may also be secured from the ASTM website (www.astm.org/COPYRIGHT/).

## Appendix B - Excerpt from a Canadian Lifeguard Manual

Chapter 4

Lifequarding Skills and Procedures

In a swimming pool, patrons could be instructed to sit against the perimeters of the facility until the ambulance arrives. The yellow tape used by emergency services and construction crews might be used to create a physical barrier.

#### MANAGEMENT OF SPINAL INJURIES

Spinal injuries can result from impact with the bottom after diving into shallow water or, less frequently, from a jack-knifing of the spine upon impact. With proper management, the spinal cord which has not been severed or damaged on the initial impact, can be protected against catastrophic injury.

#### a) Principles and tasks.

Proper management of a spinal-injured victim requires the coordination of many skills into a sequence which immobilizes the spine, maintains airway, breathing and circulation, and allows for victim removal and transport. Lifeguards must use judgment in making decisions about how and when to stabilize the victim on a spineboard and remove the victim from the water. Factors which will have to be considered include:

the number of lifeguards available

- whether and how bystanders might be used
- the characteristics of the removal site (e.g., depth of water, distance from deck/dock to the surface, surf conditions)
- · the victim's condition
- the victim's size
- the lifeguards' size and strength

The above factors may alter the techniques selected but will not alter the principles of care nor the essential tasks which are:

#### ☐ Recognize

- Quick, accurate recognition of the accident and clearing of the area.
- Entry which minimizes movement of the victim (i.e., creates no waves).

#### ☐ Immobilize

 Face-up recovery of the victim at the surface with immobilization of the head and neck.

#### ☐ Maintain airway

- Assessment and ongoing maintenance of ABCs (airway, breathing, circulation).
- Effective resuscitation if necessary.
- Reassurance and continuing communication with the victim.



Immobilization and airway management are the essential tasks when handling a spinal-injured victim. Photo: Peter Cooper.

Contact emergency medical services.

#### ☐ Stabilize

- Minimal movement of the victim.
- Recruit help if required.
- Effective lifeguard teamwork (and supervision of bystanders, if used) stabilization of the victim on a spineboard and removal from the water.

#### b) Number of rescuers.

The first responder immobilizes the victim in a face-up position at the surface using one of the techniques described in *The Canadian Lifesaving Manual*. Thereafter, which rescuer does what depends on the number of lifeguards available and the condition of the victim.

Always, the first step is to assess and maintain ABCs. An ABC problem takes priority – immobilization is maintained insofar as it is possible under the circumstances. (With only one lifeguard, immobilization may not be possible.)

Normally, a back-up lifeguard assesses ABCs. If the victim is responsive and breathing, the second lifeguard may support the victim's hips at the surface. If the victim is unresponsive and non-breathing, the victim requires immediate CPR. The second lifeguard should administer 2 rescue breaths and the victim should be removed quickly on a spineboard with just a chest strap and head support to minimize neck movement. Begin chest compressions as soon as the victim is removed from the water.

If there is no ABC problem, the second rescuer brings the spineboard to the shallow water removal point, while a third lifeguard takes over head support from the first lifeguard, ensuring constant immobilization of the head and neck throughout. However, in the slant-board procedure (see below), the transfer of head support happens after the victim is placed on the board.

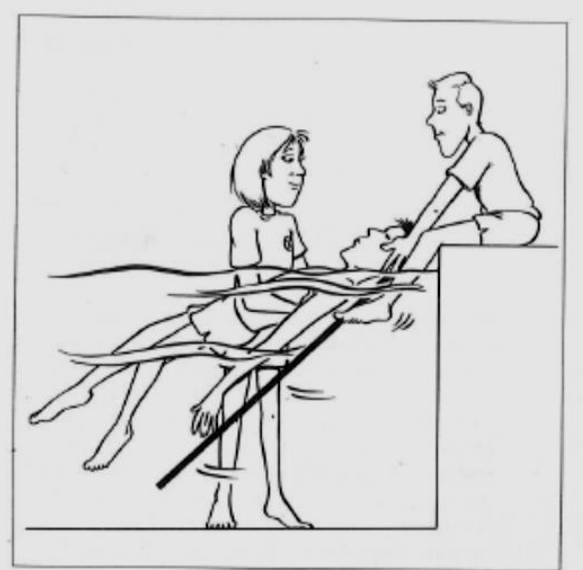
The first lifeguard, freed from head support, is responsible for the placement of the spineboard under the victim. Additional assistance for this task is desirable. With fewer than three lifeguards, it is advised that suitable bystander assistance be recruited, especially for the removal.

#### ☐ Flat-board procedure

Position the spineboard alongside and parallel to the victim. Knife the board on an angle below the surface under the victim. Control the board as it floats upward to support the victim.



The slant board spinal procedure can be performed by two lifeguards. The first lifeguard positions the victim over the slanted spineboard.



Control of the head is transferred to the second lifeguard who is on the pool edge. The first lifeguard then secures the victim to the spineboard.

#### ☐ Slant-board procedure

Knife the foot of the spineboard vertically into the water at the shallow water removal point, and stabilize it on a slant with your feet (if sitting) or arms (if kneeling). Alternatively, having entered shallow water, support the head of the slanted board on your lap or knees. The lifeguard carrying the victim positions the victim over the submerged slanted spineboard, while a second lifeguard helps guide the victim into position. Both lifeguards control the raising of the submerged portion of the spineboard and ensure the victim is centred on it.

Bystander assistants may not even have to get wet if they work from the deck or dock. In waterfront, surf, or waterpark situations, assistants will have to wade into shallow water with the board and then follow the lifeguard's instructions. The slant-board procedure can be performed in deep water if the transport of the victim to shallower water is impossible or impractical.

## Strapping the victim on the spineboard

Strap the victim in place beginning with the chest and hips. (If the head were strapped first, an unexpected movement of the body might cause neck injury.) Use an appropriate cervical immobilization device to stabilize the head and neck. Strap the feet last.

ABC complications can be managed quickly by applying just a chest strap and quick head support for immediate removal to permit care on land.

## ☐ Removal of the victim from the water

Wherever possible, remove a spinal-injured victim from shallow water. The spineboard removal requires a minimum of two people, but three or four are desirable. Usually two rescuers are in the water with one lifeguard on the deck or dock. Once the victim is secure, position the board perpendicular to the pool or dock edge. As the two lifeguards in the water sink the foot of the spineboard, the lifeguard on land carefully guides the board onto the deck or dock. If the board/edge does not permit sliding, rescuers will have to lift the board.

Take care to ensure that the straps are firmly fastened and that no jolting or jarring occurs during the removal.

Lifeguards should have a solid footing while maintaining a firm grasp of the

In deep water with no access to a low edge (e.g., far off shore, beyond the surfline, in a high walled deep tank), lifejackets or other flotation devices might be used to support the rescuers. Removal can be made vertically if necessary with immobilization maintained. Dry the victim and treat for shock while completing a victim assessment.

#### c) Victim on land.

If the victim is found on land, advise the victim not to move and immobilize the victim in the position found. Do not attempt to place the victim on a spineboard unless danger requires immediate removal. If the victim is standing, help immobilize the head and neck and assist the victim to a sitting or laying position on the ground.

Leave a prone or side-lying victim in this position unless presented with an ABC problem that cannot be managed in the position found. Careful repositioning is required with immobilization provided if possible

# MISSING PERSON AND SEARCH PROCEDURES

Lifeguard response to a missing persons report will vary with the aquatic facility and the nature of the report. The immediate concern is whether or not the missing person is in the water.

#### a) Guidelines for swimming pools.

In a swimming pool, check the water first and immediately. The need for a full underwater search is extremely unlikely, since lifeguards will close the pool if they cannot see the bottom clearly. One of the following options should be used:

- Signal to initiate a safety stop and scan the pool bottom from lifeguard chairs or the deck.
- Signal other guards you are leaving your post. Don mask or goggles and enter the water to check the swimming pool bottom.

If the missing person is not in the water, initiate the land search procedures outlined below.

## Appendix C – Sensitivity Analyses for Decision Matrices Spinal Board Geometry

a)

Criteria	Weight	Conventional	Curve	Porthole	Combination
Simplicity	0.2	5	3	4	3
Capacity to immobilize	0.15	5	8	5	8
Knife and slant rescues	0.2	5	7	9	10
Land rescue	0.2	5	8	5	8
Ease of maneouverability in water	0.25	5	8	6	9
Total	1	5	6.8	5.85	7.65

b)

Criteria	Weight	Conventional	Curve	Porthole	Combination
Simplicity	0.25	5	3	4	3
Capacity to immobilize	0.15	5	8	5	8
Knife and slant rescues	0.2	5	7	9	10
Land rescue	0.2	5	8	5	8
Ease of maneouverability in water	0.2	5	8	6	9
Total	1	5	6.55	5.75	7.35

c)

Criteria	Weight	Conventional	Curve	Porthole	Combination
Simplicity	0.25	5	3	4	3
Capacity to immobilize	0.1	5	8	5	8
Knife and slant rescues	0.15	5	7	9	10
Land rescue	0.2	5	8	5	8
Ease of maneouverability in water	0.3	5	8	6	9
Total	1	5	6.6	5.65	7.35

# Harnessing System

a)

Criteria	Weight	Conventional	Pin Lock	Twist Lock
Similarity to conventional	0.4	10	6	8
board				
Ease of use	0.3	5	3	4
Modularity/adjustability	0.3	5	9	9
Total	1.0	7.0	6.0	7.1

b)

Criteria	Weight	Conventional	Pin Lock	Twist Lock
Similarity to conventional	0.3	10	6	8
board				
Ease of use	0.4	5	3	4
Modularity/adjustability	0.3	5	9	9
Total	1.0	6.5	5.7	6.7

c)

Criteria	Weight	Conventional	Pin Lock	Twist Lock
Similarity to conventional	0.25	10	6	8
board				
Ease of use	0.35	5	3	4
Modularity/adjustability	0.4	5	9	9
Total	1.0	6.25	6.15	7.0

## Appendix D – Static Fluids Calculations for Board Geometry Design

clc clear %Constants P H20=1000; G=9.81;P HUMAN=1042; %average healthy male body composition COM HUMAN=1.9\*0.414; %average proportion from head, applied to 99% male M HUMAN=128; %99% male V HUMAN=M HUMAN/P HUMAN; %99th percentile male %All volumes, masses, COMs, rotational inertias determined by SolidWorks %mass properties function %%%%%%Analysis of board during knife rescue, (parallel to bottom)%%%%%% %unloaded %find maximum board mass that will allow board to float %unloaded v disp=0.03339; vb1=v disp; syms mb1 fb1=v disp\*P H2O\*G; fq1=mb1\*G; fnet1=fb1-fg1==0;sol1=solve(fnet1(1), 'mb1'); mb1=eval(sol1) %find that board must weigh less than 33kg to float unloaded %want to find the maximum weight that the board can support loaded mb total=6.90417; %assume 99% male human volume (worst case scenario, as someone very %large would likely have a larger volume) syms mh fb2=v\_disp\*P\_H2O\*G + V\_HUMAN\*P\_H2O\*G; fg2=mb total\*G + mh\*G;fnet2=fb2-fg2==0;sol2=solve(fnet2, 'mh'); mh=eval(sol2) %find that maximum load supported by board in water before sinking %is 149 kg; safety mh=mh\*0.9 %with 10% safety factor appled, maximum floation is 134 kg or

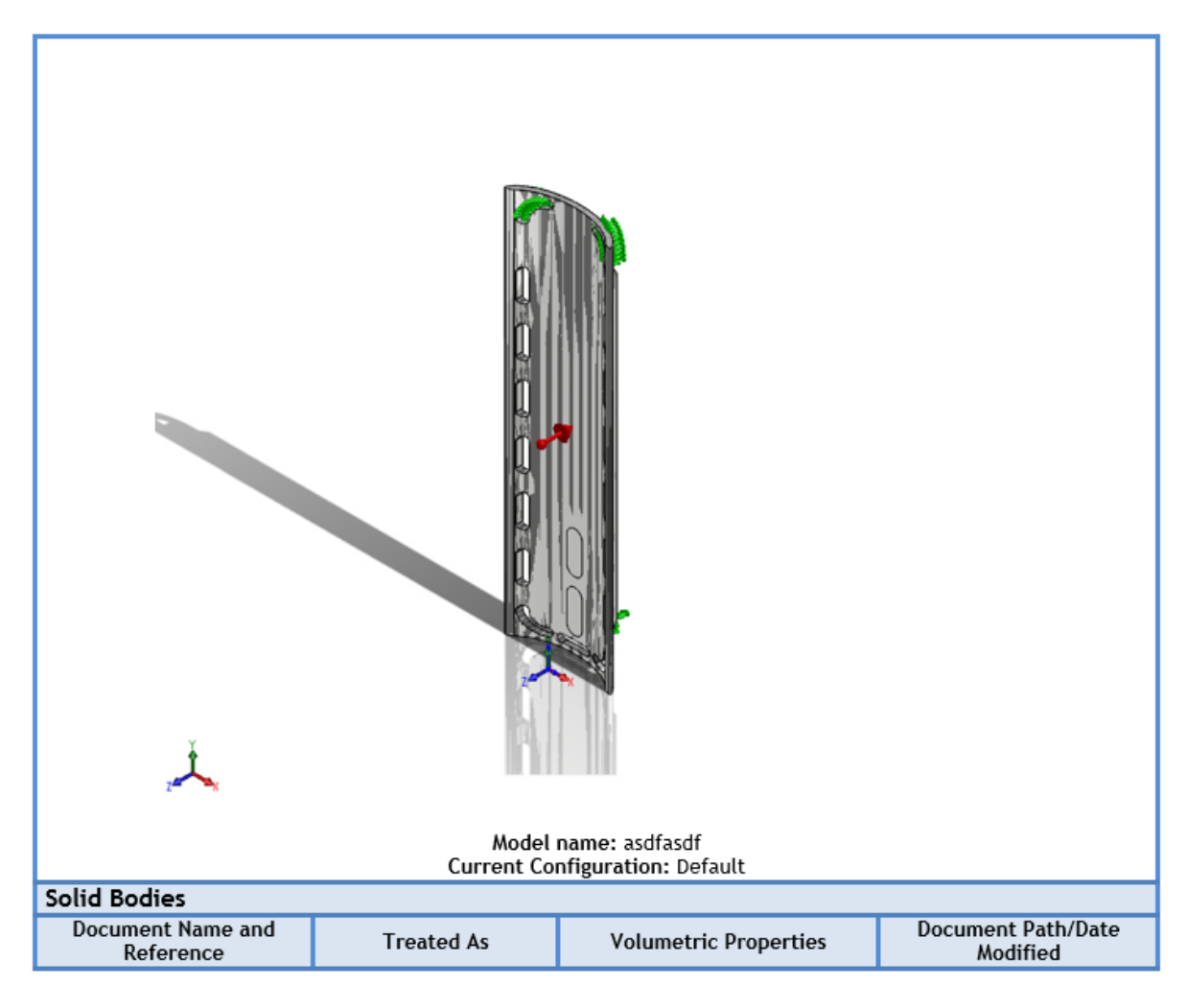
%~3001bs

```
%objective: have "foot end" of board sink when unloaded if porthole is
   %open
   THETA=45;
   H=1;
   L=1.9;
   L AIR=L-0.486;
   L p = L - 0.1;
       %check board without porthole (default)
          vsub d=0.0215+0.0037;
          com d=0.95209;
          ixx d= 2.04557;
          centroidsub d=(0.7309*0.6222 + 0.7090*4.5711)/(0.6438+4.5711);
          1 \text{ com}2p = L p - \text{com d};
          ixx_dp= ixx_d + mb_total*l_com2p^2;
          msub d=0.6438+4.5667;
          fg d= mb total*G;
          fb d=vsub d*P H2O*G;
          d fgd= L p - com d;
          d_fbd= L_p - centroidsub_d;
          syms aa d
          mnet= aa d*ixx dp - (sind(THETA)*(fg d*d fgd - fb d*d fbd))==0;
          sol d=solve(mnet, 'aa d');
          aa d=eval(sol d)
          %find that default board would rotate up by +21 \text{ rad/s2}
      % determine how submerged volume/centroid would have to change for
       % sinking to occur
          syms vsub p
          syms centroidsub p
          fb p=vsub p*P H2O*G;
          d fbp=L p - centroidsub p;
          fg p=fg_d;
          d fgp=d fgd;
          aa p=0;
          mnet= aa_p*ixx_dp - (sind(THETA)*(fg_p*d_fgp - fb_p*d_fbp)) == 0;
          sol p= solve(mnet, 'vsub p');
          vsub p=sol p
          %plot relationship between centroid location and submerged
```

```
%volume to determine possible options
            fun=vsub p;
            ezplot(fun, [0, 1.9]);
            %realize that realistically, a countersink must be added in
            %addition to 2 portholes; recalculate to determine how much
                vsub p2=0.0207+0.0035;
                com d=0.95209;
                ixx^{-}d = 2.04557;
                centroidsub p2=(0.7456*0.6222 +
0.7217*4.5711)/(0.6438+4.57\overline{11});
                1 com2p = L p - com d;
                ixx dp= ixx d + mb total*l com2p^2;
                 msub d=0.6222+4.5667;
                fg p2= mb total*G;
                fb_p2=vsub_p2*P_H2O*G;
                d fgd= L p - com d;
                d_fbp2= L_p - centroidsub_p2;
                syms msink
                aa d=0;
                mnet= aa d*ixx dp - (sind(THETA)*( fg p2*d fgd - fb p2*d fbp2
+ G*msink*1.9)) == 0;
                sol p2=solve(mnet,'msink');
                msink=eval(sol p2)
```

# Appendix E – Sample SolidWorks FEA Summary

### **Model Information**



LPattern1	Solid Body	Mass:0.834894 kg Volume:0.0278298 m^3 Density:30 kg/m^3 Weight:8.18196 N	H:\41X\curve board5 skinny.SLDPRT Mar 23 19:32:45 2015
Shell Bodies			
Document Name and Reference	Formulation	Volumetric Properties	Document Path/Date Modified
Surface-Trim2[7]	Thin	Thickness:3 mm Weight:0.409687 N Volume:3.34438e-005 m^3 Mass:0.0418048 kg Density:1250kg/m^3	C:\Users\dowlingj\AppDat a\Local\Temp\swx6776\V C~~\asdfasdf\shell^asdfas df.sldprt Mar 23 19:32:42 2015
Surface-Knit1	Thin	Thickness:3 mm Weight:88.4396 N Volume:0.00721956 m^3 Mass:9.02444 kg Density:1250kg/m^3	C:\Users\dowlingj\AppDat a\Local\Temp\swx6776\V C~~\asdfasdf\shell^asdfas df.sldprt Mar 23 19:32:42 2015

## **Study Properties**

- ·	
Study name	Static 1
Analysis type	Static
Mesh type	Mixed Mesh
Thermal Effect:	On
Thermal option	Include temperature loads
Zero strain temperature	298 Kelvin
Include fluid pressure effects from SolidWorks Flow Simulation	Off
Solver type	FFEPlus
Inplane Effect:	Off
Soft Spring:	Off
Inertial Relief:	Off
Incompatible bonding options	Automatic
Large displacement	Off
Compute free body forces	On
Friction	Off
Use Adaptive Method:	Off
Result folder	SolidWorks document (H:\41X)

## Units

Unit system:	SI (MKS)
Length/Displacement	mm
Temperature	Kelvin
Angular velocity	Rad/sec
Pressure/Stress	N/m^2

**Material Properties** 

Model Reference	Prop	erties	Components
	Name: Model type: Default failure criterion: Tensile strength: Compressive strength: Elastic modulus: Poisson's ratio: Mass density:	BioFoam Linear Elastic Isotropic Unknown 3.3e+007 N/m^2 200000 N/m^2 3.2e+006 N/m^2 0.3 30 kg/m^3	SolidBody 1(LPattern1)(curve board5 skinny-1)
Curve Data:N/A			
	Name: Model type: Default failure criterion: Yield strength: Tensile strength: Elastic modulus: Poisson's ratio: Mass density: Shear modulus:	PLA Linear Elastic Isotropic Unknown  5.78e+007 N/m^2 5e+007 N/m^2 3.5e+009 N/m^2 0.3 1250 kg/m^3 2.4e+009 N/m^2	SurfaceBody 1(Surface- Trim2[7])(shell^asdfasdf-1), SurfaceBody 3(Surface- Knit1)(shell^asdfasdf-1)
Curve Data:N/A			

## Loads and Fixtures

Fixture name	Fi	ixture Image		Fixture De	etails
Fixed-1	, ,			Entities: Type:	
Resultant Forces	5				
Componer		Χ	Y Z Resultant		Resultant
Reaction for	ce(N)	0.000102997	0.000167847	3530.61	3530.61
Reaction Mome	ent(N.m)	0	0	0	1e-033

Load name	Load Image	Load De	tails
Gravity-1			Front Plane 0 0-9.81 SI
Distributed Mass-1		Type: Coordinate System: Translation Values: Rotation Values: Reference coordinates: Remote Mass:	coordinates ,, mm ,, deg 0 0 0 mm 350 kg 0,0,0,0,0,0 kg.m^2

### **Connector Definitions**

No Data

## **Contact Information**

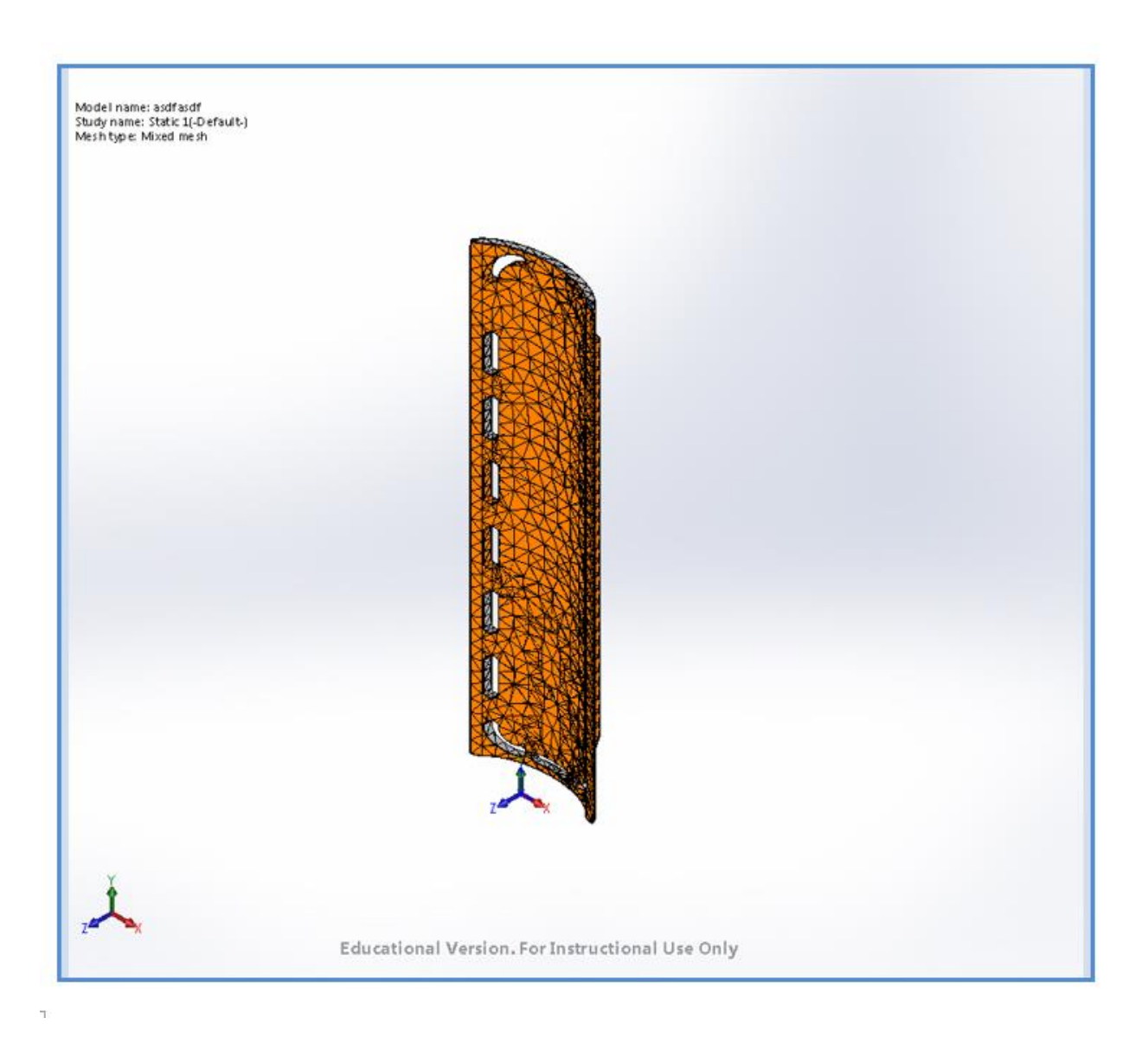
Contact	Contact Image	Contact Properties
Global Contact		Type: Bonded Components: 1 component(s) Options: Compatible mesh

## **Mesh Information**

Mesh type Mixed Mesh	
Mesher Used:	Curvature based mesh
Jacobian points	4 Points
Jacobian check for shell	On
Maximum element size	86.3445 mm
Minimum element size	17.2689 mm
Mesh Quality	High
Remesh failed parts with incompatible mesh	Off

### Mesh Information - Details

Total Nodes	15807
Total Elements	7493
Time to complete mesh(hh;mm;ss):	00:00:11
Computer name:	SOE-T2313-28



## **Resultant Forces**

### **Reaction Forces**

Selection set	Units	Sum X	Sum Y	Sum Z	Resultant
Entire Model	N	0.000102997	0.000167847	3530.61	3530.61

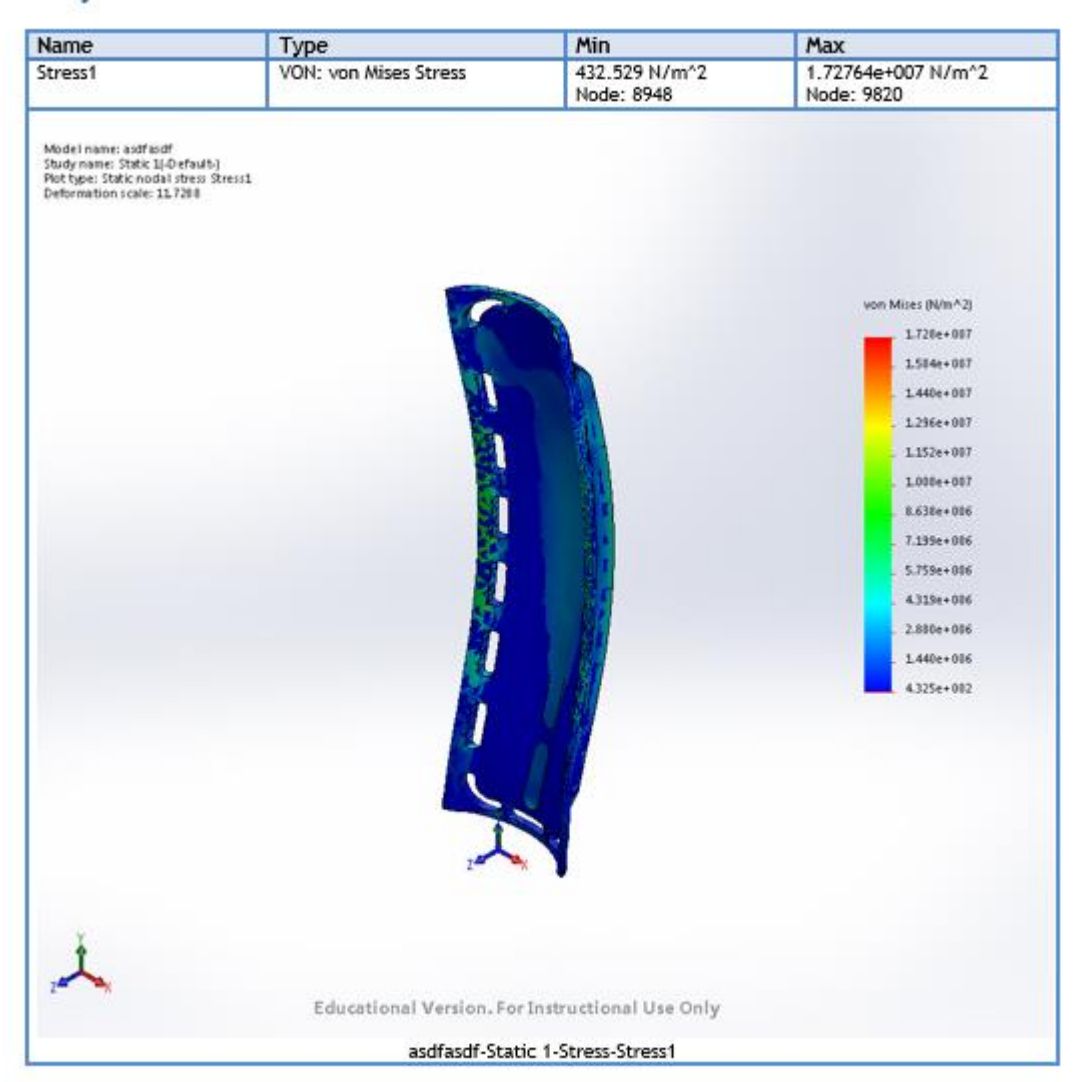
### **Reaction Moments**

Selection set	Units	Sum X	Sum Y	Sum Z	Resultant
Entire Model	N.m	0	0	0	1e-033

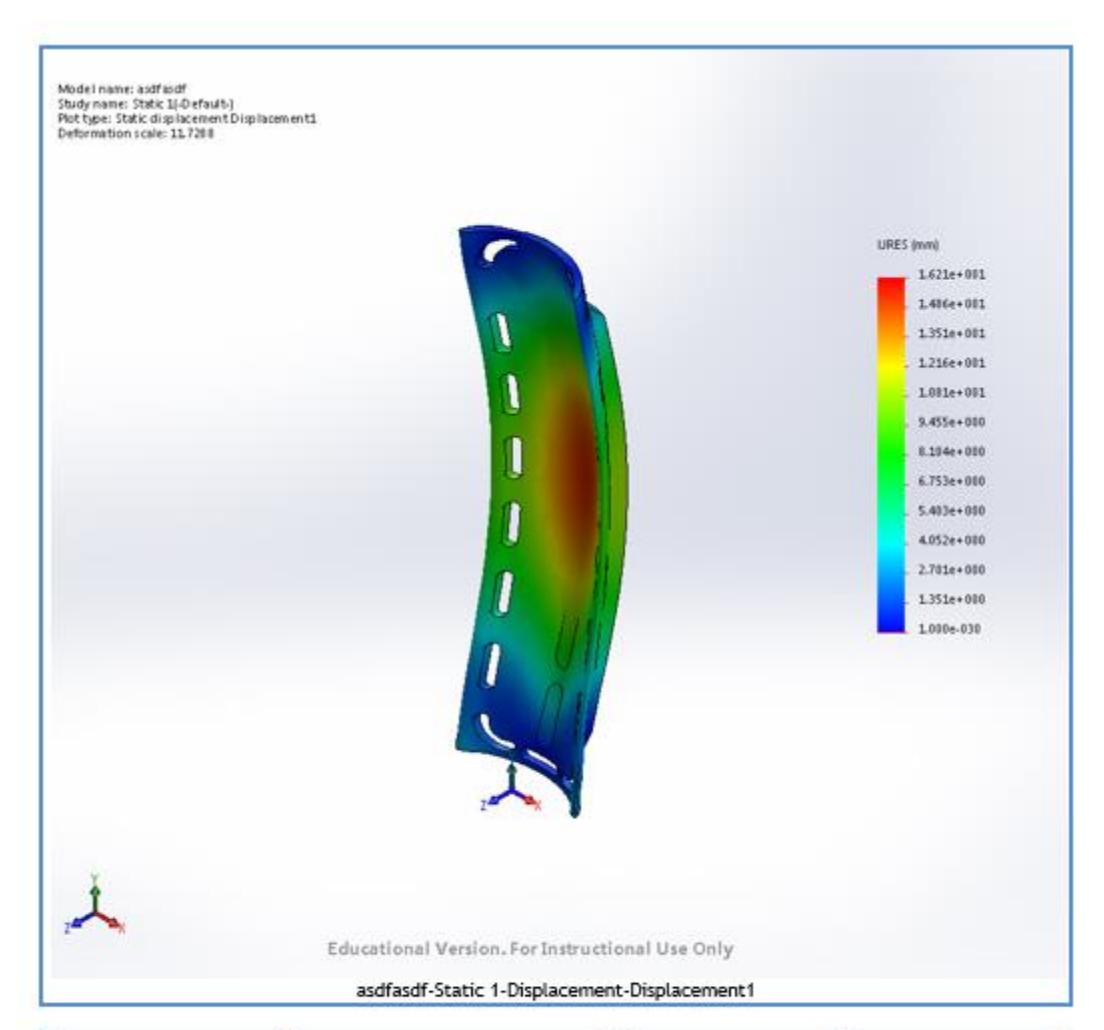
### **Beams**

No Data

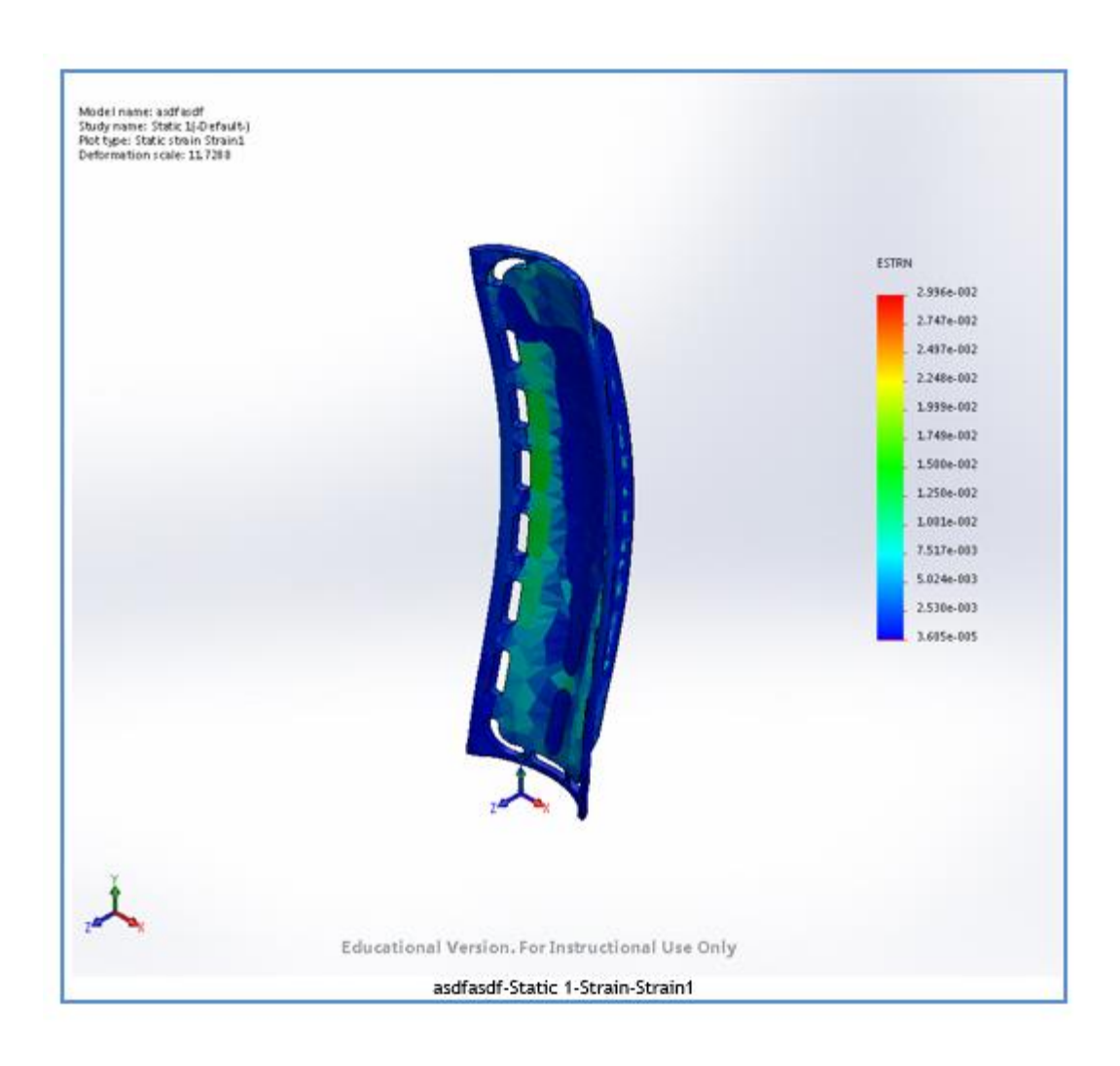
## **Study Results**



Name	Туре	Min	Max
Displacement1	URES: Resultant Displacement	0 mm Node: 266	16.2084 mm Node: 3914



Name	Туре	Min	Max	
Strain1	ESTRN: Equivalent Strain	3.60511e-005 Element: 7488	0.0299609 Element: 3480	



# Appendix F – Lifeguard Survey

# LIFEGUARD SURVEY 1: Conventional Spinal Board

### 31 March 2015

	oroximately how ma or)?	ny years of expe	erience do you h	ave working as a	a lifeguard (round to nearest half-
Eac	th of the following q	uestions pertains	s to the unmodif	ied spinal board.	
1.	Please circle how d	ifficult you think	it would be to s	ecure the straps	tightly on this board.
	1	2	3	4	5
imp	ossible		neutral		very easy;
2.	Please circle how d this board.	ifficult you think	t it would be to o	obtain the "ideal	" strap position for any victim on
	1	2	3	4	5
imp	ossible		neutral		very easy;
3.	Please circle how on number of steps re				ne using this board. Consider the em.
	1	2	3	4	5
exti	remely complex		neutral		easy to use
4.	Overall, describe yo	our satisfaction v	vith this board c	onfiguration as a	a lifeguard.
	1	2	3	4	5
diss	satisfied;		neutral		satisfied;
pre	fer not to use				prefer to use

### **LIFEGUARD SURVEY 2**

### 31 March 2015

Each of the following questions pertains to the prototype spinal board.

1.	Please circle how d	ifficult you think	it would be to se	ecure the straps	tightly on this board.
	1	2	3	4	5
imp	oossible		neutral		very easy;
2.	Please circle how d this board.	ifficult you think	it would be to o	obtain the "ideal	" strap position for any victim on
	1	2	3	4	5
imp	oossible		neutral		very easy;
3.	Please circle how on number of steps re-		•		e using this board. Consider the em.
	1	2	3	4	5
extı	remely complex		neutral		easy to use
4.	Overall, describe yo	our satisfaction v	vith this board co	onfiguration as a	ı lifeguard.
	1	2	3	4	5
diss	satisfied;		neutral		satisfied;
pre	fer not to use				prefer to use

# Appendix G – LCA Results Spinal Board LCA (QTY 1)

Table 10 Overview of the CO2 emission of a spinal board

Phase	Total CO2 (kg)
Manufacture	29.8
Transport	2.92
Use	0
Disposal	0.102

Table 11 Manufacturing and disposal of a spinal board

Part name	Material	Part mass	Qty	CO2
Strap buckle	HDPE, Recycled	0.03kg	6	0.6kg
Material:	HDPE, Recycled Injection			0.266kg
Process:	Moulding 0% recycled			0.331kg
Disposal:	100% landfilled			0.0024kg
Strap	Polyester fabric	0.01kg	6	0.413kg
Material:	Polyester fabric Cutting/machining			0.257kg
Process:	(10% scrap) 0% recycled, 100%			0.155kg
Disposal:	landfilled			0.0008kg
Spinal Board	HDPE, Virgin	7kg	1	27.4kg
Material:	HDPE, Virgin Injection			14.4kg
Process:	Moulding 0% recycled, 100%			0.552kg
Disposal:	landfilled			0.0933kg
Mount Unit	HDPE, Virgin	0.08kg	4	1.07kg
Material:	HDPE, Virgin Injection			0.472kg
Process:	Moulding 0% recycled, 100%			0.589kg
Disposal:	landfilled			0.00427kg
BioFoam	HDPE, Virgin	0.07kg	1	0.239kg
Material:	HDPE, Virgin Injection			0.144kg
Process:	Moulding			0.0934kg

0% recycled, 100%

Disposal: landfilled 0.000933kg

Table 12 CO2 emissions from the transportation of PLA from supplier.

Phase	Assembly Transported	Mode	Distance	CO2
NatureWorks, Minnetonka, MN (PLA supplier) to Guelph, ON (manufacture and warehouse)	Raw PLA	Lorry 7.5-16t, EURO5	1452 km	2.47kg
Symbra Tech (BioFoam) to Guelph, ON	BioFoam	Air freight, intercontinen tal	6038 km	0.451kg

## Spinal Board LCA (QTY 1000)

Table 13 Overview of the CO2 emission of 1000 spinal board

Phase	Total CO2 (kg)
Manufacture	160000
Transport	2920
Use	0
Disposal	102

Table 14 Manufacturing and disposal of 1000 spinal board

Part name	Material	Part mass	Qty	CO2
Strap buckle	HDPE, Recycled	0.03kg	6000	600kg
Material:	HDPE, Recycled Injection			266kg
Process:	Moulding 0% recycled			331kg
Disposal:	100% landfilled			2.4kg
Strap	Polyester fabric	0.01kg	6000	413kg
Material:	Polyester fabric Cutting/machining			257kg
Process:	(10% scrap) 0% recycled, 100%			155kg
Disposal:	landfilled			0.8kg
Spinal Board	HDPE, Virgin	7kg	1000	27400kg
Material:	HDPE, Virgin			14400kg

Process:	Injection Moulding 0% recycled, 100%			552kg
Disposal:	landfilled			93.3kg
<b>Mount Unit</b>	HDPE, Virgin	0.08kg	4000	1070kg
Material:	HDPE, Virgin Injection			472kg
Process:	Moulding 0% recycled, 100%			589kg
Disposal:	landfilled			4.27kg
BioFoam	HDPE, Virgin	0.07kg	1000	239kg
Material:	HDPE, Virgin Injection			144kg
Process:	Moulding 0% recycled, 100%			93.4kg
Disposal:	landfilled			0.933 kg

Table 15 CO2 emissions from the transportation of PLA from supplier.

Phase	Assembly Transported	Mode	Distance	CO2
NatureWorks, Minnetonka, MN (PLA supplier) to Guelph, ON (manufacture and warehouse)	Raw PLA	Lorry 7.5-16t, EURO5	1452 km	2480kg
Symbra Tech (BioFoam) to Guelph, ON	BioFoam	Air freight, intercontinen tal	6038 km	451kg

## Appendix H - KineMat MATLAB Toolbox

### Angle peak-to-peak determination

```
%Assign coordinates to segments (s1neutr, s2neutr)
load neutral.txt;
HN = neutral(1, (1:9));
TN=neutral(1,(10:18));
%Assign coordinates to segments (s1mov, s2mov)
file1 = csvread('DRAG TEST 2.csv',5,2);
HM1 = file1(:,1:9);
TM1 = file1(:,10:18);
%Apply Butterworth filter
[bb,aa]=butter(2,.1);
HM1F=filter(bb,aa,HM1);
TM1F=filter(bb,aa,TM1);
%Run Angle Analysis
[Angle1, Helix1] = cardan(HN, TN, HM1F, TM1F, 'zxy');
%Normalize to beginning of trial
X1 = sum(Helix1(1:100,1))/100;
Y1 = sum(Helix1(1:100,2))/100;
Z1 = sum(Helix1(1:100,3))/100;
A1 = Helix1(:,1) - X1;
B1 = Helix1(:,2) - Y1;
C1 = Helix1(:,3) - Z1;
%Find peak 2 peak values
AA1=peak2peak(A1);
BB1=peak2peak(B1);
CC1=peak2peak(C1);
```

#### Cardan.m

```
function[angles, helicang] = cardan(s1neut, s2neut, s1mov, s2mov, sequence)
% function[angles,helicang]=cardan(s1neut,s2neut,s1mov,s2mov,sequence)
% Description: This program calculates the intersegmental motion expressed
                in terms of Cardan angles (joint coordinate system) and
helical
       angles (Woltring, 1994) between two segments.
% Input: slneut: markers of segment 1 in anatomical position
       s2neut: markers of segment 2 in anatomical position
                 markers of segment 1 during the movement
       s1mov:
       s2mov:
                 markers of segment 2 during the movement
응
        sequence: string e.g. 'xyz' would mean:
응
                          - first rotation about x-axis of segment 1
응
                          - y is floating axis
응
                          - last rotation about z-axis of segment 2
응
       Note that segment 1 and 2 may contain a redundant number of
       markers (>3).
% Output: angles: amount of rotation about x,y,z axes (alpha,beta,gamma)
      helicangles: helical angles (Woltring, 1994)
% Author: Christoph Reinschmidt, HPL, The University of Calgary
          November, 1995
% Last Changes: November 28, 1996
% Version: 1.0
% References:
               (1) Grood, E.W., and Suntay, W.J. (1983) A joint coordinate
            system for the clinical description of three-dimensional
응
            motions: applications to the knee.
응
            J. biomech. Engng 105, 136-144.
        (2) Woltring, H.J. (1994) 3-D attitude representation of
응
                    human joints: A standardization proposal.
응
                    J. Biomechanics 27, 1399-1414.
[a1,b1]=size(s1mov);
[a2,b2] = size(s2mov);
[c1,d1]=size(s1neut);
[c2,d2] = size (s2neut);
if \sim ((a1==a2) \& (b1==d1) | (b2==d2))
 disp('The matrices of the segments do not agree! Try again!'); return
for i=1:size(s1mov, 1)
  % Calculating the Cardan angles
  T1=inv(soder([s2neut;s2mov(i,:)])) * soder([s1neut;s1mov(i,:)]);
  eval(['angles(i,:)=r' sequence 'solv(T1);']);
  % Woltring's (1994) helical convention (helical angles)
  [n1, point1, phi1, t1] = screw(T1); helicang(i, 1:3) = n1(1:3, 1)'.*phi1;
end
```

#### Soder.m

```
function [T, res] = soder(data)
% function [T, res] = soder(data)
% Description: Program calculates the transformation matrix T containing
        the rotation matrix (3x3) and the translation translation
응
       vector d (3x1) for a rigid body segment using a singular
응
       value decomposition method (Soederkvist & Wedin 1993).
% Input:
           data:
                   columns represent the XYZ positions and the rows
                   represent time.
% Output:
           T:
                   4x4 Matrix containing the rotation matrix R and the
응
                    translation d: T = [R,d; 0 0 0 1]
응
                   norm of residuals (measure of fit; "rigidity" of body
           res:
응
% References:
                 Soderkvist I. and Wedin P. -A., (1993). Determining the
                 movements of the skeleton using well-configured markers.
응
                  Journal of Biomechanics, 26:1473-1477
% Author:
           Christoph Reinschmidt, HPL, The University of Calgary
                (Matlab code adapted from Ron Jacobs, 1993)
% Date:
           February, 1995
% Last Changes: December 09, 1996
% Version:
               3.1
if (size(data, 2)/3) \sim = fix(size(data, 2)/3),
   disp('ERROR: input has to be multiple of 3 (XYZ coordinates)'); return
end
A=[reshape(data(1,:)',3,size(data,2)/3)]';
B=[reshape(data(2,:)',3,size(data,2)/3)]';
% Checking for NaNs and also checking if still 3 pts left and if not
% T=[NaN...];
cut=[0];
qA=isnan(A); qB=isnan(B); qAB=[qA,qB];
qsum=sum(qAB'); cut=find(qsum~=0);
A([cut],:)=[]; B([cut],:)=[];
if size (A, 1) < 3,
return:
end
Amean=mean(A)'; Bmean=mean(B)';
 for i=1:size(A,1)-size(cut,2),
        Ai(:,i) = [A(i,:) - Amean']';
       Bi(:,i) = [B(i,:) - Bmean']';
end
C=Bi*Ai';
[P,T,Q]=svd(C);
R=P*diag([1 1 det(P*Q')])*Q';
```

```
d=Bmean-R*(Amean);
T=[R,d;0 0 0 1];
% Calculating the norm of residuals
A=A'; A(4,:)=ones(1,size(A,2));
B=B';
Bcalc=T*A; Bcalc(4,:)=[]; Diff=B-Bcalc; Diffsquare=Diff.^2;
%DOF=3*(number of points)-6 unknowns (Hx,Hy,Hz,alpha,beta,gamma):
DOF=size(B,1)*size(B,2)-6;
res=[sum(Diffsquare(:))/DOF].^0.5;
```

#### Screw.m

```
function [n,point,phi,t]=screw(T,intersect);
% Calculation of the screw axis
% function [n,point,phi,t]=screw(T)
% Input:
          T matrix containing the rotation matrix and transl. vector
                [R; [t1, t2, t3]'; 0 0 0 1]
                   location of the screw axis where it intersects either the
        intersect
x=0 (intersect=1),
                        the y=0 (intersect=2), or the z=0 (intersect=3)
plane.
            default: intersect=3
응
% Output:
              unit vector with direction of helical axis
           n
           point point on helical axis
           phi
                  rotation angle (in deg)
응
                    amount of translation along screw axis
            +
% Comments:
                Note that phi is b/w 0 and 180 deg. Right handed screw
                axis system. The "sign" of phi can be checked with direction
응
                of the unit vector (n).
% References:
               (1) Spoor and Veldpaus (1980) Rigid body motion calculated
                    from spatial co-ordinates of markers.
응
                    J Biomech 13: 391-393
응
                (2) Berme, Cappozzo, and Meglan. Rigid body mechanics
응
                    as applied to human movement studies. In Berme and
                    Cappozzo: Biomechanics of human movement.
% Author:
             Christoph Reinschmidt, HPL, UofCalgary
                Oct. 03, 1994
% Date:
% Last Changes: Nov-20-96
if nargin==1, intersect=[3]; end
R=T(1:3,1:3);
% tmp is matrix in equ. 31 (Spoor and Veldpaus, 1980)
tmp=[R(3,2)-R(2,3);R(1,3)-R(3,1);R(2,1)-R(1,2)];
%calculating n using equ. 31 and 32 (Spoor and Veldpaus, 1980)
n=tmp/norm(tmp);
% calculating phi either with equ. 32 or 34 (Spoor and Veldpaus, 1980)
% depending if sin(phi) smaller of bigger than 0.5*SQRT(2)
if norm(tmp) <= sqrt(2)</pre>
      phi=rad2deg(asin(0.5*norm(tmp)));
else phi=rad2deg(acos(0.5*(R(1,1)+R(2,2)+R(3,3)-1)));
end
%if phi approaches 180 deg it is better to use the following:
% (see Spoor and Veldpaus Eq. 35,36)
if phi>135;
  b=[0.5*(R+R')-cos(deg2rad(phi)) * eye(3)];
  b1=[b(:,1)]; b2=[b(:,2)]; b3=[b(:,3)];
  btmp=[b1'*b1;b2'*b2;b3'*b3];
   [bmax, i] = max(btmp);
   n=b(:,i)/sqrt(bmax);
```

```
if sign(R(3,2)-R(2,3)) \sim sign(n(1,1)); n=n.*(-1); end; end t=n'*T(1:3,4); % calculate where the screw axis intersects the plane as defined in 'intersect' Q=R-eye(3); Q(:,intersect)=-n; point=Q\[T(1:3,4).*[-1]]; point(intersect,1)=[0];
```

## Appendix I - Full Experimental Results

Table 16: Full results of peak-to-peak angles

Toot	Angle	Conventional Board [°]		Modified Harness [°]			Padded Board [°]			
Test	Angle	Trial 1	Trial 2	Trial 3	Trial 1	Trial 2	Trial 3	Trial 1	Trial 2	Trial 3
	Flexion / Extension	8.1647	7.2953	4.2117	5.2148	5.7485	4.2009	6.218	3.304	4.5221
Drag	Rotation	3.8848	4.3612	2.7767	6.2529	8.5554	16.530	3.702	2.0386	2.4903
	Lateral Bend	2.7998	2.3626	2.7677	2.3775	2.484	12.190	1.8432	1.1966	1.4061
	Flexion / Extension	7.2458	7.7374	5.8222	8.114	4.6246	4.9709	4.2666	14.910	3.9566
Tip	Rotation	2.1086	1.7418	3.3039	2.4851	2.2127	1.601	2.298	5.9889	2.1793
	Lateral Bend	2.5283	2.6059	6.0656	1.9567	1.2893	1.4096	1.8981	5.8671	1.5589
	Flexion / Extension	8.9453	6.9672	5.3247	14.8296	16.159	17.461			
Puke	Rotation	6.2054	5.2645	7.6861	22.3274	18.970	21.957			
	Lateral Bend	6.8946	5.4109	4.2418	10.0838	9.7133	10.715			

Note: Red font denotes trials that were omitted in mean calculations as outliers. Outliers were defined as trials in which a calculated angle was at least 3 times greater the same angle calculated for each other trial under the same test conditions.

Table 17: Full results of body displacement

Tost	Displacement	Conventional Board [mm]			Modified Harness [mm]		
Test	Displacement	Trial 1	Trial 2	Trial 3	Trial 1	Trial 2	Trial 3
Drag	Longitudinal	Lost markers	55.3058	53.6658	49.571	53.5333	Lost markers
Tip	Longitudinal	64.2806	55.1758	70.8233	72.0929	61.2175	58.8842
Puke	Lateral	15.2238	30.1538	30.1706	12.8917	17.529	17.4431

Note: Red font denotes trials that had large gaps in the sternum (ST) and bottom centre (BC) markers and could therefore not calculate a vector between these positions accurately.